

Rowan University

Rowan Digital Works

Theses and Dissertations

5-2-2017

Effects of bioengineering scaffolds releasing neurotrophins and body weight supported treadmill training on H-reflex after spinal cord injury

Jaclyn Ann Witko

Follow this and additional works at: <https://rdw.rowan.edu/etd>



Part of the [Biomedical Engineering and Bioengineering Commons](#)

Recommended Citation

Witko, Jaclyn Ann, "Effects of bioengineering scaffolds releasing neurotrophins and body weight supported treadmill training on H-reflex after spinal cord injury" (2017). *Theses and Dissertations*. 2394. <https://rdw.rowan.edu/etd/2394>

This Thesis is brought to you for free and open access by Rowan Digital Works. It has been accepted for inclusion in Theses and Dissertations by an authorized administrator of Rowan Digital Works. For more information, please contact graduateresearch@rowan.edu.

**EFFECTS OF BIOENGINEERING SCAFFOLD RELEASING
NEUROTROPHINS AND BODY WEIGHT SUPPORTED TREADMILL
TRAINING ON H-REFLEX AFTER SPINAL CORD INJURY**

by

Jaclyn Ann Witko

A Thesis

Submitted to the
Department of Mechanical Engineering
College of Engineering
In partial fulfillment of the requirement
For the degree of
Master of Science in Mechanical Engineering
at
Rowan University
July 14, 2016

Thesis Chair: Tom Merrill, Ph.D.

© 2016 Jaclyn Ann Witko

Acknowledgments

I would like to thank my advisor Dr. Anita Singh, for all of her hard work and dedication to this project. It was your determination and motivation that kept me extremely excited about the project and field of study. I would also like to thank Brittany King for making this very long journey more fun and enjoyable. From all the long days and nights, I probably would not have made it through without all the fun and laughter we had. I would also like to thank my thesis committee members, Dr. Thomas L. Merrill and Dr. Jennifer Vernango, for their participation and advice throughout this journey. I would also like to thank Karl Dryer for his expert skills in designing treadmills and problem solving and the Vivarium staff. I would also like to thank Rowan University and Rowan School of Osteopathic Medicine for the opportunity to follow my dreams of obtaining a higher-level degree.

Lastly, I would like to thank my parents, family, and friends for all their support and encouragement throughout these years. Without them I would not have made it through this long couple of years. To my parents, thank you for everything you have taught me and has made me into the person I am today, and the late-night phone calls complaining how over this I am. To my friends, thank you for always encouraging me and listening even though you never understood what the heck I was talking about most of the time.

Abstract

Jaclyn Ann Witko

EFFECTS OF BIOENGINEERING SCAFFOLDS RELEASING NEUROTROPHINS AND
BODY WEIGHT SUPPORTED TREADMILL TRAINING

2015 - 2016

Tom Merrill, Ph.D.

Master of Science in Mechanical Engineering

Changes in monosynaptic reflex, often used to study spasticity, has been tested through the H-reflex in spinal cord injury (SCI) patients after rehabilitation training, such as body weight support treadmill training or cycling. The combinational effects of rehabilitation training and a bioengineered scaffold on spasticity in SCI animal model have not been studied. We used a clinically relevant animal model of spinal cord moderate contusion at T9/T10 with BWSTT and the bioengineered scaffold PNIPAAm-g-PEG loaded with the growth factors BDNF/NT-3 to measure the efficiency of the combinational bioengineered approach to treat spasticity. Five animal groups were included in the study: sham, injury, SCI + BWSTT, SCI + PNIPAAm-g-PEG with BDNF/NT-3 (Transplant), and SCI + BWSTT/PNIPAAm-g-PEG with BDNF/NT-3 (combinational). Results indicate that there was an increase in the over ground BBB test scores from the BWSTT, and combinational groups from weeks 6-8, but not in the transplant only or injury groups when compared to the sham. There was also a decrease in habituation of the H-reflex and restoration of rate depression properties in both the BWSTT and combinational groups.

Table of Contents

Abstract.....	iv
List of Figures.....	viii
List of Tables.....	xii
Chapter 1: Introduction.....	1
Background.....	1
Problem Statement.....	3
Hypothesis.....	3
Organization of Thesis.....	3
Chapter 2: The Spinal Cord.....	4
Anatomy.....	4
Vertebral Column (Spine).....	4
Nervous System.....	10
Spinal Cord Injury.....	18
Epidemiology.....	18
Injury Types.....	20
Animal Models of Spinal Cord Injuries.....	21
Pathophysiology of SCI.....	25
Spasticity After SCI.....	26
Current Treatments.....	27
Pharmaceutical.....	27
Transplant.....	28
Rehabilitation.....	29

Table of Contents (Continued)

Chapter 3: Reflexes and Spasticity	30
Overview	30
Spasticity	32
Reflexes	33
M-Wave	33
H-Wave	34
Human Studies	36
Animal Studies	43
Chapter 4: Therapeutic Approaches to Treat Spasticity in Spinal Cord Injury	54
Rehabilitation	54
Body Weight-Support Treadmill Training (BWSTT)	54
Functional Electrical Stimulation (FES)	55
Cycling	55
Transplant	56
Cell-Based Therapies	56
Hydrogel-Based Biomaterials	64
Self-Assembling Peptides	81
Combinational Biomaterials	82
Chapter 5: Using Bioengineered Scaffold Loaded with Neurotrophins to Enhance Functional Recovery after Locomotor Training in Spinal Cord Injury	
Animals	85
Abstract	85

Table of Contents (Continued)

Introduction.....	86
Methods and Materials.....	88
Spinal Cord Injury (Contusion) And Animal Care.....	88
Transplantation	90
Behavioral Analysis.....	90
Treadmill Training.....	90
Electrophysiology (H-Reflex).....	93
Statistical Analysis.....	95
Results.....	96
Behavior Test-Overground BBB Test	96
H-Reflex.....	97
Discussion.....	102
Conclusion	109
Chapter 6: Future Work	111
References.....	113
Appendix: Definitions.....	120

List of Figures

Figure	Page
Figure 1. Vertebral column and its five regions (Moore, 1980)	5
Figure 2. Movements of vertebral column (Moore, 1980)	6
Figure 3. Curvatures of vertebral column (Moore, 1980).....	6
Figure 4. Surface anatomy of curvatures of vertebral column (Moore, 1980)	7
Figure 5. Typical vertebra represented by the 2 nd lumbar vertebra (Moore, 1980)	8
Figure 6. Lateral view of the lumbar vertebrae (Moore, 1980)	9
Figure 7. Structure and function of IV discs (Moore, 1980)	10
Figure 8. Multiple motor neurons synapsing (Moore, 1980).....	12
Figure 9. Basic organization of the spinal cord (Moore, 1980)	13
Figure 10. Spinal cord nuclei and laminae (Anatomy)	14
Figure 11. Spinal cord and spinal meninges (Moore, 1980).....	15
Figure 12. Myelinated and unmyelinated nerve fibers (Moore, 1980).....	17
Figure13. Arrangement and ensheathment of myelinated nerve fibers (Moore, 1980)....	17
Figure 14. Spinal cord gray matter, spinal roots, and spinal nerves (Moore, 1980).....	18
Figure 15. Causes of spinal cord injuries (Christopher and Dana Reeves Foundation, April, 2009).....	19
Figure 16. Causes of paralysis (Christopher and Dana Reeve Foundation, April 2009).....	20
Figure 17. American Spinal Injury Association scale for Spinal Cord Injury.....	21
Figure 18. Contusion and compression injuries of the spinal cord usually involve exposing the spinal cord with a dorsal laminectomy, typically in the thoracic region but sometimes in cervical or lumbar spinal cord	24
Figure 19. Mechanism of spinal cord injury (Sabapathy et al., 2015).....	26
Figure 20. Response of H-reflex for a non-injured animal with increasing stimulus frequency.....	31
Figure 21. Electrical stimulation of a mixed nerve.....	35

Figure 22. A nerve cell that shows the direction of orthodromic and antidromic direction (http://nervecell-assessment.weebly.com/2d-labelled-diagram.ht)	35
Figure 23. Summary of absolute peak-to-peak reflex electromyographic amplitude (SRPP), absolute Hmax value, and Mmax of each subject group	38
Figure 24. Summary of relative peak-to-peak stretch reflex sizes and H/M ratios for each subject group.....	38
Figure 25. Persons with incomplete SCI: percentage decrease in H/M ratio while walking in BWSMAT environment compared with unassisted overground environment	39
Figure 26. Characteristics of M-wave and H-reflex under control conditions and during sinusoidal hip stretches.....	40
Figure 27. Standing i-SCI vs. non-injured control.....	41
Figure 28. M wave to H reflex response sensitivity graphs.....	42
Figure 29. Changes in baseline H/M ration after varying degrees of SCI.....	45
Figure 30. Overlapping representative H-reflex waveforms of uninjured control (A) and 4-week Mild SCI (B) animals measured at 0.1, 1 and 5 Hz stimulus frequencies	45
Figure 31. Alteration of H-reflex rate depression over time after varying degrees of SCI	46
Figure 32. Averages of 16 consecutive responses following tibial nerve stimulation recorded in plantar muscles in representative animals in each group	47
Figure 33. Graph of the mean and standard deviation of the H-reflex at 1 Hz, 5 Hz and 10 Hz stimulation frequency as a percent of the response observed at 0.3 Hz stimulation frequency	48
Figure 34. Averages of H-reflex recordings	49
Figure 35. H-reflex amplitude at 0.2, 1, 5, and 10Hz for intact animals (CONTROL, open circles), and 15 (Tx + Ex 15D, filled diamonds), 30 (Tx + Ex 30D, filled circles), 45 (Tx + Ex 45D, filled triangles), 60 (Tx + Ex 60D, filled plus signs) and 90 (Tx + Ex 90D, filled squares) days of MBET, and 90 days without MBET (Tx ONLY 90D, open squares)	50
Figure 36. H-reflex amplitude at 0.2, 1, 5, and 10Hz for CONTROL (open circles), 30 days without MBET (Tx only 30D, filled squares), and 30 days with MBET (Tx + Ex 30D, filled diamonds)	51

Figure 37. (a) Representative H-reflex recordings of animals tested 7 days after transection (Tx)	52
Figure 38. H-reflex amplitude at 0.2, 1, 5 and 10Hz in intact (control, filled circles), Tx 7D (squares), Tx 14 D (diamonds) and Tx 30D (triangles) groups.....	53
Figure 39. Application of mesenchymal stromal stem cells (MSCs) as a treatment for spinal cord injury	62
Figure 40. Hydrogel properties considered relevant for drug and cell delivery to the central nervous system	65
Figure 41. Chemical structure of poly (lactic acid) (PLA)	66
Figure 42. Chemical structure of poly (lactic-co-glycolic acid) (PLGA).....	68
Figure 43. Chemical structure of poly [N-2- (hydroxypropyl) methacrylamide] (PHPMA)	69
Figure 44. Chemical structure of poly (2-hydroxyethyl methacrylate) (PHEMA).....	70
Figure 45. Chemical structure of poly (ethylene glycol) (PEG).....	72
Figure 46. Chemical structure of agarose	74
Figure 47. Chemical structure of alginate.....	75
Figure 48. Collagen triple helix structure	76
Figure 49. Fibrinogen and fibrin formation	78
Figure 50. Chemical structure of chitosan	79
Figure 51. Chemical structure of hyaluronic acid.....	81
Figure 52. Custom treadmill and body weight support (BWS)	91
Figure 53. Custom body weight support (BWS) treadmill with components labeled	92
Figure 54. Rat undergoing BWSTT	92
Figure 55. Bipolar hook electrode	93
Figure 56. Set up of A-M Systems Isolated Pulse Stimulator Model 2100, A-M Systems Differential Amplifier Model 1700, and Tektronix TDS 310 oscilloscope used for H-reflex	94
Figure 57. NI USB-6212 used to collect M and H waves	95

Figure 58. A schematic diagram of how the M and H waves are stimulated and the path it travels to the spinal cord to produce the response 95

Figure 59. BBB scores 97

Figure 60. Averages of H-reflex recording at 0.3 and 10 Hz100

Figure 61. H ratio – 10/0.3 Hz for each group.....101

Figure 62. H/M Ratios at 0.3 and 10 Hz for control (circles), injury (square), BWSTT (diamond), transplant (asterisk) and combinational (triangle).....102

List of Tables

Table	Page
Table 1. Summary of the current SCI animal models that are used in research to mimic the clinical human SCI	23
Table 2. Therapeutic potential of combinational approaches based on cell therapy and biomaterials for spinal cord injury treatment (Assunção-Silva et al., 2014) ...	84
Table 3. Number of animals in each group.....	89

Chapter 1

Introduction

Background

Spinal cord injury (SCI) affects an estimated 40 cases per million population in the United States with about 12,500 new cases reported each year, according to the National Spinal Cord Injury Statistical Center. Studies have shown that vehicle crashes are the leading cause of injury, and spinal cord injuries are the second leading cause of paralysis among Americans (Christopher and Dana Reeve Foundation, April 2009). There is no known cure for spinal cord injuries and available treatments just help minimize pain and discomfort, thereby slowing the progression of secondary damage. One such secondary problem that results after SCI is spasticity, which is reported in 65 -78% of patients (Adams et al., 2005). Treatment options are currently available to decrease spasticity and the associated pain and discomfort. One of those treatments is an activity based rehabilitation therapy, which includes body weight support treadmill training. Body weight support treadmill training after an incomplete spinal cord injury can help retrain the complex circuitry and connections within the spinal cord (SC), resulting in functional improvement. Since greater sparing within the SC after injury can result in higher functional improvement (Nógrádi et al., 2000-), neuroprotection and regeneration transplantation treatment strategies, combined with training, should improve the outcomes after body weight support treadmill training. Transplantation of cells that have been genetically engineered to deliver neurotrophins, such as brain derived nerve growth factor, (BDNF) or neurotrophin-3 (NT-3), because they have neuroprotective and neuroregenerative properties. BDNF has been studied and shown to stimulate growth of

vestibulospinal fibers (Boyce et al., 2014), which are fibers found within the vestibulospinal tract that runs along each side of the central nervous system (Pease, 2006). BDNF has also been found to cause increased excitability of motor neuron in an injured spinal cord, but has no effect on the strength of synaptic projections to motor neurons, unlike NT-3. NT-3 will enhance the strength of synaptic projection to the motor neurons and will increase corticospinal fiber growth (Boyce et al., 2014). These fibers are found in the corticospinal tract, which consists of four columns of motor fibers that run along either side of the spinal cord (Pease, 2006). The BDNF and NT-3 will work together after injury to protect and minimize the secondary damage of the pathways, while promoting growth of new pathways based on their properties of repairing the spinal cord (Boyce et al., 2014). These neurotrophins have the potential to help reduce spasticity because it is caused by the damage that occurs to the nerve pathways (Reese et al., 2006). Previous studies conducted by Skinner et al., 1996 and Phadke et al., 2006, among others have shown that if there are more spared pathways within the injury site that are preserved, the less severe spasticity the patient will experience.

Many different cell types pose a problem when tested in animal models in regards to rejection, regulation of release among others (Assunção-Silva et al., 2014). To overcome these problems, our study uses the bioengineered scaffold poly N-(isopropylacrylamide) – poly (ethylene glycol) (PNIPAAm-PEG) loaded with neurotrophins as a transplant because it has shown to be highly biocompatible, and when functionalized to secrete a neurotrophic factor, it can promote regeneration and functional recovery in a surgically induced spinal cord injury animal model (Comolli et al., 2009).

Problem statement. To study changes in monosynaptic, also known as H-Reflex, reflex pathway after combinational treatment using bioengineered scaffold (PNIPAAm-PEG) secreting neurotrophins (BDNF+NT3) and rehabilitation training using body weight support treadmill training (BWSTT) in a clinically relevant contusion spinal cord injury (SCI) animal model.

Hypothesis. Neurotrophins secreting scaffold will protect and minimize the secondary damage that the descending pathways undergo, while promoting growth of new pathways that together will help restore the H-reflex response after body weight support treadmill training (BWSTT).

Organization of thesis. This first chapter is an outline of why our research is relevant to spinal cord injuries. It states the problem statement along with the hypothesis proposed. Chapter 2 discusses the spinal cord in detail, including injury types, anatomy, and current treatments for spinal cord injuries. Chapter 3 discusses the reflexes and spasticity that occur in the spinal cord, how they are studied, and how they relate to the current problem statement and hypothesis. Chapter 4 presents therapeutic approaches to treat spasticity in spinal cord injuries, including rehabilitation, transplant, and combinational biomaterials. Chapter 5 is the manuscript, and provides a draft for future publication. Lastly, Chapter 6 is conclusions and future work, and discusses where the research will lead in the future and more studies that are needed in order to enhance spinal cord injury research.

Chapter 2

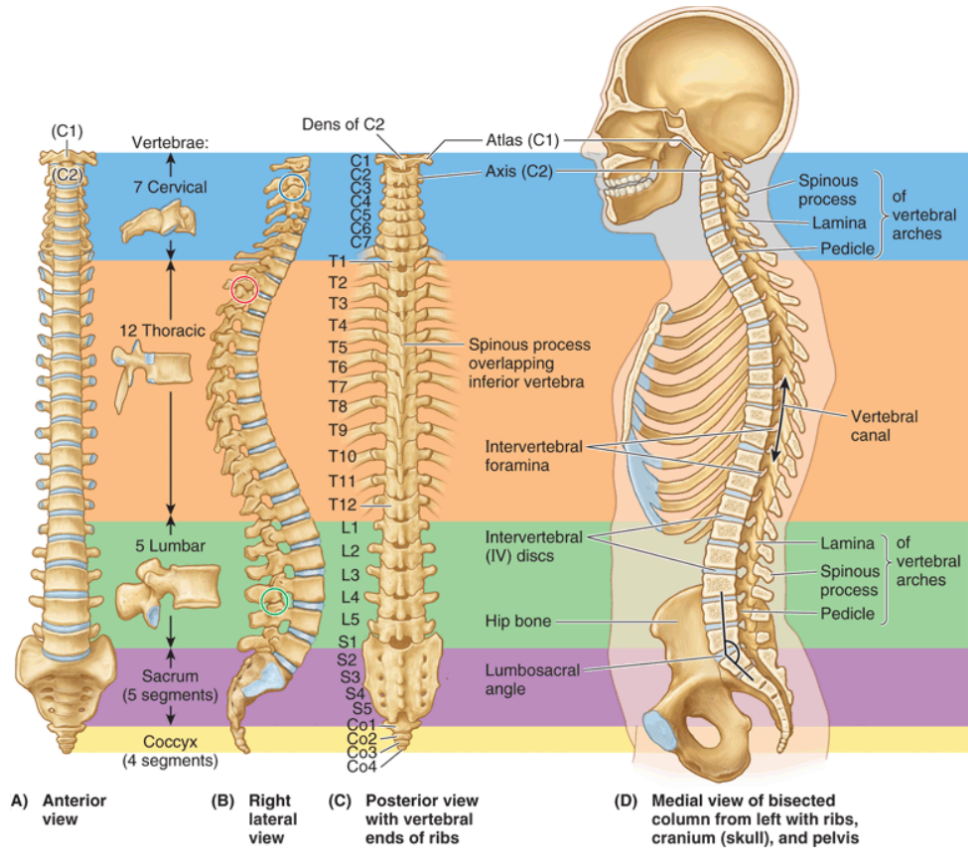
The Spinal Cord

Anatomy

Vertebral column (spine). The vertebral column, commonly known as the spine, consists of vertebrae and intervertebral (IV) discs. The vertebrae of the spine are broken down into five different sections: cervical, thoracic, lumbar, sacrum, and coccyx. They can be seen in Figure 1 from both the anterior and right lateral views. The five sections of the spine will be discussed in more detail in the upcoming sections (2.1.1.1). The spine runs from the base of the skull to the bottom of the coccyx, and typically measures 72 -75 cm long (Figure 1D). The intervertebral discs account for approximately one quarter of the spine. There are five different joints of the vertebral column (Moore, 1980). The vertebral column is capable of producing six different motions: flexion, extension, lateral flexion and extension, and rotation. These movements can be seen in Figure 2.

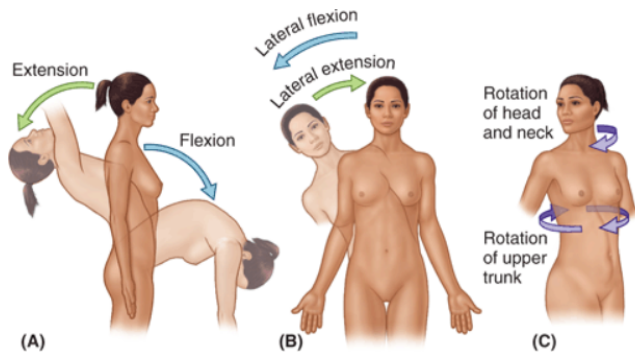
There are a total of four curvatures of the adult spine: thoracic, sacral kyphosis, cervical, and lumbar lordosis. Figure 3 illustrates the development of the curvatures in the spine throughout infancy, childhood and adulthood. Figure 4 shows the surface anatomy of the four curvatures. The thoracic and sacral kyphosis are concaved anteriorly and are considered primary curvatures that develop during the fetal period. The other two curvatures, cervical and lumbar lordosis, are secondary curvatures that are concave posteriorly. These secondary curvatures result from the extension from the flexed fetal

position. The curvatures of the vertebral column also provide additional flexibility (shock-absorbing resilience) in combination with the intervertebral discs (Moore, 1980).



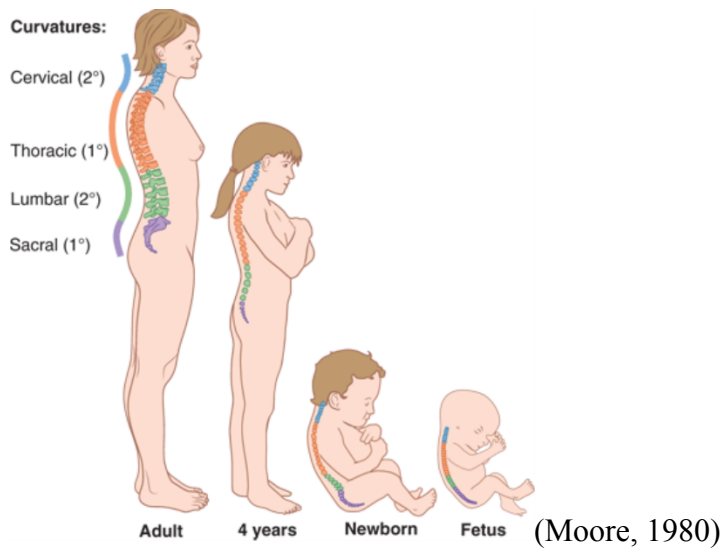
(Moore, 1980)

Figure 1. Vertebral column and its five regions (Moore, 1980).



(Moore, 1980)

Figure 2. Movements of vertebral column (Moore, 1980).



(Moore, 1980)

Figure 3. Curvatures of vertebral column (Moore, 1980).

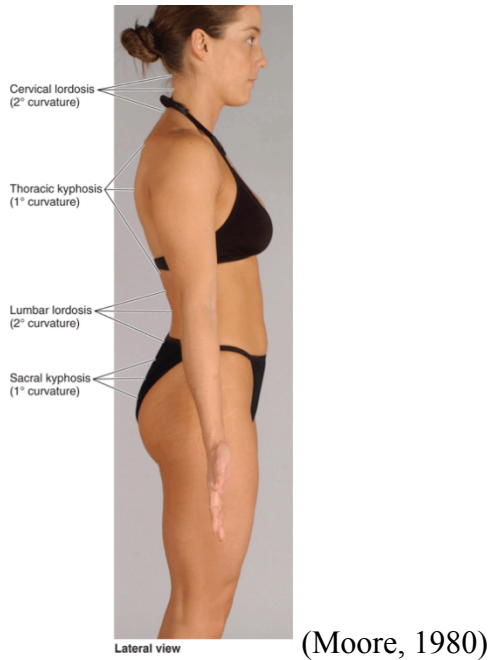
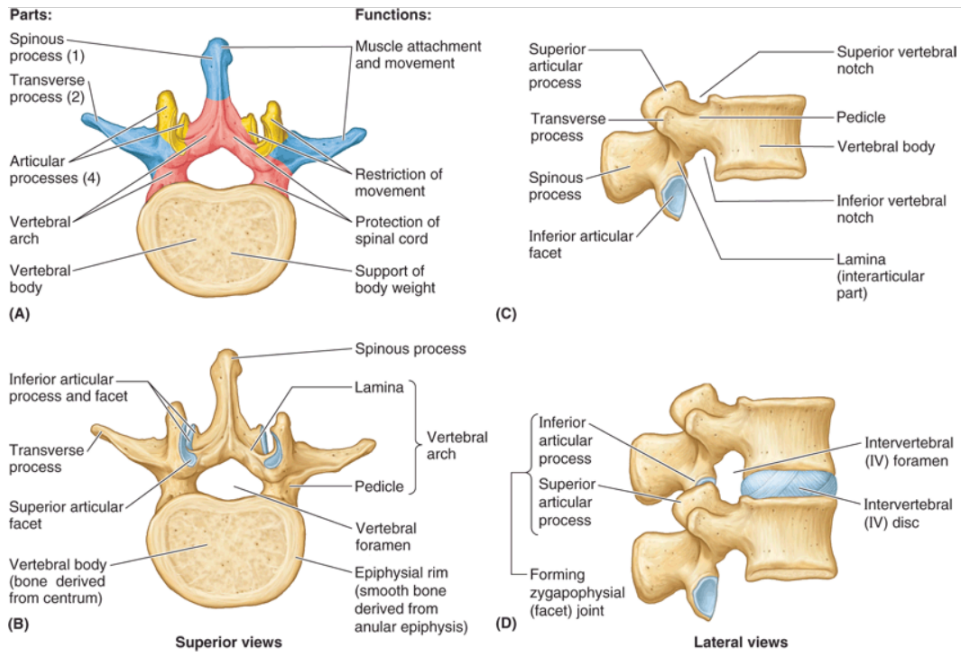


Figure 4. Surface anatomy of curvatures of vertebral column (Moore, 1980).

Vertebrae. Vertebrae are one of the components that make up the vertebral column. There are a total of 33 vertebrae in five different regions. The cervical region has 7, 12 of which are in thoracic, 5 in lumbar, 5 in sacral and 4 in coccygeal. The vertebrae in the cervical, thoracic and lumbar regions are considered superior vertebrae. These regions are where the most amount of movement is seen, and the sacral and coccygeal regions are considered inferior vertebrae. The vertebrae in the sacral and coccygeal regions will eventually fuse together, about age 30, to form the sacrum and coccyx. As shown in Figure 1A, there is an increase in size of the vertebrae as one moves down the vertebral column to the sacrum where they become smaller. Figure 5 illustrates a typical structure of the vertebrae, including of a vertebral body, a vertebral arch and seven processes (Moore, 1980).



(Moore, 1980)

Figure 5. Typical vertebra, represented by the 2nd lumbar vertebra (Moore, 1980).

Intervertebral (IV) discs. IV discs can be found in between the vertebral bodies (Figure 6). The discs made up between 20 -25% of the entire vertebral column. The main roles of intervertebral discs are to allow movement between adjacent vertebrae and provide an extra layer of “cushion” to absorb the shock. The IV disc has two parts: the annulus fibrosus and nucleus pulposus. The nucleus pulposus is the inner gelatinous central mass and is surrounded by the annulus fibrosus. The annulus fibrosus is a ring made up of concentric layers of fibrocartilage, which protects the nucleus pulposus, located at the core of the disc. The nucleus pulposus is a very important part of the vertebrae because it is responsible for the flexibility and resilience of the IV disc and the vertebral column, due to its semifluid nature. The core of the disc is constantly deforming

due to vertical forces. When the vertebral column is compressed it becomes broader, and when it is stretched it is thinner. The structure and function of the IV discs can be seen in Figure 7 (Moore, 1980).

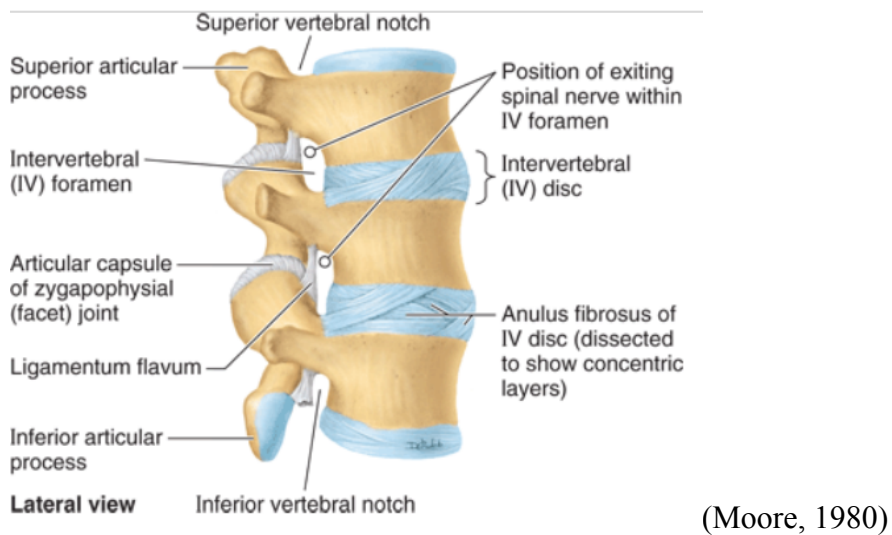
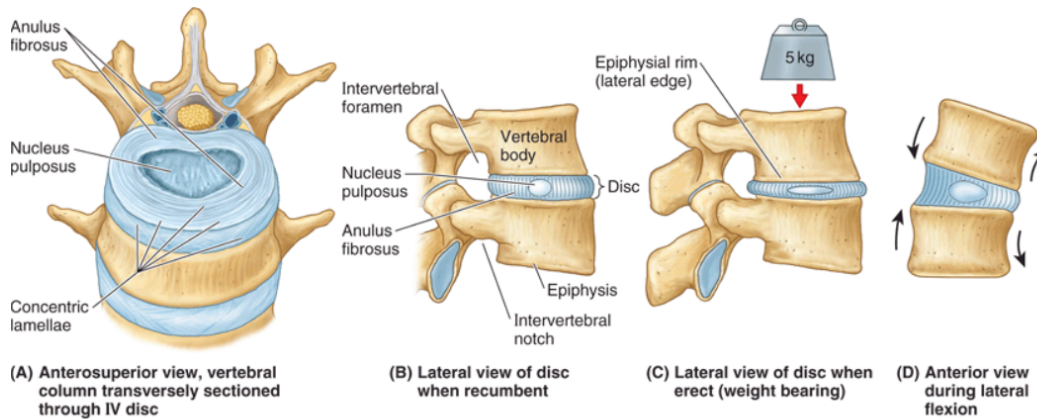


Figure 6. Lateral view of the lumbar vertebrae (Moore, 1980).



(Moore, 1980)

Figure 7. Structure and function of intervertebral (IV) discs (Moore, 1980).

Nervous system. The nervous system can be broken down into two separate parts the central nervous system (CNS) and the peripheral nervous system (PNS). The CNS consists of the brain and the spinal cord, and the PNS contains nerve fibers and cell bodies outside the central nervous system. Figure 9 shows the basic organization of the nervous system. Both the CNS and PNS will be discussed in more detail in the next two sections (Moore, 1980).

Nervous tissue contains two main cell types - neurons and neuroglia. Neurons are known for their rapid communication and are classified into two main groups - multipolar motor neurons and pseudounipolar sensory neuron. Neurons are all comprised of a cell body and an axon. The cell body has extensions named dendrites, which carry impulses to the cell body, and the axon carries the impulse away from the cell body. Some axons of the neurons will be encapsulated by a myelin sheath, which consists of layers of lipids

and proteins. This myelin sheath increases the velocity of the impulse conduction. These neurons will communicate with each other through synapses. Synapses are simply just the points of contact between neurons. Figure 8 show a pictorial representation of a multipolar motor neurons synapsing. During a synapse, communication occurs through neurotransmitters that have been secreted by a neuron. The communication is received by another neuron. This process keeps continuing until communication is finished and a new synapse occurs. Neuroglia, which are more commonly known as glial cells, function to support the neurons. They are five times more abundant than neurons are. There are different neuroglia within the CNS and PNS. In the CNS, they include oligodendroglia, astrocytes, ependymal cells, and microglia. In the PNS they can include satellite cells and Schwann cells (Moore, 1980).

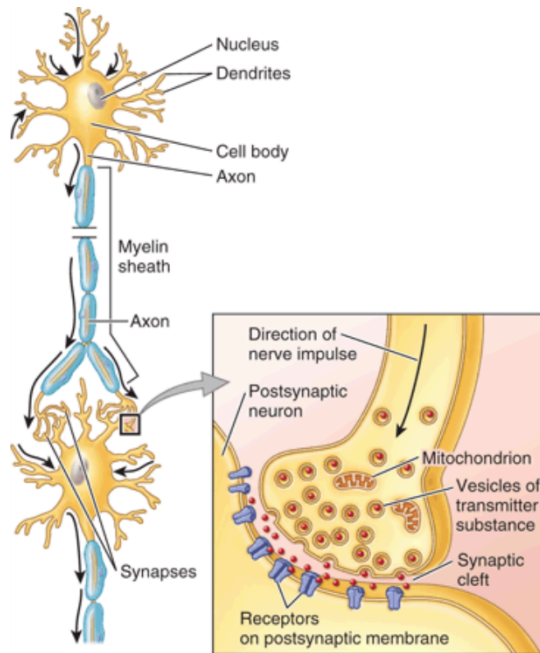
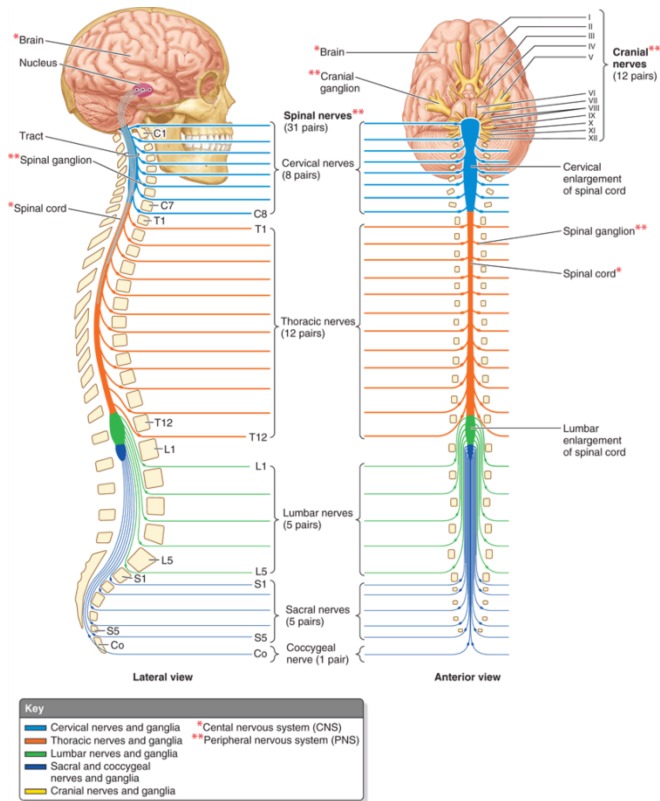


Figure 8. Multiple motor neurons synapsing (Moore, 1980).

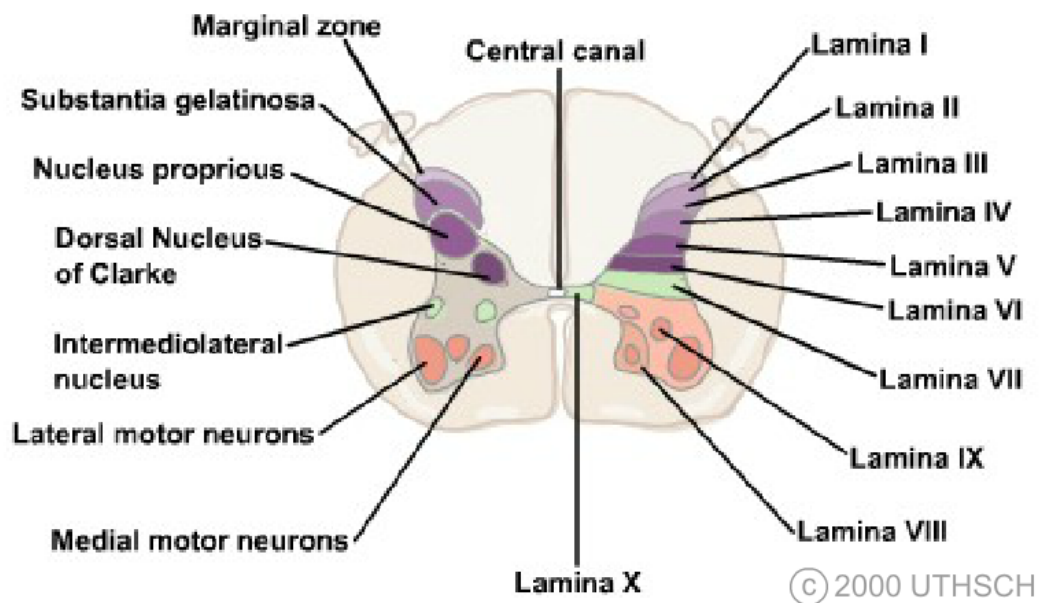


(Moore, 1980)

Figure 9. Basic organization of the spinal cord (Moore, 1980).

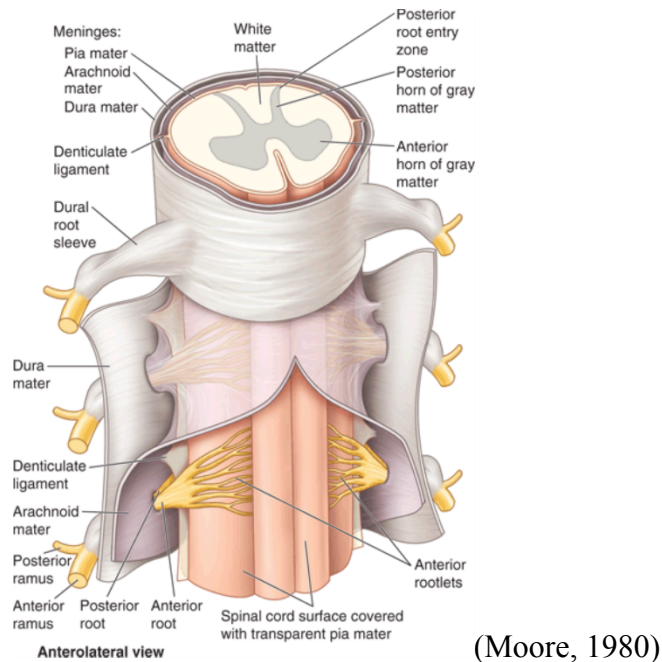
Central nervous system (CNS). The CNS consists of the brain and spinal cord, and allows incoming and outgoing neural signals to coordinate to produce movements, as well as to carry out higher mental functions. The brain and the spinal cord are composed of gray and white matter. The gray matter, at the center of the spinal cord, resembles the shape of the letter H, and is composed of nerve cell bodies (Moore, 1980). The arrangement of the gray matter is organized into nine distinct laminae, labeled I through IX (Figure 10); (Nógrádi et al., 2000-). The white matter surrounds the gray matter and is an interconnecting fiber tract system. The CNS is protected by meninges and the

cerebrospinal fluid (CSF). The meninges are a three-layered membrane that is made up of the pia mater, arachnoid mater and dura mater. The pia mater is the inner most layer and is directly covers the spinal cord. The arachnoid mater is the middle layer, and the outermost layer is the dura mater. The dura mater is very tough, unlike the pia mater which is very delicate. The cerebrospinal fluid is found between the pia mater and the arachnoid mater. The meninges are shown in Figure 11 (Moore, 1980).



(Anatomy)

Figure 10. Spinal cord nuclei and laminae (Anatomy).



(Moore, 1980)

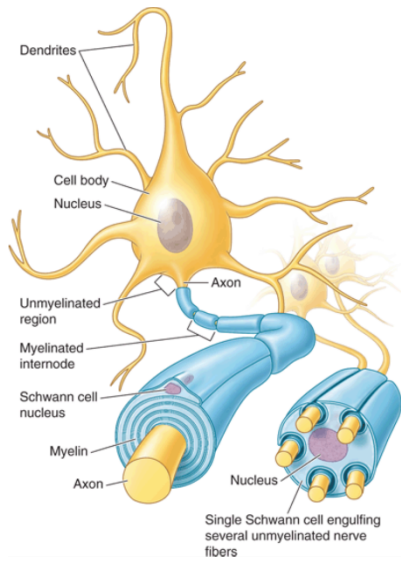
Figure 11. Spinal cord and spinal meninges (Moore, 1980).

Peripheral nervous system (PNS). The PNS consists of the nerve fibers and cell bodies that lie outside the brain and spinal cord. In Figure 9, the different part of the PNS is marked by two red asterisks. This system can either conduct impulses to or away from the brain and spinal cord. PNS is an organization of nerves (Moore, 1980).

A nerve is composed of nerve fibers which have three parts - an axon, its neurolemma, and endoneurial connective tissue. A neurolemma is another term for Schwann cell. The Schwann cells have two forms they can take, which then gives rise to two different nerve fibers, myelinated and unmyelinated. The difference between the two nerve fibers is their ability to produce myelin. As stated previously, myelin increases the speed at which the impulses are conducted. Myelinated nerve fibers have Schwann cells that are specific to a particular axon and an unmyelinated nerve fiber has Schwann cells

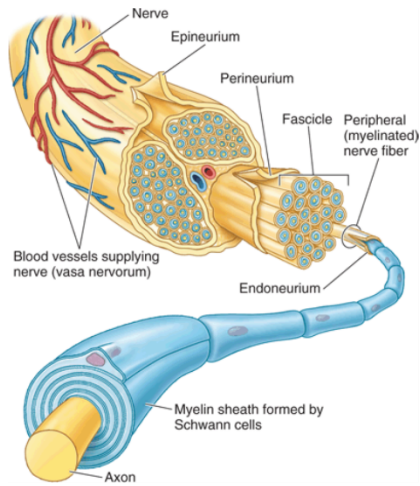
that are not specific to just one axon. An illustration of myelinated and unmyelinated nerve fibers is shown in Figure 13. Nerves are simply a bundle of nerve fibers that are surrounded by a connective tissue covering loaded with blood vessels that nourish the entire nerve. The connective tissue covering is divided into three parts - endoneurium, perineurium and epineurium. These three parts together allow the nerve to be fairly strong and resilient. Figure 13 shows the endoneurium as the innermost layer surrounding the nerve fiber and the epineurium being the outermost layer (Moore, 1980).

The nerves of the peripheral nervous system are broken down into two main sections - cranial nerves and spinal nerves. Spinal nerves exit the vertebral column and are known as rootlets, which then form two nerve roots. The two nerve roots are anterior (ventral) and posterior (dorsal). The anterior (ventral) nerve root has motor (efferent) fibers that convey neural impulses from the brain and spinal cord to effector organs, which include muscles and glands. The posterior (dorsal) nerve root has sensory (afferent) fibers that convey neural impulses to the brain and spinal cord from sensory organs and sensory receptors. Figure 14 shows how the nerve roots form from the rootlets and stem from either side of the grey matter (Moore, 1980).



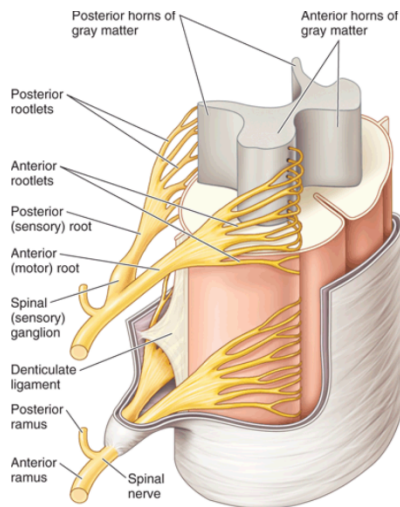
(Moore, 1980).

Figure 12. Myelinated and unmyelinated nerve fibers (Moore, 1980).



(Moore, 1980)

Figure 13. Arrangement and ensheathment of myelinated nerve fibers (Moore, 1980).



(Moore, 1980)

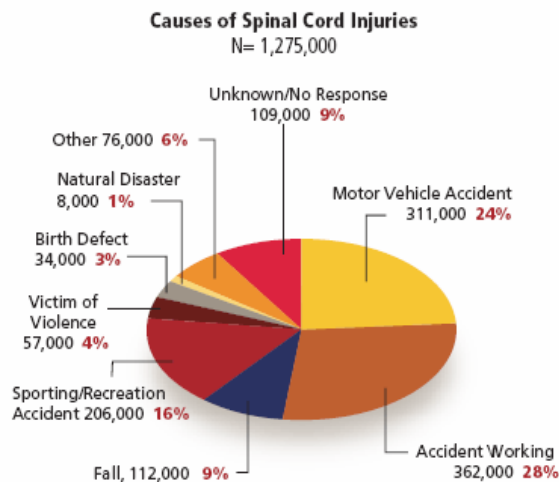
Figure 14. Spinal cord gray matter, spinal roots, and spinal nerves (Moore, 1980).

Spinal Cord Injury

Epidemiology. SCI is reported in 25.5 cases per million or about 40 million people worldwide. The average age of these people is 31.7 years, mainly ranging from 20 to 35 (Assunção-Silva et al., 2014; Nas et al., 2015). Spinal cord injuries are more commonly seen in young men (Assunção-Silva et al., 2014), but 1% of the reported cases are children (Nas et al., 2015). In children 60-80% of injuries occur in the cervical region, and the remaining 20-45% are split evenly between the thoracic and lumbar regions (Nas et al., 2015). The number one cause of spinal cord injuries is due to motor vehicle accidents (24%), followed by accident working (28%) and sporting/recreation (16%) (Christopher and Dana Reeve Foundation, April 2009). Another major number for spinal cord injuries are that they are the second leading cause of paralysis (23%) after stroke (29%). The exact breakdown of the numbers per cause of spinal cord injuries and cause

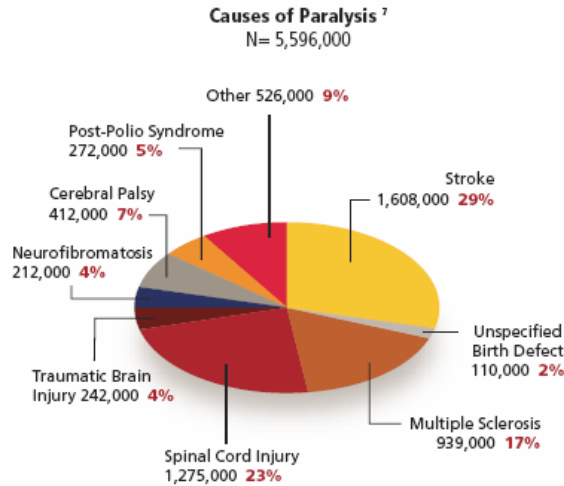
of paralysis can be seen in the two pie charts below (Figures 15 and 16) (Christopher and Dana Reeve Foundation, April 2009).

Spasticity is reported in over a half a million people in the United States and over 12 million people all over the world (Voerman et al., 2005). Literature also report that it affects 42.7%, 65-78%, 70% and 80% of people living with spinal cord injuries (Kakebeeke et al., 2005; Adams et al., 2005; Hagen, 2015; Elbasiouny et al., 2015; respectively). Even after 10 years post injury, 35% of patients still reported having spasticity as a side effect (Kakebeeke et al., 2005).



(Christopher and Dana Reeve Foundation, April 2009)

Figure 15. Causes of Spinal Cord Injuries.



(Christopher and Dana Reeve Foundation, April 2009)

Figure 16. Causes of Paralysis.

Injury types. Spinal cord injuries are classified into two main types, complete and incomplete. A complete injury is considered to be traumatic and an incomplete injury is non-traumatic (Sabapathy et al., 2015). When a person has a complete spinal cord injury they have a complete loss of motor and sensory functions from the point of injury down to the distal point of the spinal cord. On the other hand, an incomplete spinal cord injury has partial motor and sensory functions below the level of neurological disrupt and in the lower sacral segments (Kirshblum et al., 2011; Nas et al., 2015). Typically, spinal cord injuries are caused by flexion, compression, hyperextension or flexion-rotation mechanisms. This initial response of these mechanisms is known as the primary damage. The secondary damage is the response from the body because of the primary damage. Secondary damage is seen in the form of hemorrhaging, inflammation and the release of different chemicals from the body (Nas et al., 2015).

American spinal injury association (ASIA). Spinal cord injury patients are classified using the Spinal Injury Association (ASIA) scale (Kirshblum et al., 2011; Nas et al., 2015). This scale was last revised in 2011 (Nas et al., 2015). The scale ranges from A-E, where A is the most severe injury and E is completely normal. The table below outlines each level of the scale and what classifies a patient in the different levels (Kirshblum et al., 2011; Nas et al., 2015).

ASIA-A	Complete. There is no sensory or motor function preserved in the sacral segments of S4-S5
ASIA-B	Sensory incomplete. Motor deficit without sensory loss below the neurological level, including the sacral segments of S4-S5 (light touch, pin sensation or deep anal pressure at S4-S5), and there is no protected motor function from three levels below the motor level at each half of the body
ASIA-C	Motor incomplete. Motor function is preserved below the neurological level ¹ and more than half of the muscles below this level have strength lower than 3/5 (0, 1 or 2)
ASIA-D	Motor incomplete. Motor function is preserved below the neurological level ¹ and at least half of the muscles (half or more) below this level have strength higher than 3/5
ASIA-E	Normal. Sensory and motor function as assessed by ISNCSC in all segments are normal and in patients with pre-existing deficits there is "E" degree of ASIA. Initially one without a spinal cord injury does not have an ASIA degree

(Nas et al., 2015)

Figure 17. American Spinal Injury Association scale for spinal cord injury

Animal Models of Spinal Cord Injuries

Different animal models are used depending on the research that is being performed. There are four main types of models that are used for spinal cord injury research, which include hemi-section, compression, contusion, and transection. Table 1 below shows a summary of the current spinal cord injury animal models that are used to

mimic human spinal cord injuries. To simulate an incomplete spinal cord injury, the hemi-section, compression and contusion models are typically used, and for a complete injury a transection model is used. For our study, we performed a moderate contusion injury at T9/T10 using a weight drop system. In a hemi-section model, a portion of the spinal cord is removed at the desired level, simulating an incomplete injury where the transection model removes the entire cross-section of the spinal cord at a particular level. In the compression and contusion models, a dorsal laminectomy is performed first to expose the spinal cord. In the compression models, calibrated forceps are used to compress the exposed spinal cord, and in the contusion model a weight drop device is dropped on the particular level of injury desired. The weight drop system can account for a mild, moderate, or severe injury depending on the height it is dropped from. Figure 18 shows a contusion and compression injury being performed (Blight, 2000).

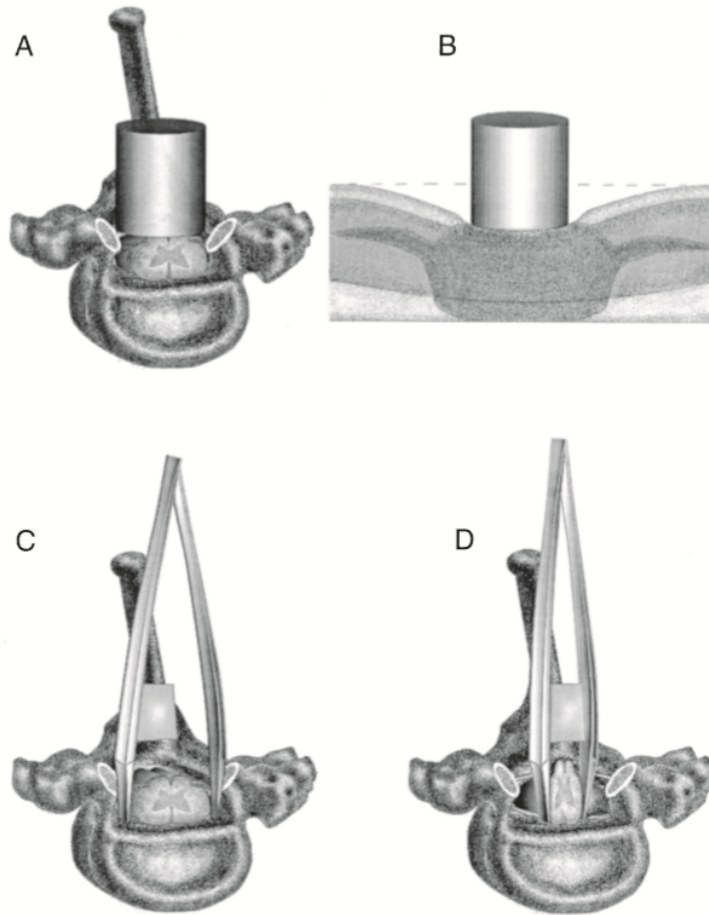
Table 1

Summary of the current SCI animal models that are used in research to mimic the clinical human SCI.

Model	Description	Advantages/Disadvantages
Contusion	Induced with an impactor i.e. weight-drop from a Specified height (Allen, 1911), thoracic contusion is most commonly used (Behrmann <i>et al.</i> , 1993; Jakeman <i>et al.</i> , 2000) Clip Induced with clips calibrated to exert a force of 50/35g-	Impact from contusion can be difficult to assess pain behaviour due to variation of distance
Clip compression	Induced with clips calibrated to exert a force of 50/35g -50g = severe response and 35g = moderate response The clip is closed over the entire cord for 1 minute (Bruce <i>et al.</i> , 2002)	Allows for precise control of injury Does not resemble injury seen in humans
Balloon compression	Uses different volumes of balloon inflation and different compression durations of expression to create contusion (Lim <i>et al.</i> , 2007)	Controlled environment Non-invasive method of creating SCI
Computer controlled contusion	Uses an animal trap that delivers a set weight to the exposed spinal cord; the computer monitors the (Stokes and Jakeman, 2002)	Reproducible, controlled environment But equipment is expensive
Spinal cord displacement	impact attempts to regulate trauma impact by Controlling displacement length of the spinal cord (Nakae <i>et al.</i> , 2011)	Controlled displacement and monitoring of biochemical parameters at the time of impact helps reduce outcome variability-controlled environment
Transection	Complete spinal transection, performed using spring scissors (Kang <i>et al.</i> , 2011; Nakae <i>et al.</i> , 2011)	Widely used to assess regeneration (Talac <i>et al.</i> , 2004) but it is clinically irrelevant (Poon <i>et al.</i> , 2007)
Photochemical	The use of a dye induces the photochemical reaction by activating an argon laser to produce single oxygen molecules on the endothelial surface of spinal cord vessels (Watson <i>et al.</i> , 1986)	Reliable and reproducible Does not induce mechanical trauma to the cord Extent of injury is difficult to control
Excitotoxic	Intraspinal/intrathecal injection of excitotoxins e.g., quiscolic acid (Bhatoe, 2009)	Long-lasting spontaneous pain, thermal hyperalgesia and mechanical allodynia (Fairbanks <i>et al.</i> , 2000; Yeziarski <i>et al.</i> , 1998) Has ability to correlate specific areas of tissue damage
Spinothalamic tract lesions	Lesions core pain pathway; spinothalamic tract area using tungsten microelectrode (Nakae <i>et al.</i> , 2011; Zeilig <i>et al.</i> , 2011)	Resembles allodynia and hyperalgesia Provides useful and novel insights into the underlying biological mechanisms of SCI
Canal stenosis	Is entrapment of the cauda equine and/or lumbar Nerve roots by hypertrophy of osseous and soft tissue structures surrounding the lumbar spinal cord that reduces blood flow (Sekido <i>et al.</i> , 2012)	This model helps clarify pathophysiology of chronic, light pressure to the spinal cord (Sekiguchi <i>et al.</i> , 2004)

(Kundi *et al.*, 2013)

Note: These animal models are used to assess, behavior, histology and genetic alterations following SCI, but more importantly to assess neural and molecular outcomes. These models are more frequently developed on Rat and Mice and less frequently on larger animals such as Cats and Dogs (Kundi *et al.*, 2013).



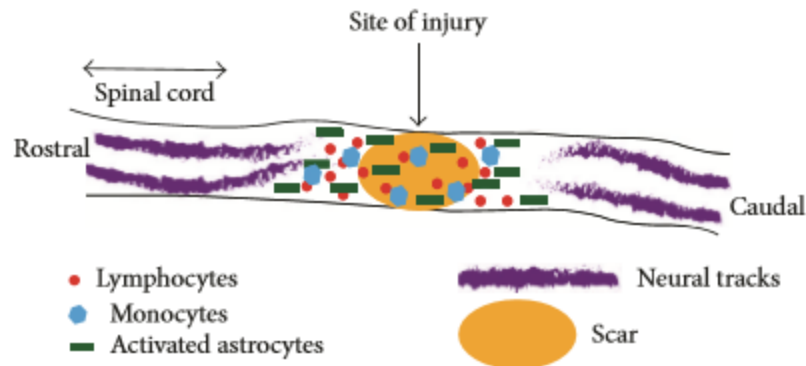
(Blight, 2000)

Figure 18. Contusion and compression injuries of the spinal cord usually involve exposing the spinal cord with a dorsal laminectomy, typically in the thoracic region but sometimes in cervical or lumbar spinal cord. The spinal cord is then compressed, either from the dorsal surface (A, B) or from the sides (C,D). In contusion injury, a cylindrical weight (A) is dropped from a given height into the spinal cord or a similar cylinder may be depressed with a motor, controlled by a computer. In static compression injuries a heavier weight is simply placed onto the spinal cord. In both cases, the dorsal surface of the spinal cord is displaced downward. This produces distributed hemorrhage in the spinal cord at the site of compression. The compression also produces a displacement of the central contents of the cord in cranial and caudal directions (B), particularly in a narrow region above and around the central canal. Lateral compression injury can be produced with calibrated forceps that are inserted on either side of the spinal cord (C) and closes together(D) inducing a similar central hemorrhagic necrosis and displacement of the centrally located, damage tissue in cranial and caudal directions (Blight, 2000).

Pathophysiology of SCI

In an event of a trauma to the spinal cord, there is primary and secondary damage. When the initial injury occurs, the body triggers a series of cellular and biochemical events that allow a lesion or injury site to form in the spinal cord. Some of the immediate changes that occurs after this primary damage are disrupted blood vessels and extensive apoptosis (Assunção-Silva et al., 2014). After the primary damage is done secondary damage starts to set in. The secondary damage changes depending on the severity of the primary damage, and can be divided into three different sections - acute phase, subacute phase, and chronic phase. Each of these phases has a timeline associated with them- acute: 2 hours to 2 days, subacute: days to weeks, and chronic: months to years (Sabaphathy et al., 2015). Initially, in the secondary damage in the acute phase, an inflammatory environment occurs because of cellular and molecular interaction of macrophages, neutrophils and leukocytes (Assunção-Silva et al., 2014; Sabaphathy et al., 2015). The purpose of these interactions is to phagocyte cell debris and to prevent further tissue damage. Then, in the subacute phase, a fluid-filled cyst forms at the injury site, where a glial scar forms around the cyst. The glial scar is mainly made up of reactive astrocytes and is supposed to stabilize and protect the damaged spinal cord. In reality, the glial scar and its cells release inhibitory proteins such as chondroitin sulfate proteoglycans (GSPGs) and axonal growth inhibitors. These proteins and inhibitors do not allow axonal regeneration and remyelination along the damaged spinal cord (Assunção-Silva et al., 2014). Figure 19 below is a pictorial representation of the mechanism of a spinal cord injury. At the injury or lesion site, the neural tracks have been

severed, the formation of the glial scar appeared and lymphocytes, monocytes and activated astrocytes appeared to help minimize injury. These three cells tend to appear within the subacute phase (Sabapathy et al., 2015).



(Sabapathy et al., 2015)

Figure 19. Mechanism of spinal cord injury (Sabapathy et al., 2015).

Spasticity after SCI. The cause of spasticity is still unknown, but from the previous epidemiology section we know it greatly affects spinal cord injury patients. Spasticity is one of the symptoms of the upper motor neuron syndrome and is seen in the form of exaggeration of the stretch reflex, secondary to hyper-excitability of spinal reflexes (Adams et al., 2005; Elbasiouny et al., 2010). It can also be seen in forms other than reflexes, such as hyperreflexia, clonus, clasp-knife responses, long-lasting cutaneous reflexes, and muscle spasms. Spasticity develops gradually, starting in the subacute phase. After injury, the spinal cord is in spinal shock, which is seen by the loss of tendon reflexes below the injury site. Muscle paralysis and flaccid muscle tone occurs. Over the

span of the subacute and chronic phases, new reflexes start to appear, like the tendon reflex among others. This causes the threshold of the flexor reflexes to decrease over time, which can cause long-lasting contractions. Later the extensor reflexes start to occur, which makes the flexor/extensor muscles co-contract and become more prominent. Other stimulus, such as heat/cold and bladder distention can also cause these muscle spasms that we know as spasticity. There are many factors that affect spasticity and its severity (Elbasiouny et al., 2010).

Current Treatments

There are three different categories of current treatments for spinal cord injuries. The three categories are pharmaceutical, transplant, and rehabilitation. Pharmaceutical treatment only includes one drug, methylprednisolone more commonly known as Medrol. Transplant and rehabilitation treatments are part of the therapeutic approaches to treat spinal cord injuries. Transplant treatments include cell-based therapies, hydrogel-based biomaterials and combinational biomaterials. Rehabilitation strategies include body weight support treadmill training, functional electrical stimulation and cycling. Next three sections, will elaborate more on the different categories of current treatments. In Chapter 4, the therapeutic approaches will be discussed in further detail.

Pharmaceutical. The only pharmaceutical that is used for treatment in spinal cord injuries is methylprednisolone (Medrol). There were three large randomize clinical trials - the National Acute Spinal Cord Injury Studies (NASCIS) I, II, III - that made this drug the standard for spinal cord injuries. In the first NASCIS trial, patients were examined for changes in their motor function and sensation. This trial produced results

that showed no benefit, which was thought to be due to the dosage being below the therapeutic threshold. The second phase of the NASICS trial used a higher dose of Medrol administered through a 24-hour infusion within 12 hours after injury (Hugenholtz, 2003). Results from this trial showed no benefit except during post hoc analysis. Post hoc analysis showed that within 8 hours of injury there was a small gain in the motor and sensory score. The NASCIS II allowed Medrol to become the standard care for acute spinal cord injuries. NASCIS III further refined the protocol that was used to administer Medrol (Framptom et al., 2006; Hugenholtz, 2003). Even though Medrol became the standard, many other clinical trials have provided conflicting evidence. Even though it is used today, it is still a controversial drug and its ability to help spinal cord injury patients is still uncertain (Hugenholtz, 2003; Hugenholtz et al., 2002).

Transplant. Transplantation therapies in animal models of SCI are currently being investigated extensively for their translation capabilities. Some of the therapies being researched for transplantation are cell-based therapies, which include stem cells, hydrogel-based biomaterials, which include both natural and synthetic hydrogels, and the combination of both cell-based therapies and hydrogels. When looking at cell-based treatments they must be able to possess the ability to 1) minimize the secondary injury, 2) replace and minimize the survival of damaged cells and 3) alter the local environment to be more conducive for regeneration (Sabapathy et al., 2015; Tam et al., 2014). In general, stem cells have been tested from different origins to see if they are capable of nerve regeneration and possess the ability to restore the complex circuitry of the spinal cord when transplanted into the injury site. More on the specific outcomes from the

different types of stem cells can be found in Chapter 4. Hydrogel-based biomaterials have become popular in spinal cord repair because hydrogels have great physical properties and chemical composition. The physical properties allow the hydrogel to have the ability to mimic the environment of the central nervous system and its chemical composition is easily integrated into the extracellular matrix. Hydrogels, because they are a biomaterial, still have to overcome biocompatibility, mechanical and physicochemical properties, porosity and permeability, and biodegradability. The hydrogel-based biomaterials are extensively outlined in Chapter 4 under the hydrogel-based biomaterials section (Assunção-Silva et al., 2014).

Rehabilitation. Rehabilitation is currently the most widely used treatment for spinal cord injuries. This therapeutic rehabilitation includes body weight support treadmill training, functional electrical stimulation, and cycling. These approaches have shown to have the capability to decrease symptoms of spinal cord injury, especially spasticity. More on these three rehabilitation strategies can be found in Chapter 4.

Chapter 3

Reflexes and Spasticity

Overview

The Hoffmann (H) - reflex is a monosynaptic reflex (Lee et al., 2005; Gozariu et al., 1998) elicited by the synaptic activation of motor neurons by muscle afferents following stimulation of muscle nerves (Reese et al., 2006; Skinner et al., 1996) that was first studied in the 20th century by Paul Hoffman on the triceps surae. In 1973, Hoffman published “Methodology of the Hoffman Reflex in Man” which became the guidelines of parameters for achieving the H-reflex (Tucker et al., 2005; Gozariu et al., 1998).

In a non-injured patient, the expected outcome of the H-reflex is decrease in the amplitude with increasing stimulus frequency of 1Hz or higher (Reese et al., 2006) while the M-wave amplitude remains constant (Figure 20). The M- and H-wave are obtained through an electrical stimulation of a peripheral nerve that innervates the muscle where the H-reflex is recorded. When a single stimulus is initiated, it generates a short latency M-wave and long latency H-wave. The M-wave appears because of the direct stimulation of the motor axons innervating the muscle, and the H-wave is the measure of the alpha motor neurons activated by Ia afferents (Lee et al., 2005). After injury, the H-wave amplitude become less sensitive to stimulation, which results in a higher H/M ratio, and the ratio becomes higher at the baseline stimulus frequency (Lee et al., 2005). The M- and H-wave will be discussed in more detail in the Section 3.3.

Spasticity is a common side effect of spinal cord injuries and can be seen when testing the H-reflex. Spasticity is measured through the habituation that occurs during electrical stimulation. When there is no habituation that occurs at higher frequencies it is known that spasticity occurred because of the spinal cord injury. This habituation can be seen by observing the M- and H-wave during testing (Yates et al., 2008). Spasticity can cause loss of mobility and produce pain from muscle spasms (Mukherjee et al., 2010). From Chapter 2 we know that spasticity occurs after injury to the spinal cord and is also the most observed phenomena after injury. There is no one exact cause of spasticity, it occurs from a combination of effects. Spasticity effects over a half a million spinal cord injury patients in the United States and over 12 million worldwide (Voerman et al., 2005). More on spasticity and how it relates to the H-reflex and the effects of different rehabilitation strategies will be discussed later in this chapter in Section 3.4.

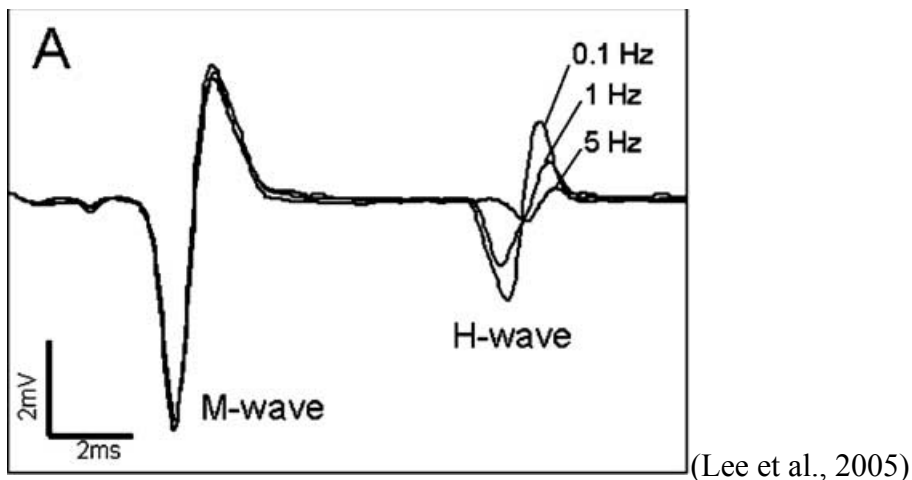


Figure 20. Response of H-reflex for a non-injured animal with increasing stimulus frequency. The H-wave decrease with increasing frequency while the M-wave remains constant (Lee et al., 2005).

Spasticity

Spasticity is known to be one of the secondary symptoms that occur after spinal cord injuries and occurs in 65-78% (Adams et al., 2005) of patients who have had a chronic spinal cord injury for more than a year. It has been reported that in complete spinal cord injuries spasticity starts to appear 2-6 months after injury (Hagen, 2015). Spasticity has many definitions, but the most commonly agreed upon within the scientific community is that it is “a velocity-dependent increase in the tonic stretch reflexes (muscle tone) with exaggerated tendon jerks, resulting from the hyper-excitability of the stretch reflex as one component of the upper motor neuron (UMN) syndrome” (Adams et al., 2005; Mukherjee et al., 2010; Voerman et al., 2005). The upper motor neuron syndrome is the motor changes that occur in the descending motor pathways after injury to the spinal cord (Purves et al., 2001). In simpler terms, spasticity can affect both muscles and joints by having an abnormal increase in muscle tone or stiffness of the muscles. This can cause pain and discomfort, can interfere with movement or speech, and cause deformities and abnormal movements (NINDS; Voerman et al., 2005). Spasticity is typically caused by the damage that occurs to the nerve pathways. Some of the symptoms that occur with spasticity include hypertonicity (increased muscle tone), hyper-reflexia (Reese et al., 2006), clonus (a series of rapid muscle contractions), exaggerated deep tendon reflexes, muscle spasms, scissoring (involuntary crossing of the legs) and fixed joints (contractures). Spasticity does not just occur in spinal cord injuries, but also in patients with multiple sclerosis, cerebral palsy and others (NINDS). Today there is no current treatment that is used to cure spasticity, only treatments to reduce the symptoms. These treatments include medications, physical therapy and surgery. One important thing

to keep in mind is that no one treatment will be effective for all spinal cord injuries. The key is to manage each case based on the unique goal of the patient (Adams et al., 2005; NINDS). The next two sections will discuss spasticity and the reflexes of both humans and animals in different spinal cord injury models. Chapter 4 Section 4.1, will discuss spasticity after a therapeutic approach has been used, and its outcomes.

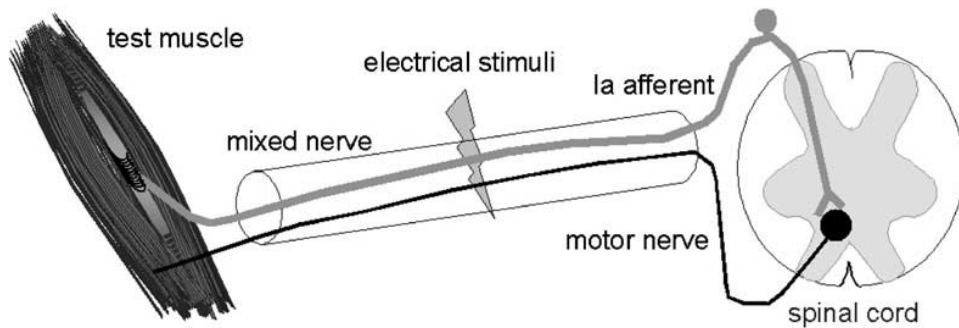
Reflexes

M-wave. One of the responses of stimulating a mixed nerve within the triceps surae is the M-wave. An electrical current is passed through a mixed nerve, including both muscle spindle afferents and motor efferents of the test muscle, initiating the response. The concept of mixed nerve is shown in Figure 21. When comparing the M-wave and the H-wave, the M-wave will appear at a higher stimulation than the H-wave because of the relatively thinner size of the motor nerves, compared with the muscle spindle Ia afferents. It also occurs at shorter latency (< 4 ms, Skinner et al., 1996; Gozariu et al., 1998; 5-8 ms, Tucker et al., 2005) with a maximal amplitude occurring in the range of 6-8 mV (Gozariu et al., 1998), because it has to travel only along the motor axons, approximately 5-8 milliseconds in the soleus muscle (Tucker et al., 2005).

The M-wave is used in studies to normalize the H-reflex results obtained. When normalizing the results, the H-reflex is a ratio of the maximum M-wave (M-max, H/M-max). When the M-wave was initially studied it was believed that it was a successful and accurate way of measuring the total muscle activation. Further investigation showed that the maximum M-wave changes during experiments due to the different limb positions and/or during different levels of muscle contractions. This variability seen in the

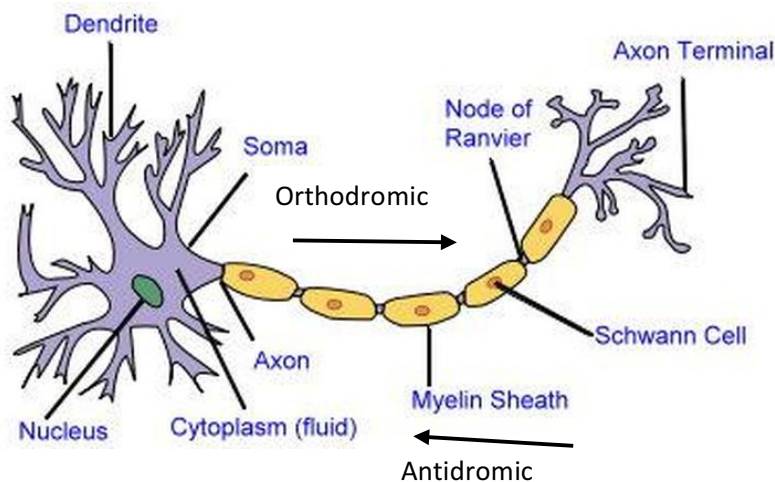
maximum M-wave is due to the changes in the angle of the muscle fibers and electric stimulation. Other factors affecting the maximum M-wave are the experimental time, the decrease of the maximum M-wave value over time, time of day the experiment is conducted, and temperature of the muscle being tested. Many factors can change the value of the maximum M-wave, so when it is used as a normalization factor it should be recorded in all condition to obtain the most accurate results (Tucker et al., 2005).

H-wave. The second response of electromyography testing is the H-reflex, which is a long latency (> 4 ms, Skinner et al., 1996; 11-12 ms, Gozariu et al., 1998; 3-4 ms, Tucker et al., 2005) compound electromyographic response with a maximal amplitude ranging from 1.5-2.5 mV (Gozariu et al., 1998; Yates et al., 2008). The H-reflex is a longer latency response because the volley begins in the afferent fibers, as shown in Figure 21. The response has to travel in both orthodromic and antidromic directions. From Figure 22 below, the orthodromic and antidromic directions are shown by the indicating arrows. The orthodromic direction is considered the normal direction and is towards the axon terminal, and the antidromic direction is away from the axon terminal (Tucker et al., 2005). The H-reflex measures the alpha motoneurons activated by Ia afferents, and is seen when the peripheral nerve is stimulated by an electrical stimulation (Lee et al., 2005) and evoked by muscle afferents (Reese et al., 2006; Yates et al., 2008).



(Tucker et al., 2005)

Figure 21. Electrical stimulation of a mixed nerve. The mixed nerve contains Ia afferents and motor neurons. Action potential within the mixed nerve is then evoked by an electrical current depending on the thickness of the fibers in the nerve. Once the electrical current is large enough to elicit the action potential in the nerve fibers, the potential volley travels in both the orthodromic and antidromic directions to elicit the response (Tucker et al., 2005).

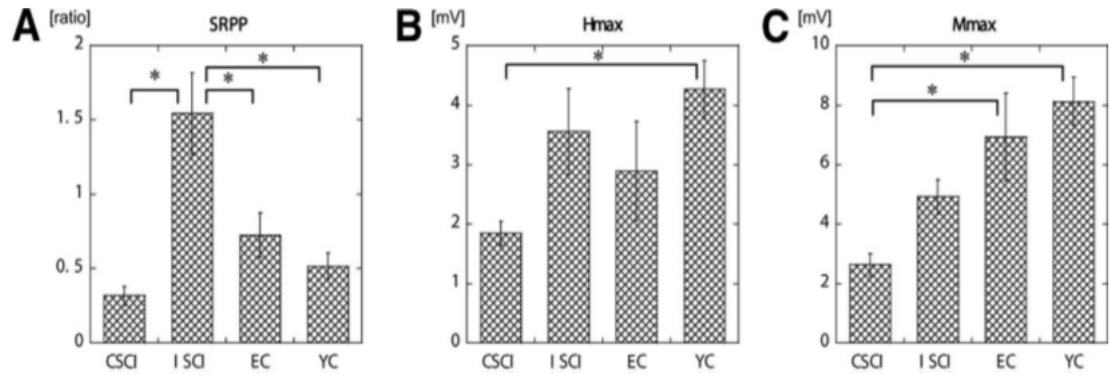


(<http://nervecell-assesment.weebly.com/2d-labelled-diagram.ht>)

Figure 22. A nerve cell that shows the directions of orthodromic and antidromic directions.

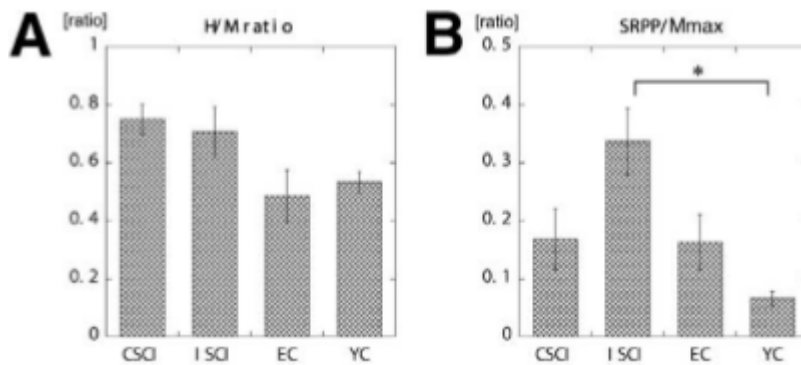
Human studies. Many studies have been conducted on human volunteers with different spinal cord injuries along with different environments tested. A study conducted by Nakazawa et al., 2006 compared the excitability stretch reflex of the soleus muscle in patients with clinically complete and incomplete spinal cord injury, elderly healthy patients, and young healthy patients. They mechanically and electrically induced stretch reflex, H-reflex, and M-wave responses in electromyographic activity of the right soleus muscle for all groups. Nakazawa et al. found that the incomplete spinal cord injury group had a greater absolute stretch reflex electromyographic amplitude than its relative value of the M_{max} . The H/M ratio were comparable between the incomplete and complete groups, but were greater than those in the younger and elderly groups (Figure 23 and 24). Another study conducted by Phadke et al., 2007 compared the soleus H-reflex in incomplete spinal cord injury patients in two different walking environments: treadmill activity with body weight support and over ground walking. A total of 8 motor incomplete spinal cord injury patients and 8 control patients were tested for their mean soleus H-reflex amplitude. H/M ratio was recorded during mid-stance and mid-swing phases of walking. The results showed that with manual assistance and body weight support on the treadmill in stance phase, the H/M ratio was 33% smaller and swing phase was 56% smaller than over ground incomplete spinal cord injury patients. The two different walking environments of the control group did not change the soleus H-reflex modulation significantly (Figure 25). Another study looked at the effects of sinusoidal hip stretches on the soleus H-reflex modulation pattern in people with clinically incomplete spinal cord injuries (Knikou et al., 2007). Seven clinically incomplete spinal cord injury patients with lesions from cervical (C) 5 to thoracic (T) 11 participated in the

study. The study showed that when a sinusoidal stretch is imposed, it started a hip-phase dependent modulation of the soleus H-reflex (Figure 26). A study conducted by Phadke et al., 2006 looked at the different H-reflex modulation with different percentages in leg loading of the body weight support system in people with motor incomplete spinal cord injuries. The study included 8 people with injury and 5 non-injured controls ranging from 42-60 of age. Phadke et al. compared 0% (100% body weight load) and 40% (60% body weight load) body weight support. The results showed that there was a significance difference in the amplitude of the soleus H-reflex in the injured and non-injured group, but no significance change was seen on the H/M ratios in either the injured/non-injured groups with 0% or 40% body weight support. This study suggests that a 40% body weight support load does not alter the soleus H-reflex excitability (Figure 27). The H-reflex is a very reproducible response, but not always the most accurate. Querry et al., 2008 wanted to develop a model that was precise and accurate during the stimulation of the H-reflex during specific times during the gait cycle using robotic body weight support treadmill training in both patients with and without spinal cord injuries. This study used the Lokomat system to determine the mid-stance and mid-swing points of the gait cycle. The H-reflex of the soleus was synchronized to the mid-stance and mid-swing, and tested at 1.8 and 2.5 km/h for 50 cycles. The results showed that the stimulation accuracy was within 0.5° of the defined hip joint position, and $>85\%$ of the 50 H-reflex cycles met the $\pm 10\%$ M-wave criterion that was determined during standing (Figure 28).



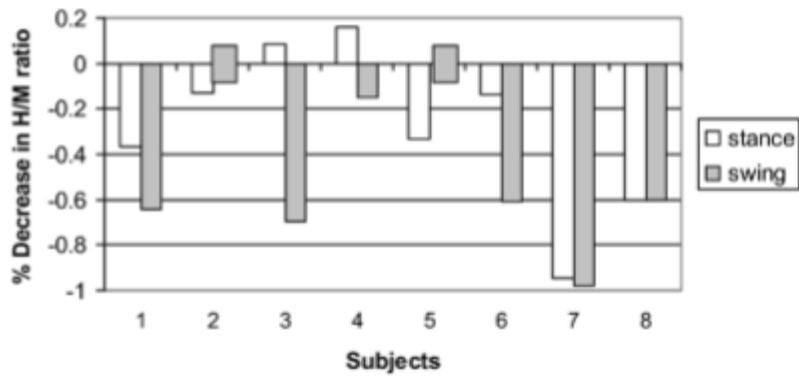
(Nakazawa et al., 2006)

Figure 23. Summary of absolute peak-to-peak reflex electromyographic amplitude (SRPP), absolute Hmax value, and Mmax of each subject group. Bar height show mean and error bars represent the SEM. ANOVA indicated there were statistically significant intergroup differences in the absolute reflex electromyographic amplitude, Hmax, and Mmax. Abbreviations: CSCI, complete spinal cord injury; EC, elderly healthy subjects, ISCI, incomplete spinal cord injury; YC, young health subjects. *Significant between-group differences revealed by Scheffé post hoc comparison ($P < .05$) (Nakazawa et al., 2006).



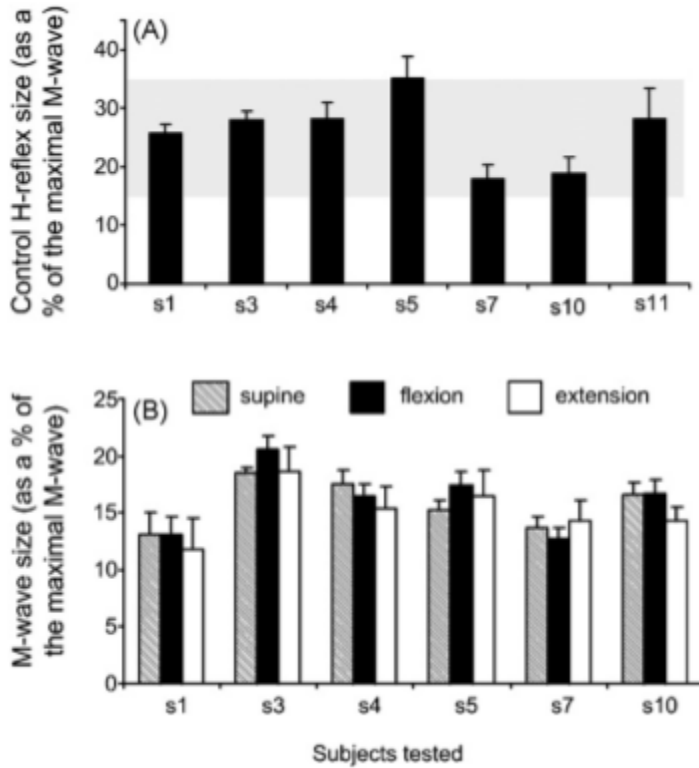
(Nakazawa et al., 2006)

Figure 24. Summary of relative peak-to-peak stretch reflex sizes and H/M ratios for each subject group. Bar height show mean and error bars represent the SEM. There were statically significant inter-group differences in the relative peak-to-peak stretch reflex sizes and H/M. *Significant ($P < .05$) between-group difference revealed by Scheffé post hoc comparison ($P < .05$) (Nakazawa et al., 2006).



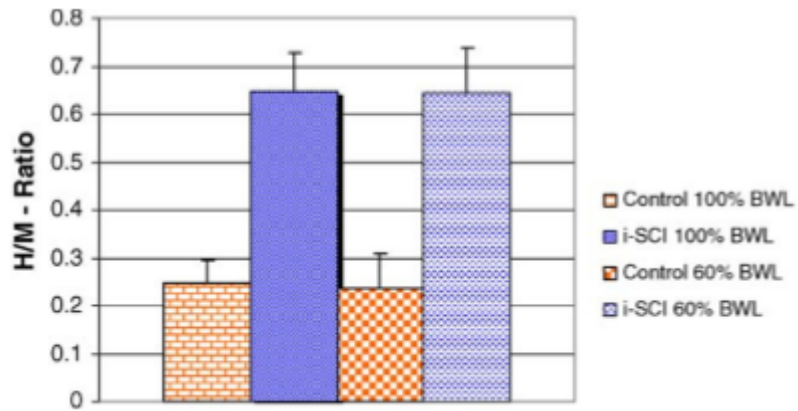
(Phadke et al., 2007)

Figure 25. Persons with incomplete SCI: percentage decrease in H/M ratio while walking in BWSMAT environment compared with unassisted overground environment. In subjects 3 and 4, the H/M ratio increased in stance phase, and, in subjects 2 and 5, the H/M ratio did not change in the swing phase of walking in the BWSMAT environment (Phadke et al., 2007).



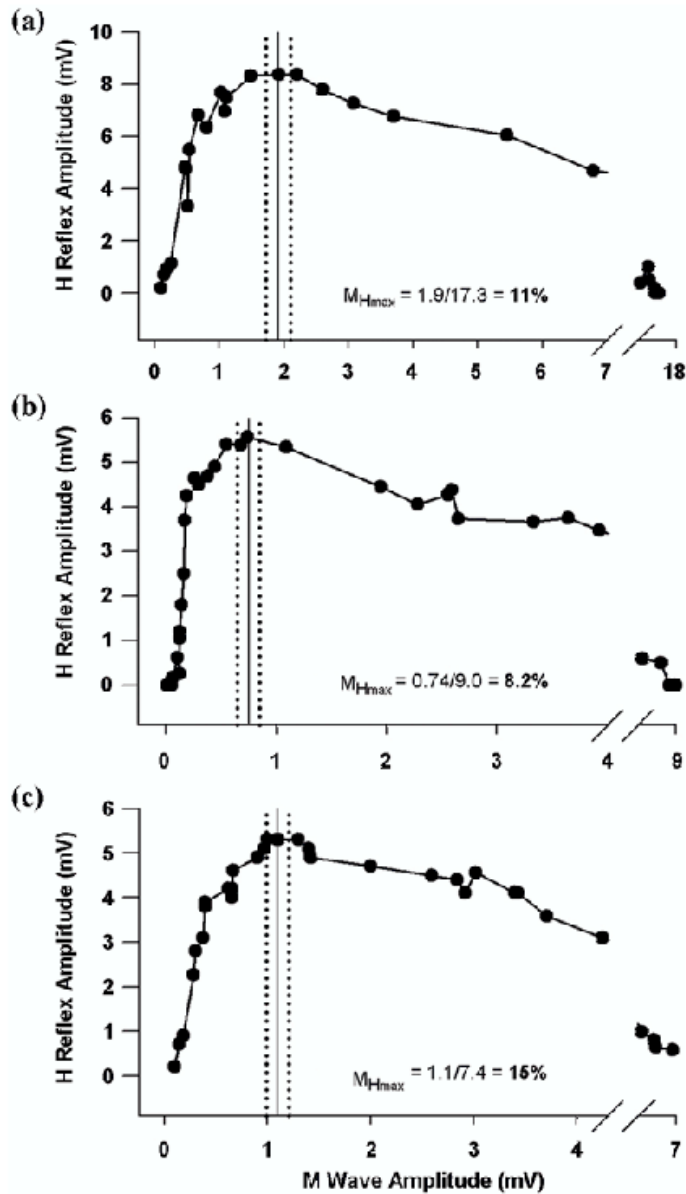
(Knikou et al., 2007)

Figure 26. Characteristics of M-wave and H-reflex under control conditions and during sinusoidal hip stretches. For each subject identified on the abscissa, the average control H-reflex (A) and M-wave recorded during control conditions and following imposed sinusoidal hip stretches (B) are illustrated as a percentage of the maximal M-wave. Control H-reflexes varied from 18 to 35% of the maximal M-wave across subjects. The M-wave was not statistically significantly different across experimental conditions ($P > 0.05$). In subject 11, the M-wave was not present at these stimulus intensities (Knikou et al., 2007)



(Phadke et al., 2006)

Figure 27. Standing i-SCI vs. non-injured control. Comparison of H/Mmax values between the two BWL conditions in non-injured subjects with i-SCI. Standard error bars shown (Phadke et al., 2006).



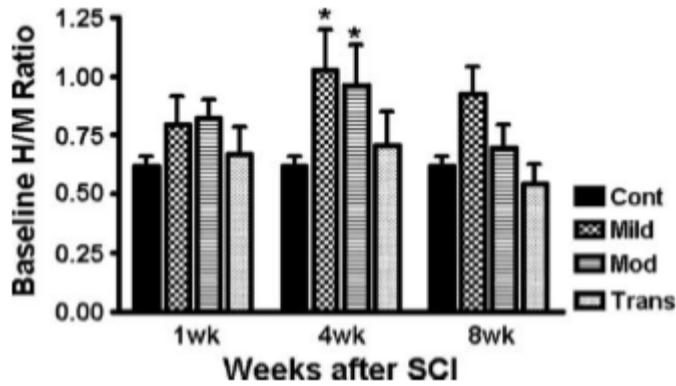
(Querry et al., 2008)

Figure 28. M wave to H reflex response sensitivity graphs. Data represent tibial-nerve stimulation ramping protocol from no M wave to maximal M wave amplitude (M_{max}). Presented are typical responses of subjects (a) without spinal cord injury (SCI), (b) with American Spinal Injury Association (ASIA) A (motor complete) SCI, and (c) with ASIA C (motor incomplete) SCI. Solid vertical line represents measured M wave that elicited maximal H reflex (M_{Hmax}). Dotted vertical line represents $\pm 10\%$ of M_{Hmax} percentage of M_{max} is calculated (Querry et al., 2007).

Animal studies. There are several studies in animal models of spinal cord injuries, most in contusion or weight drop spinal cord injury model at the T8/T9 level. This is the most widely studied since it closely resembles the most common human spinal cord injuries (Magnuson et al., 1999). In all animal models, except the complete transection, the animals eventually regain most of their motor functions. This phenomenon is not seen in humans, but is actually the opposite, where even a partial injury to the spinal cord leads to spasticity. A negative aspect of the complete transection model is that the animals need much more care after injury, and very often experience complications. This is not to say that a complete transection model for animals is never studied, but it is more common to see hemi-sections, partial transections, or contusion injuries (Eaton, 2003).

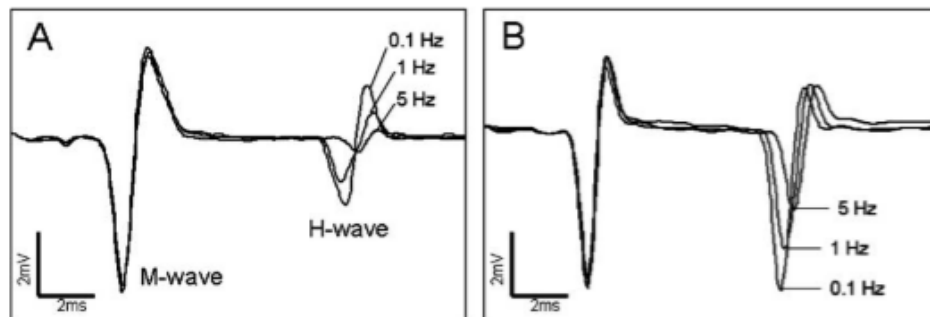
A study conducted by Lee et al., 2005 studied how the severity of the spinal cord injury affects the H-reflex at different times after injury. Four groups (Control, Mild Contusion, Moderate Contusion, and Transection) of adult female Sprague-Dawley rats were evaluated 1, 4, and 8 weeks after injury. The results showed that the H-reflex rate depression was seen as abnormal in all three injured groups at each time period tested. Week 8 is where the difference of more H-reflex rate depression was seen in the transected group than those of the mild contusion group. The study also showed that the baseline H-reflex amplitude was increased in the mild and moderate contusion group (Figure 29, 30, and 31). This result was also seen in Nakazawa et al., 2006 outlined in Section 3.3.3. A study conducted by Skinner et al., 1996 looked at the effects of exercise

on the H-reflex in chronically spinalized adult rats. The rats underwent a complete spinal cord transection at T10 level and were put on a training regimen for 3 months. The rats received 60 minutes of motorized bicycle exercise training a day for 5 days per week. Reflex testing took place after the 3 months of training occurred. The results of the H-reflex test showed that exercise training was capable of restoring frequency-dependent depression of the H-reflex as in normal non-injured animals (Figure 32 and 33). A follow up study to Skinner et al., 1996 was the “Restoration of frequency-dependent depression of the H-reflex by passive exercise in spinal rats” conducted by Reese et al., 2006. This study aimed to investigate the time frame of passive exercise that would have similar outcomes as Skinner et al., 1996. Adult rats underwent a complete transection at the T10 level followed by motorized bicycle exercise training for 1 hour per day, 5 days per week for either 15, 30, 45, 60, or 90 days. After training ended the H-reflex was tested. The results of this study showed that after 30 days of exercise, statistically significant low frequency-dependent depression of the H-reflex was seen. Overall there was a linear decrease in low frequency-dependent depression of the H-reflex with passive exercise (Figure 34, 35, and 36). A study by Yates et al., 2008 used a complete transection model to assess the hyper-reflexia, a component of spasticity after injury. The study was able to establish a time frame for the onset of the hyper-reflexia. They used adult rats that underwent complete transection at T10 level and the H-reflex was tested at 7, 14, and 30 days’ post-transection. Results showed that the rats did in fact have spasticity in the form of hyper-reflexia, and it was observed to decrease when tested at 10 Hz after 14 and 30 days. This study reports that between 7 and 14 days, the rats developed hyper-reflexia (Figure 37 and 38).



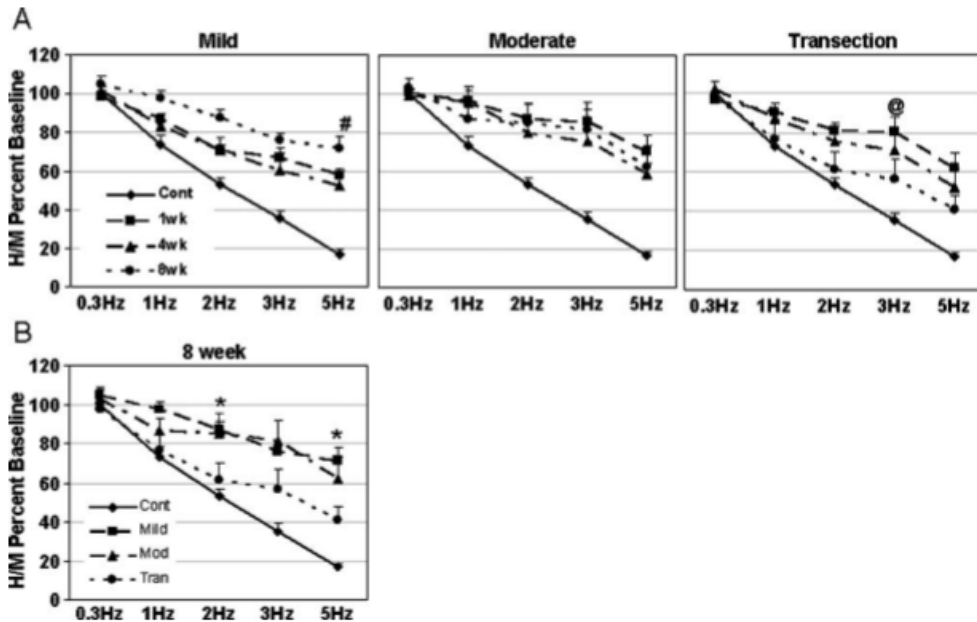
(Lee et al., 2005)

Figure 29. Changes in baseline H/M ratio after varying degrees of SCI. There was a significant increase in baseline H/M ratio at 4 weeks after a Mild and Moderate SCI. Mild injury continued to display an increased baseline H/M ratio at 8 weeks, although not significantly different from controls. Transection SCI did not differ from controls at any time points tested. At 8 weeks, transection SCI had significantly lower baseline H/M ratio compared to Mild SCI. ** $P < 0.01$, * $P < 0.05$ compared to controls unless noted otherwise. Two-way ANOVA with Bonferonni post-test (Lee et al., 2005).



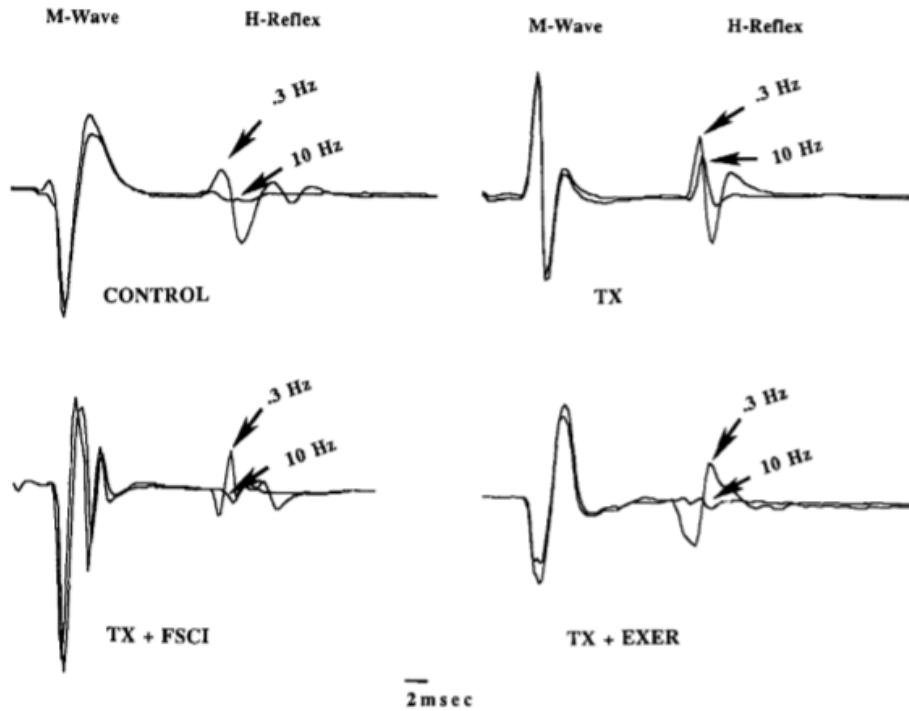
(Lee et al., 2005)

Figure 30. Overlapping representative H-reflex waveforms of uninjured control (A) and 4-week Mild SCI (B) animals measured at 0.1, 1 and 5 Hz stimulus frequencies. The amplitude of the M-wave remains unchanged, while the H-wave amplitude steadily decreases with increasing stimulus frequency. After SCI, this rate depression property of the H-reflex is significantly diminished compared to uninjured controls. In addition, at 4 weeks after SCI, the baseline amplitude (0.1 Hz) is higher than uninjured controls (Lee et al., 2005).



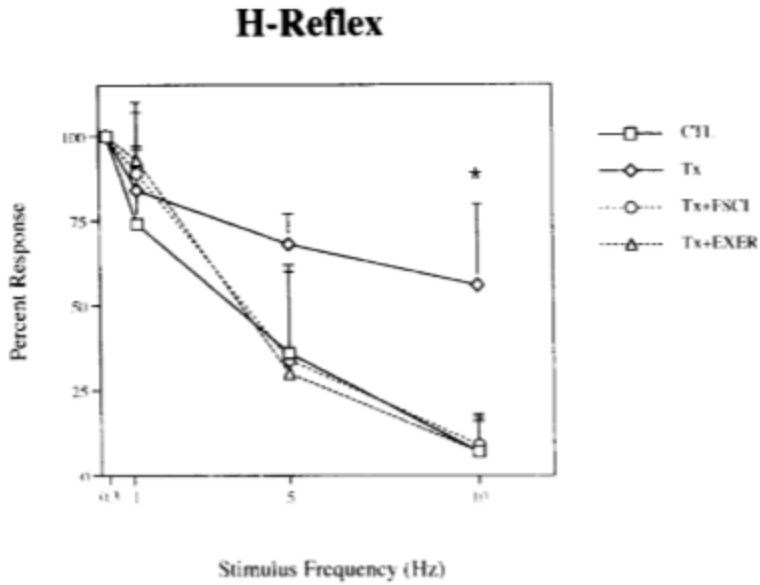
(Lee et al., 2005)

Figure 31. Alteration of H-reflex rate depression over time after varying degrees of SCI. Higher H/M percent values on the y axis indicates less H-reflex rate depression, whereas lower values indicate more rate depression. H-reflex rate depression becomes more abnormal over time after a mild SCI, but more normal after a transection (A). At 8 weeks, mild injury displayed the most abnormal rate depression, while transection injury was closest to controls. All three injury groups had significantly less rate depression compared to uninjured controls at all three time points. Two-way ANOVA with Bonferonni post-test. # $P < 0.05$ comparing 8 weeks to 4 weeks, @ $P < 0.05$ comparing 8 weeks to 1 week, * $P < 0.05$ comparing transected to mild (Lee et al., 2005).



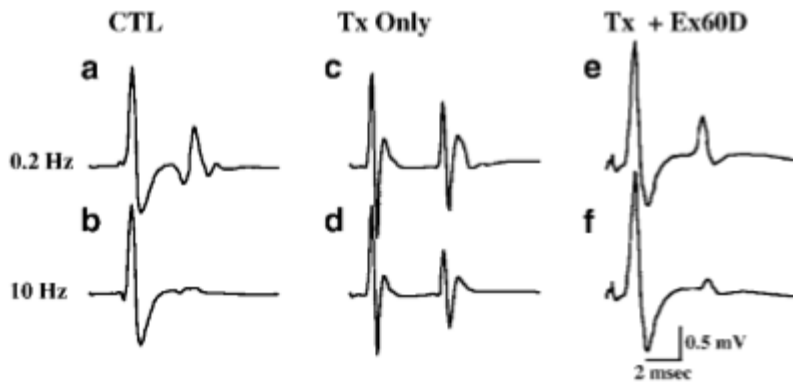
(Skinner et al., 1996)

Figure 32. Averages of 16 consecutive responses following tibial nerve stimulation recorded in plantar muscles in representative animals in each group. The earlier M-wave (~ 2 ms latency) was followed by the H-reflex (~7 ms latency). Averages of stimulation frequencies of 0.3 Hz and 10 Hz are superimposed for each animal. Note that the 10 Hz average in the control record is decreased (due to frequency-dependent depression) compared to the 0.3 Hz average (top left). On the other hand, the 10Hz average in the Tx animal did not decrease as much compared to the 0.3 Hz average (top right). The 10 Hz averages in both treated animals, Tx + FSCI and TX + EXER (bottom left and right) decreased as in the control animal. Calibration bar 2 ms for all records (Skinner et al., 1996).



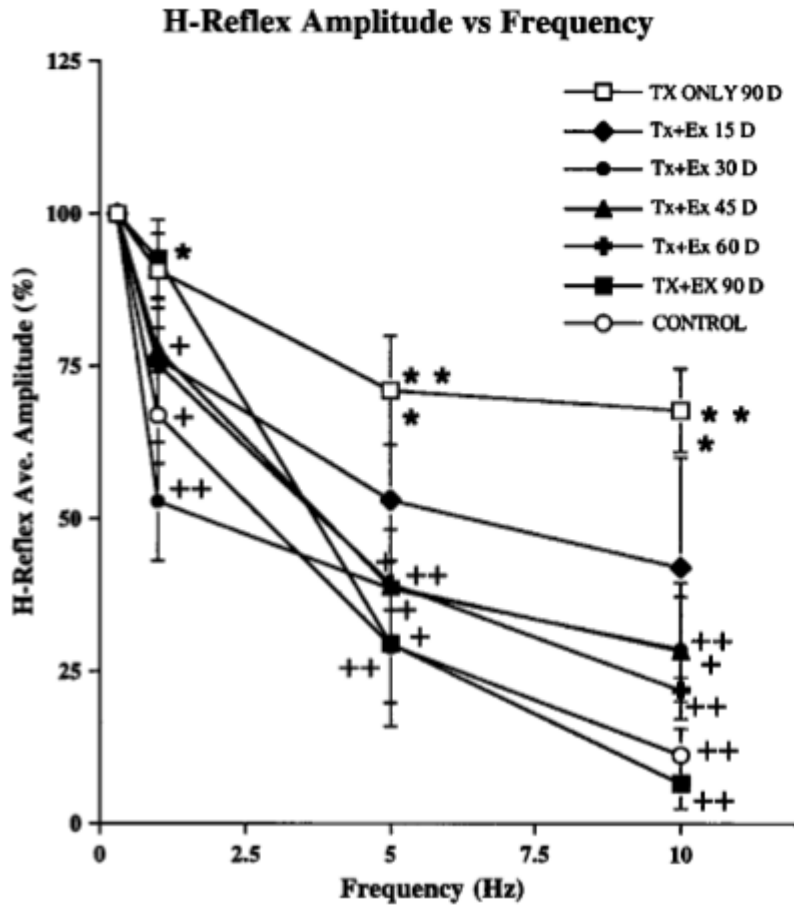
(Skinner et al., 1996)

Figure 33. Graph of the mean and standard deviation of the H-reflex at 1 Hz, 5 Hz and 10 Hz stimulation frequency as a percent of the response observed at 0.3 Hz stimulation frequency. Animals in the CTL group (square) showed marked decrease of the H-reflex amplitude as the stimulation frequency increased. After transection (Tx, diamond), there was decreased habituation of the H-reflex at 10 Hz (asterisk, $P < 0.01$) compared to the CTL as well as the two treatment groups (Tx + RCI, circle: Tx + EXER, triangle) (Skinner et al., 1996).



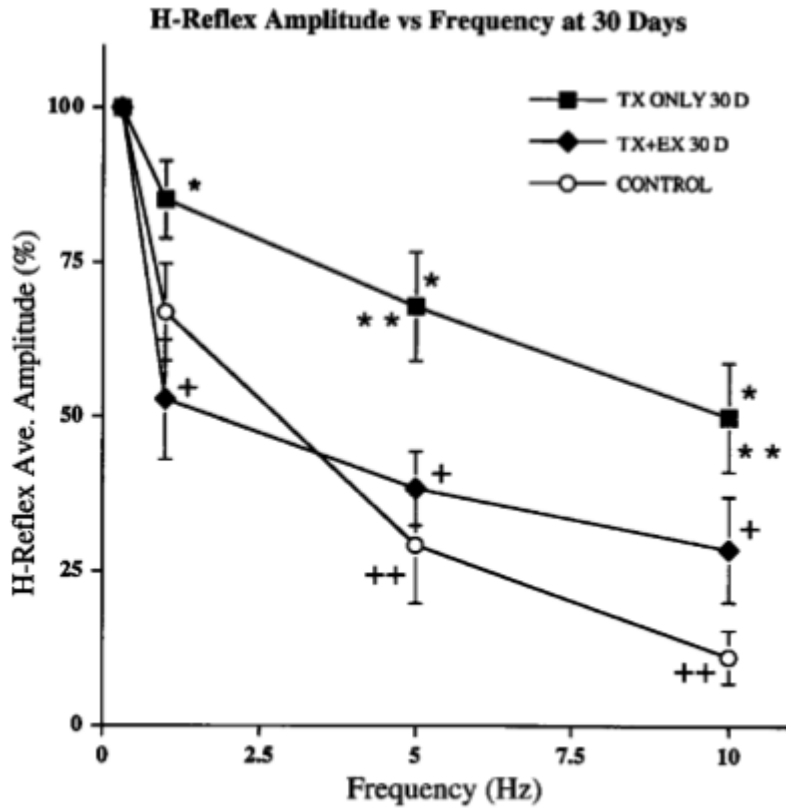
(Reese et al, 2006)

Figure 34. Averages of H-reflex recordings. Evoked muscle potentials included an early M-wave and a later H-reflex following stimulation. (a) Averaged responses to stimulation at 0.2Hz in a control rat. (b) Averaged responses to stimulation at 10Hz in the same control rat. Note the decrease in amplitude (frequency-dependent depression) of the H-reflex at 10Hz compared to 0.2Hz. (c) Averaged responses to stimulation at 0.2Hz in a Tx only 60D rat. (d) Averaged responses to stimulation at 10Hz in the same Tx only 60D rat. Note the greater amplitude (decrease in frequency-dependent depression) of the H-reflex at this frequency compared to 10Hz in the intact animal (b). (e) Averaged responses to stimulation at 0.2Hz in a Tx +Ex 60D rat. (f) Averaged responses to stimulation at 10Hz in the same Tx + Ex 60D rat. Note the return of frequency-dependent depression of the H-reflex after 60 days of MBET. Calibration bars vertical 0.5mV, horizontal 2ms (Reese et al., 2006).



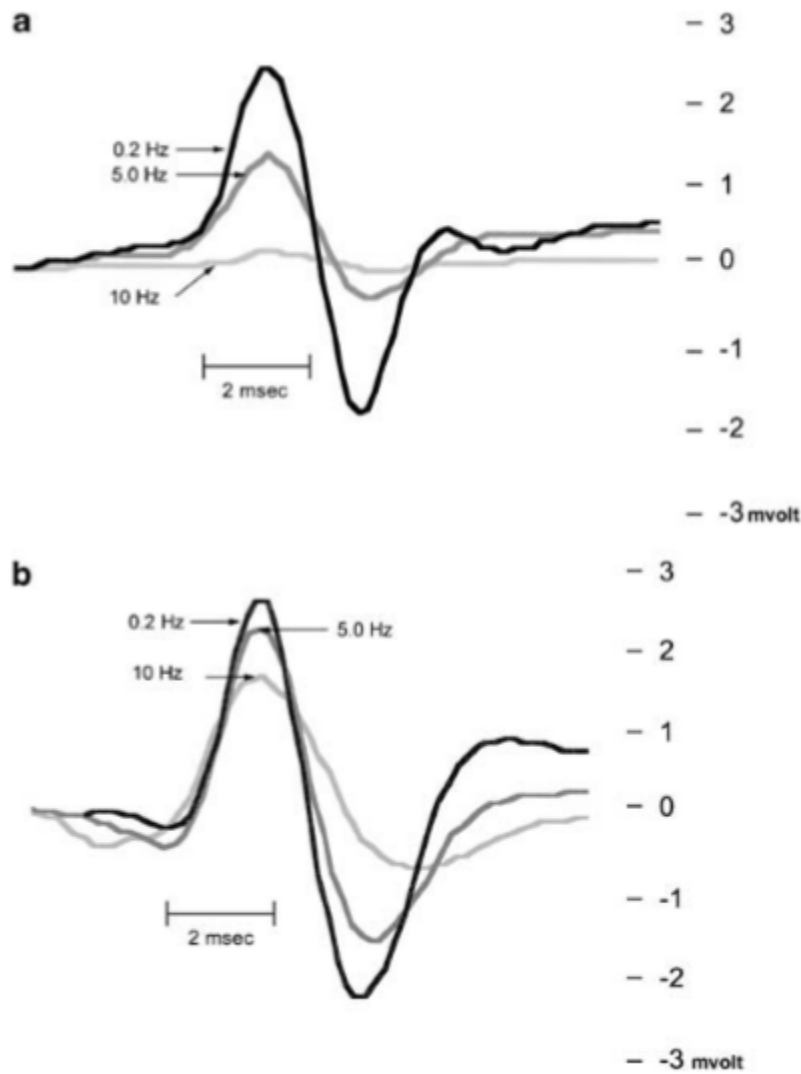
(Reese et al., 2006)

Figure 35. H-reflex amplitude at 0.2, 1, 5, and 10Hz for intact animals (control, open circles), and 15 (Tx + Ex 15D, filled diamonds), 30 (Tx + Ex 30D, filled circles), 45 (Tx + Ex 45D, filled triangles), 60 (Tx + Ex 60D, filled plus signs) and 90 (Tx + Ex 90D, filled squares) days of MBET, and 90 days without MBET (Tx only 90D, open squares). Frequency-dependent depression of the H-reflex at 0.2Hz was designated 100%, and all statistical comparisons in this figure made against the Tx only 90D group. At 1Hz, the Tx only 90D group (*) differed significantly from the Tx + Ex 45D, Tx + Ex 60D, and control groups at the P<0.05 level (+); and from the Tx + Ex 30D group at the P<0.01 level (++). At 5Hz, the Tx only 90D group (*) differed from the Tx + Ex 45D, and Tx + EX 60D groups at the P<0.05 (+), and was also different (**) from the Tx + Ex 30D and control group at the P<0.01 level (++). At 10Hz, the Tx only 90D group (*) differed from the Tx + Ex 45D group at the P<0.05 level (+), and differed (**) from the Tx + Ex 30D, Tx + Ex 60D, Tx + Ex 90D, and control groups at the P<0.01 level (++) (Resse et al., 2006).



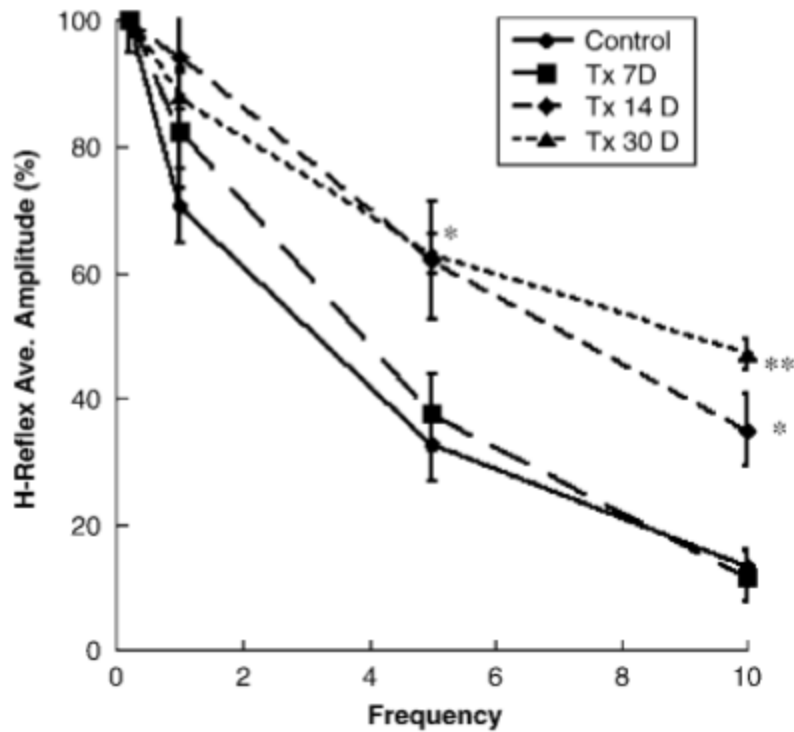
(Reese et al., 2006)

Figure 36. H-reflex amplitude at 0.2, 1, 5, and 10Hz for control (open circles), 30 days without MBET (Tx only 30D, filled squares), and 30 days with MBET (Tx + Ex 30D, filled diamonds). Frequency-dependent depression of the H-reflex at 0.2Hz was designated 100%, and all statistical comparisons in this figure made against the Tx only 30D group. At 1Hz, the Tx only 30D group (*) differed from the Tx + Ex 30D group at the $P < 0.05$ level (+), but not the control group. At 5Hz, the Tx only 30D group (*) differed from the Tx + Ex 30D group at the $P < 0.05$ level (+) and from the CONTROL at the $P < 0.01$ level (++). At 10Hz, the Tx only 30D group (*) differed from the Tx + Ex 30 group at the $P < 0.05$ level (+), and from the control at the $P < 0.01$ level (++) (Reese et al., 2006).



(Yates et al., 2008)

Figure 37. (a) Representative H-reflex recordings of animals tested 7 days after transection (Tx). The H-reflex was observed 8–10ms after the stimulus. The H-reflex amplitudes at the different frequencies have been superimposed for comparison. The black line represents the H-reflex recorded at 0.2Hz. The dark gray line represents recording at 5Hz, and the light gray line represents recording at 10Hz. Note the decrease in amplitude as frequency of stimulation was increased, indicative of low frequency-dependent depression present at 7 days post-Tx. (b) Representative H-reflex recording of animals tested 14 days after Tx. The H-reflex responses at the different frequencies have been superimposed for comparison. The black line represents H-reflex recorded at 0.2Hz. The dark gray line represents recording at 5Hz, and light gray line represents recording at 10Hz. Note lack of decrement in amplitude as frequency of stimulation was increased, indicative of a decrease in frequency-dependent depression. The x-axis represents time in milliseconds, the y-axis amplitude in millivolts (Yates et al., 2008).



(Yates et al., 2008)

Figure 38. H-reflex amplitude at 0.2, 1, 5 and 10Hz in intact (control, filled circles), Tx 7D (squares), Tx 14 D (diamonds) and Tx 30D (triangles) groups. The y-axis shows amplitude expressed as a percent of the amplitude at 0.2Hz designated as 100 percent, and all statistical comparisons in this figure were made against the control group. At 5Hz, the Tx 14D and Tx 30D groups differed from the control group and the Tx7D ($P<0.05$). At 10Hz, the Tx 14 D group differed from the control group and Tx 7D ($P<0.05$), and the Tx 30 D group differed from the control and Tx7D group ($P<0.01$). *indicates $P<0.05$; **indicates $P<0.01$. Note the lack of habituation of the H-reflex at 10Hz in the Tx 14D and Tx 30D groups compared with the control group and the Tx 7D group. Tx, transection (Yates et al., 2008).

Chapter 4

Therapeutic Approaches to Treat Spasticity in Spinal Cord Injury

Rehabilitation

Body weight-support treadmill training (BWSTT). Body weight-support treadmill training focuses on re-training standing and walking in patients with spinal cord injury (Phadke et al., 2006; Querry et al., 2008) by producing a repetitive stepping pattern like that of normal walking (Phadke et al., 2007). There are two parts to this rehabilitation, namely the body weigh-support system and the treadmill. The body weigh-support system allows a particular percentage of patient's body weight to be supported by a suspended device and harness taking pressure and weight off the legs. This system is suspended over a treadmill so the patient can walk with either manual or robotic help (Phadke et al., 2006). The robotic system is very beneficial for researchers and clinicians because it allows them to be able to monitor joint position, torques, and the overall performance of the patient with better accuracy and precision. This robotic training also gives a better monitored environment allowing the patients' monosynaptic reflex to be measured through H-reflex during standing and stepping, allowing assessment of the improvement throughout the body weigh-support treadmill training process. (Querry et al., 2008). After training, spasticity should normalize, which is evident by the observed changes in the H-reflex, such as the H-wave becoming more sensitive to a reapplied electrical stimulation (Knikou et al., 2007). Another benefit of body weight-support treadmill training that are typically not discussed are the physiological and psychological

benefits for patients. They can improve the overall health of the patient, not just the spinal cord injury (Hicks et al., 2008).

Functional electrical stimulation (FES). Functional electrical stimulation (FES) has always been used in orthopedic and neurological rehabilitation, and is now being used for spinal cord injuries. This rehabilitation can have a therapeutic or functional effect. This section will focus on the therapeutic effects only. The ultimate goal of using FES is to reduce muscle spasms and the effects of spasticity by obtaining responses in the nervous system. During FES, a low level of electrical current is applied to a paralyzed nerve or muscle via, an electrode controlling the neural activation, in hopes to restore or achieve function. FES is typically combined with some form of physical activity such as cycling. Cycling will be discussed more in the next section (Martin et al., 2012; Peckham, 1989). Studies have shown that functional electrical stimulation by itself, used with incomplete and complete spinal cord injury patients, causes an increase in stepping response and an activation of the central pattern generator mechanism. Patients when regularly treated also show improvement in motor and sensory scores and decrease in spasticity (Martin et al., 2012).

Cycling. Cycling movements is another rehabilitation strategy that is used in spinal cord injuries. It is a passive exercise that helps to maintain full range of motion of the joints that are immobilized (Kakebeeke et al., 2005; Rayegani et al., 2011). Studies have shown that it can reduce spasticity in patients as well as cardiac output and stroke volume, and muscle atrophy (Rayegani et al., 2011). Cycling is sometimes preferred over body weight-support treadmill training if researchers are studying the H-reflex, because it

can allow them to see all the muscles being activated. Also changing the load can increase or decrease the levels of muscle activation (Boorman et al., 1992). One study conducted by Reese et al., 2006 used motorized bicycle exercise training to measure hyper-reflexia by restoring the frequency-dependent depression of the H-reflex. They used a complete spinal cord transection model with rats that underwent training for 1 hour per day, 5 days per week for 3 months and were then tested at 15, 30, 45, 60, and 90 days after training began. The results showed that after 30 days of exercise there was a statistically significant low frequency-dependent depression of the H-reflex.

Transplant

Cell-based therapies. Stem-cell therapies have many of the qualities necessary to promote regeneration in spinal cord injuries, and are widely studied because of their differentiation potential (Assunção-Silva et al., 2014). For these therapies to be successful in spinal cord regeneration they need to 1) minimize the secondary injury, 2) replace and minimize the survival of damaged cells and 3) alter the local environment to be more conducive for regeneration (Sabapathy et al., 2015; Tam et al., 2014). Combining stem-cell with growth factors allows a strategy to control cell fate after transplantation (Tam et al., 2014). Some transplantation strategies have been tested more than others and investigated through clinical trials. This research, though, has not yet shown a clear convincing pattern in the results of significantly promoting regeneration in spinal cord injuries. Additional studies are needed to safely and efficiently use stem-cell therapies as a possible treatment for spinal cord injury (Assunção-Silva et al., 2014). Stem-cells that are being studied include: embryonic, induced pluripotent, neural, mesenchymal, and

glial cells, which will be discussed in the upcoming sections (Assunção-Silva et al., 2014; Tam et al., 2014).

Embryonic stem cells (ESC). Embryonic stem cells (ESC) are pluripotent cells (Tam et al., 2014) that can differentiate into more than 200 different fetal cell lineages (Tewarie et al., 2008; Assunção-Silva et al., 2014). These cells are present within the inner cell mass of the blastocyst, which is formed very early on in development (Tewarie et al., 2008). Many studies have been conducted to look at ESC and their ability to specifically differentiate into neural and glial cells. Neural and glial cells and their roles in spinal cord injury repair are discussed more in later Sections 4.2.4 and 4.2.6 (Assunção-Silva et al., 2014). Through the different studies using a spinal cord injury model it has been shown that ESC offer good long-term treatments because of their ability to survive in the injured spinal cord (Tewarie et al., 2008). A study conducted by Keirstead et al., 2005 used human ESC that were differentiated into oligodendrocyte progenitor cells (a subtype of glial cells) and were implanted into the injury site of the spinal cord either 7 days or 10 months after injury. This study showed that the rats with the transplant of cells after 7 days had recovery of motor function whereas the rats with transplant after 10 months did not. The overall outcome of this study claims that embryonic stem cell have therapeutic potential with a time frame limitation in which these cells can be therapeutic.

Induced pluripotent stem cells (iPS cells or iPSCs). Induced pluripotent stem cells (iPSCs) are another type of stem cell that can be obtained directly from adult tissues and used for autologous transplantation. They are obtained by reprogramming

differentiated adult cells through the introduction of 4 transcription factors (OCT3/4, SOX2, KLF4, and MYC) that revert them to an embryonic stage (Assunção-Silva et al., 2014; Tam et al., 2014; Tewarie et al., 2008). They are similar to embryonic stem cells in their characteristics, such as pluripotency, self-renewal capacity, and gene expression (Assunção-Silva et al., 2014). Researchers are looking into using iPSCs instead of embryonic stem cells because of the ethical issues that are associated with them later (Tewarie et al., 2008). iPSCs are useful because they run no risk of immune rejection of transplants. A potential problem is the formation of tumors. Tumor formation in induced pluripotent has been widely studied and is now being studied for the use of cellular system for spinal cord injury treatment. One study implanted human induced pluripotent stem cells derived neurospheres (hiPSC-NSs) into non-obese diabetic-severe combined immunodeficient (NOD-SCID) spinal cord injury model mice. There was an improvement of the functional activity of the mice, because there was evidence of formation of synapses between the cells and the neurons, increased in the expression of neurotrophic factors, angiogenesis, axonal regrowth and myelination of the injury site. This evidence was prominent because the cells differentiated into neurons, astrocytes, and oligodendrocytes. There was also no tumor formation reported. Another study that was conducted in 2012 used pre-evaluated neural stem/progenitor cells (NS/PCs) clones that were derived from both mice and human induced pluripotent stem cells. The model used a contusion spinal cord injury in nonhuman primates. Similar results of cell survival and differentiated into neurons, astrocytes, and oligodendrocytes, were seen without evidence of tumor formation. The results were also promising with axonal

sparing/regrowth and angiogenesis at the injury site and functional recovery of the animal (Assunção-Silva et al., 2014).

Neural/progenitor stem cells (NSPCs). Neural/progenitor stem cells (NSPCs) are used in spinal cord injuries because they are multipotential and found in the central nervous system, and offer neuroprotection and axon regeneration properties. These stem cells are unique because they have been found to have the ability to differentiate into the three main neural cell lineages: neurons, oligodendrocytes, and astrocytes (Assunção-Silva et al., 2014; Tam et al., 2014; Tewarie et al., 2008). NSPCs have been tested in many spinal cord injury models including contusion, traumatic, and complete injury with promising results (Assunção-Silva et al., 2014). In contused adult rat model, the NSPCs were found to produce neurons that travel along the spinal cord. This also resulted in improvement in the patient's overall function (Kakulas, 2004). The study using a cervical contusion-induced spinal cord injury showed that human NSPCs can survive and eventually differentiate into the four neural cell lineages. It was reported that there was a decrease in the injury site, and also an increase in motor activity of the animals (Iwanami et al., 2005). In a transection spinal cord injury model of rats, fetal neural stem cells were implanted. After two months, the cells were found to form ectopic colonies. These colonies were seen dispersing into the CNS where they were dividing into several neural-cell lineage types (Lu et al., 2012). They secreted a variety of molecules that had the potential to protect cells from death, and also secrete neurotrophic factors. Both in *in vitro* and *in vivo* tests, the secretion of growth factors that the NSPCs give off was found to promote growth of the host axons, which are sensitive to neurotrophic factors. More

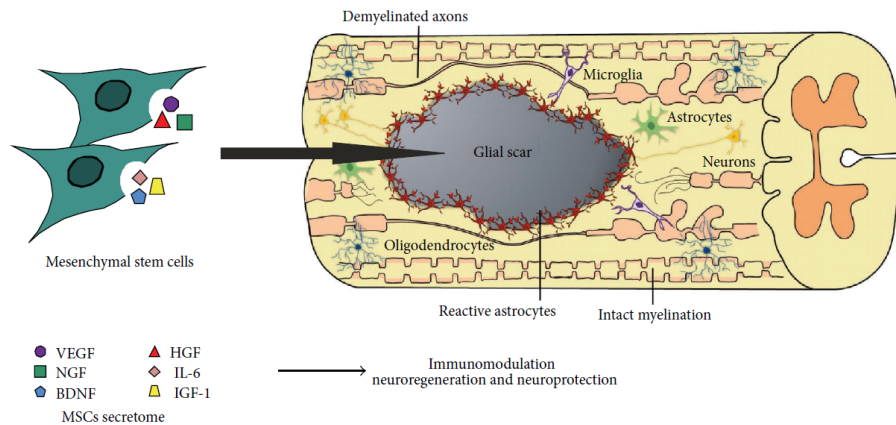
testing has shown that combinational treatment of these NSPCs, and the growth factor neurotrophin-3 (NT-3), offer extremely promising results by expanding the growth and penetration of host axons along the injury site (Assunção-Silva et al., 2014; Tewarie et al., 2008). More on combinational treatment will be discussed in Section 4.4. These NSPCs were studied in 2011 in a phase I/II clinical trial by a company in Switzerland. This company specifically used purified fetal human neural stem cells (HuCNS-SC) for the treatment of chronic thoracic spinal cord injury in both complete and incomplete patients. The clinical trial used a total of 12 patients, 7 of them having complete injuries and 5 incomplete. Results were only reported for 8 of the 12 patients. 4 of the complete injury patients showed a significant improvement in sensory function. Two patients with incomplete injuries gained sensory perception, and the third remained altered (Assunção-Silva et al., 2014).

Mesenchymal stromal stem cells (MSCs). Mesenchymal stromal stem cells (MSCs) were first thought to be only present within bone marrow, but are also found in non-marrow tissue. These cells are multipotent and can differentiate into osteoblasts, chondrocytes and adipocytes *in vitro* (Assunção-Silva et al., 2014; Tam et al., 2014). The advantage of using (MSCs) is that they are more available because they can be found in multiple tissues. There are no ethical or political issues during the isolation process (Assunção-Silva et al., 2014).

The use of MSCs and different strategies have been studied, but there is not yet a clear census of the outcomes. Some of the outcomes reported are that *in vitro* bone marrow mesenchymal stromal stem cells (BM-MSCs) differentiate into neuron-like cells

and glial cells, and *in vivo* they migrate across the blood-brain barrier, repopulate the CNS, and differentiate into microglia-like cells. Researchers are interested in their trophic activity rather than strictly using them as a therapeutic agent. MSCs secrete a set of bioactive molecules and/or microvesicles, which is called secretome. This secretome is thought to have neuroprotection and axon regeneration properties after spinal cord injury by suppressing local immune response, enhancing angiogenesis and inhibiting scarring and cell apoptosis (Assunção-Silva et al., 2014). This process can be seen in Figure 39.

When specifically looking at spinal cord injury treatment, MSCs are used in two different ways: transplantation of the cells into the injury site and administration of secretome. Many studies have been conducted for transplantation of the MSCs using either intravenous or subcutaneous injections, as well as direct injection into the injury site. All of these studies using these different techniques showed functional recovery after spinal cord injury. Studies using administration of the secretome also showed promising results. (Assunção-Silva et al., 2014).



(Assunção-

Silva et al., 2014)

Figure 39. Application of mesenchymal stromal stem cells (MSCs) as a treatment for spinal cord injury. The MSCs secretome is believed to be a key player on the promotion of neuroregeneration and neuroprotection, as well as the modulation of the inflammatory response (Assunção-Silva et al., 2014).

Glial cells.

Olfactory ensheathing cells (OECs). Olfactory ensheathing cells (OECs) are used in spinal cord injury repair because studies have shown functional recovery after transplantation. These cells are a specialized glial cell found in the olfactory system. The cells have been shown to promote axonal regeneration of olfactory nerve fibers into the olfactory bulb of the CNS, serving as a pathway for regeneration of the olfactory receptor neurons, by creating cellular channels that the axon can grow through (Assunção-Silva et al., 2014; Radtke et al., 2008). They can prevent axons from recognizing growth inhibitory molecules, and this allows them to elongate into otherwise inhibitory terrain (Tewarie et al., 2008). Additionally, they can produce different neurotrophic factors

(Radthke et al., 2008), including nerve growth factor (NGF), brain-derived neurotrophic factor (BDNF), neuregulins, and glial cell line-derived neurotrophic factor (GDNF) (Assunção-Silva et al., 2014). Olfactory ensheathing cells have been tested in phase I/II clinical trials in complete thoracic injuries and severe chronic spinal cord injuries. In the complete thoracic injuries clinical trial, the safety and feasibility was first tested. The results showed that, after one and three years, there were no safety issues observed with the procedure, no cord cyst or tumor formation, no neuropathic pain and deterioration in neurological status, and finally no functional changes in the patients. In the phase I/II pilot clinical study with severe chronic spinal cord injury patients, olfactory mucus autographs were transplanted. Results showed motor improvements in 11 of the 20, with some complications in 5 of the patients (Assunção-Silva et al., 2014).

Schwann cells (SCs). Schwann cells (SCs) are another form of glial cells just like the OECs, but they are primarily found in the PNS. These cells have become of more interest in spinal cord injuries because they may allow damaged axons in the central nervous system to regrow and remyelinate, just as it does in the PNS. Many studies have been conducted, but their results are contradictory. Some report that in the presence of astrocytes, the Schwann cells are not sustainable, but then some reports show evidence in their ability to promote regeneration. Some of the studies that support the evidence that they can promote regeneration involve transplantation of autologous SCs into thoracic injuries of cat spinal cord, human SCs grafted in a transected nude rat spinal cord, and adults SCs in a moderately contused adult rat thoracic spinal cord. These SCs, just like the OECs, have the unique property to overexpress NGF or BDNF. These genetically

modified SCs have shown a tremendous increase in axonal growth and remyelination after transplantation into adult rats with spinal cord injuries. Since there have been promising outcomes in the animal SCI models, it has been translated over to clinical trials. One study used autologous transplantation of SCs into patients with chronic spinal cord injuries. They injected the cells directly into the lesion by intramedullary delivery. The results showed no harmful effects after one and two years, and no real benefits were observed in the patients. This study ultimately showed that there is no danger associated with the procedure. In 2013, the Miami Project to Cure Paralysis performed the first ever FDA approved SC transplantation into a patient with complete thoracic spinal cord injury. This was a phase I clinical trial to test the safety and the ability to transplant the patient's own SCs. Four weeks after injury the cells were transplanted into the patient and no adverse signs were reported. The next part of the phase I clinical trial enrolled 8 more patients with acute thoracic spinal cord injuries and is currently ongoing (Assunção-Silva et al., 2014).

Hydrogel-based biomaterials. Hydrogel-based biomaterials have gained interest in spinal cord research. While using hydrogels for drug and cell delivery to the central nervous system, which is composed of the brain, spinal cord, and retina, there are many properties that need to be taken into consideration. Some of which include physicochemical and mechanical properties, biodegradability/bio absorbability, and biocompatibility. Some of these properties can be seen in Table 4.1 below. Since hydrogels possess these properties, they are an excellent candidate for neural tissue repair. In the upcoming sections, synthetic and natural-based hydrogels are outlined, and

the role they play within spinal cord injury research is discussed (Assunção-Silva et al., 2014; Tam et al., 2014).

In general, some issues/properties should be considered for developing hydrogel-based drug and cell delivery systems:

- The chemical and mechanical properties of the material, eg, to mimic the extracellular microenvironment in terms of chemical properties, such as growth factors and extracellular matrix proteins, and mechanical properties in terms of stiffness, porosity, and topography.
- The ability to load multiple drugs/biologics and control their release.
- The distribution of cells within the hydrogel, which will influence their survival and capacity to integrate with the host tissue.
- The release kinetics, the control of which allows the appropriate dose of growth factor or drugs to be released over a given period of time, eventually with different kinetic profiles at the same time for one or multiple agents.
- The ability to protect proteins against degradation.
- The biodegradability/bioresorbability of the material.
- The injectability of the delivery system, allowing for minimally invasive surgery.
- The interactions with the host immune system (biocompatibility).
- The non-toxicity of the delivery system and its degradation products.
- The stability/gelation time, the control of which ensures that the biomaterial hydrogel (and either cells or biomolecules encapsulated within) remains at the injection site to achieve local delivery.

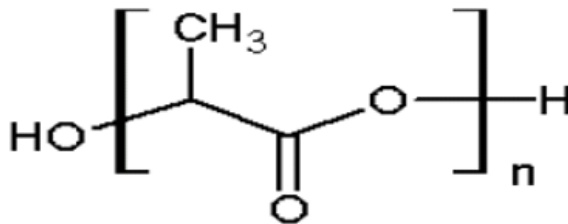
(Tam et al., 2014)

Figure 40. Hydrogel properties considered relevant for drug and cell delivery to the central nervous system (Tam et al., 2014).

Synthetic hydrogels. Synthetic hydrogels have one main advantage of being able to be manipulated to have specific mechanical and physicochemical properties (Assunção-Silva et al., 2014; Kim et al., 2014). It is also easy to blend two or more of these different synthetic polymers to create something unique with the specific properties needed. A set back that comes with these synthetic hydrogels is the fact that they are capable of producing an immune response within the body, and therefore have limitations with the FDA approval (Kim et al., 2014).

Poly (lactic acid) (PLA). Poly-lactic acid (PLA) is a biodegradable aliphatic polyester, and is a member of the α -hydroxy acid class of compounds. Its chemical

structure is shown in Figure 40 (Assunção-Silva et al., 2014; Kim et al., 2014). A disadvantage of PLA is that it is structurally unstable, fragmenting and collapsing on itself. Even with the instability it has shown that it supports axon extension and vascular growth into the graft. PLA scaffolds are used as only a temporary extracellular matrix. Implanting PLA alone, either in a hydrogel, macroporous sponge, micro- or nano-fiber or multi-walled conduit forms showed promising results. The next logical step would be to combine the poly-lactic acid with a therapeutic drug to improve the outcome. Through the research, there has not been a clear result for successful axonal regeneration in animal spinal cord injuries. Much more research is needed to optimize the results (Kim et al., 2014).



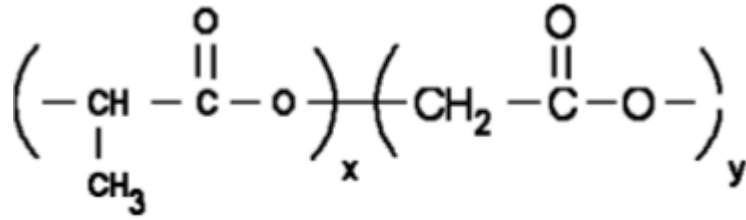
(Mahapatro et al., 2011)

Figure 41. Chemical Structure of poly (lactic acid) (PLA).

Poly (lactic-co-glycolic acid) (PLGA). Poly-lactic-co-glycolic acid (PLGA) has been approved by the FDA for the repair of human peripheral nerves. It is now being researched for use in the CNS related injuries including spinal cord injuries. PLGA is a polymer made up of two different monomers; glycolic acid (Figure 42, X) and lactic acid

(Figure 42, Y). The degradation and mechanical properties of this synthetic hydrogel can be varied depending on its particular application, by varying the ratio of the monomer units and their stereochemistry (either D- or L-form), along with varying the molecular weight distribution of the monomer chains (Assunção-Silva et al., 2014; Kim et al., 2014).

PLGA has evolved throughout the years in relation to how it's being used. It initially started off as a delivery agent of neurotrophic factors in tissue engineering (Assunção-Silva et al., 2014) and has evolved into a microsphere for drug delivery. Today it is a nanoparticle that encapsulates different therapeutic drugs. Some of the more recent studies of PLGA involve the delivery of certain stem cells, such as MSCs, neural stem cells and SCS. In a rat hemisection injury model, a PLGA scaffold containing neural stem cells showed a major improvement in spinal cord function, and in a canine model it showed that there is a possibility for spinal cord regeneration. In a rat complete transection model, PLGA hydrogels, loaded with human MSCs, showed improvement in both behavior analysis and motor-evoked potentials (MEP's). PLGA definitely has the potential in spinal cord injury repair, but needs to be studied more extensively (Kim et al., 2014).



(Mahapatro et al., 2011)

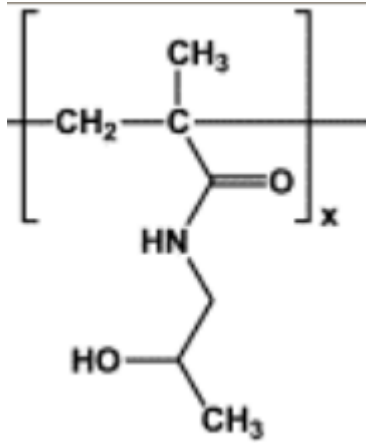
Figure 42. Chemical structure of poly (lactic-co-glycolic acid) (PLGA). X and Y represent the number of lactic acid and glycolic acid respectively (Mahapatro et al., 2011).

Methacrylate-based hydrogels.

Poly [N-2-(hydroxypropyl) methacrylamine] (PHPMA). Poly [N-2-

(hydroxypropyl) methacrylamide] (PHPMA) is a hydrophilic co-polymer, that has neuroinductive and neuroconductive effects, and the chemical structure is shown in Figure 43. There currently is a PHPMA hydrogel, that was developed for spinal cord injury, commercialized today. The hydrogel is known as NeuroGel™, and it contains PHPMA with an Arg-Gly-Asp (RGD) modification. (Kim et al., 2014). Throughout the years researching PHPMA, the results were extremely promising. In a transected rat spinal cord model, the hydrogel was found to successfully bridge the gap at the site of transection (Assunção-Silva et al., 2014). The hydrogel also helped with cell growth, angiogenesis and axonal growth, all within the microstructure of the spinal cord. This study also concluded that the growth of reparative tissue containing glial cells, blood vessels, axons, dendrites, and extra cellular matrix molecular (Assunção-Silva et al., 2014; Kim et al., 2014) was present and favored. Other studies have also reported

reduction of necrosis, motor benefits and improved locomotor BBB scores (Assunção-Silva et al., 2014).



(Ulbrich et al., 2010)

Figure 43. Chemical Structure of poly [N-2-(hydroxypropyl) methacrylamide (PHPMA)].

Poly 2-hydroxyethyl methacrylate (PHEMA)/poly 2-hydroxyethyl methacrylate-co-methyl methacrylate (PHEMA-MMA). Poly 2-hydroxyethyl methacrylate (PHEMA) hydrogel is made up of hydrophilic co-polymer that are cross-linked networks. The chemical structure is shown in Figure 44. This hydrogel is able to absorb water and retain it without dissolving, which provides a 3D substrate for cell attachment and growth. It is a known fact that most synthetic hydrogels are not biodegradable but this PHEMA hydrogel is ideal in tissue engineering because it has ideal physical properties and is very biocompatible (Assunção-Silva et al., 2014; Kim et al., 2014). An interesting property that PHEMA has is that when it is being produced into a hydrogel, it can be made to have

similar mechanical properties of the spinal cord. The more similar they are, the least likely issues are to arise after implantation (Kim et al., 2014).

Kim et al., 2014 studied both PHEMA and its co-polymer PHEMA-MMA and reported that they promoted axon regeneration. The hydrogels were then modified to obtain better mechanical strength and function by adding coiled channels (Assunção-Silva et al., 2014; Kim et al., 2014). The surface of the hydrogels were either positively charged or negatively charged. Results showed that the positively modified hydrogels were better at promoting axon growth and regeneration than both the unmodified or negatively charged hydrogels. More recently, studies have been done to assess the capability of using PHEMA and its co-polymer PHEMA-MMA to deliver therapeutic cells. One study used PHEMA with MSCs in a hemisectioned rat spinal cord model. The results showed that it promoted regeneration of the axons (Kim et al., 20114).

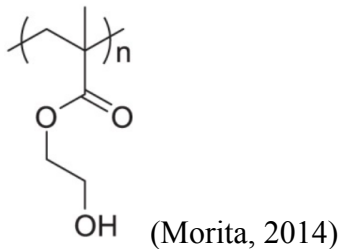


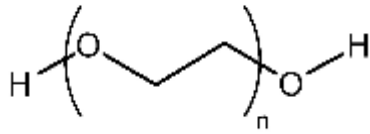
Figure 44. Chemical structure of poly (2-hydroxyethyl methacrylate) (PHEMA).

Poly (ethylene glycol) (PEG). Polyethylene glycol (PEG) shown in Figure 45 is a synthetic hydrogel used in many aspects of spinal cord injuries. It is a water-soluble

nontoxic polyether that is known to have protective effects on the spinal cord by resisting protein adsorption and cell adhesion (Assunção-Silva et al., 2014; Kim et al., 2014).

These protective effects allow a PEG hydrogel to be injected into the body without the body producing an immune response. As stated before, PEG has a natural effect on the spinal cord, so researchers started to develop different cross-links using PEG. Different cross-links were created to increase/decrease degradation rate and increase cell adhesion (Assunção-Silva et al., 2014).

PEG has a wide range of uses as a biomaterial. Studies have shown promising outcomes. An *in vivo* model using just a PEG solution injection into a spinal cord injury showed potential for accelerating and enhancing the membrane resealing process, and also restoring neuronal membrane integrity (Assunção-Silva et al., 2014). Another study reported that cross-linked PEG with poly (N-isopropylacrylamide) (PNIPAAm) in to a spinal cord injury allowed axonal growth and successful cell transplants or BDNF release (Kim et al., 2014). Another study looked at the effects of using PEG hydrogel loaded with NT-3, which was implanted into a rat model of spinal cord injury. Results from this study showed that there was an improvement in the rat's locomotor behavior and more axonal growth (Assunção-Silva et al., 2014). In our study, we used a combination of the cross-linked PEG and PNIPAAm loaded with BDNF and NT-3. In Chapter 5, the results of the study will be discussed.



(Barron, 2015)

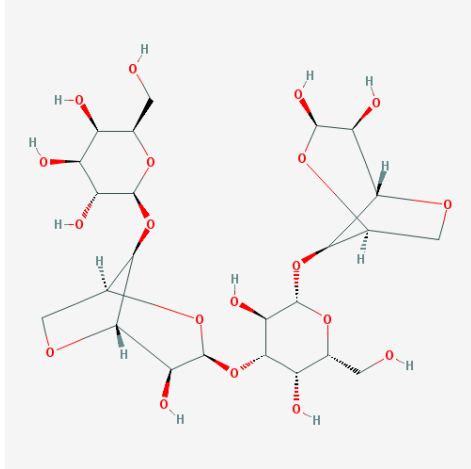
Figure 45. Chemical structure of poly (ethylene glycol) (PEG).

Natural-based hydrogels. Natural-based hydrogels are commonly made up of natural polymers (e.g. Proteins) and/or molecules that are naturally found within the human body, because it is easier for integration and interaction with the tissue already present. Most of the natural-based hydrogels are substances that are found within the bodies extra cellular matrix or have existing properties of the cells. This gives the hydrogel a seamless integration into the injury site. Another unique trait is that these hydrogels have similar properties of the soft tissue that they are replacing within the spinal cord. One problem, though, of the natural-based hydrogels is the chance for immune reactions from the existing tissue because they are derived from natural sources (Assunção-Silva et al., 2014; Kim et al., 2014).

Agrose. Agrose is a linear polysaccharide of D-galactose and 3,6-anhydro-L-galactopyranose (Figure 46) that is derived from the cell walls of red algae making it biocompatible. It is used in three different varieties as a delivery vehicle for drug or macromolecules in animal models of spinal cord injuries; encapsulation, tubular, and hydrogel. This section will focus on the hydrogel. One of the main applications of agrose hydrogel is local delivery of BDNF because of the porous nature of the structure and

mechanical properties similar to that of the tissue. One trait that intrigues researchers to study agarose hydrogel as a tissue engineering approach for spinal cord repair is their ability to polymerize *in situ* thereby adapting to the different shapes of lesion because of their ability to fill different types of neurological defects.

Previous studies involving agarose hydrogels have already proven the potential uses for them because of their ability to support neurite extension *in vivo*. In a contusion and dorsal-over hemisection rat model of spinal cord injuries, the agarose hydrogels loaded with methylprednisolone nanoparticles were able to provide a local and gradual release of the drug. The results showed that the lesion volume was reduced, as well as a decrease in the expression of proinflammatory proteins when compared to systematic methylprednisolone delivery. Another study used the agarose hydrogel delivery system to deliver lipid microtubes that have been loaded with different drugs. The main drug used was thermostabilized chondroitinase ABC (chABC) (Assunção-Silva et al., 2014; Kim et al., 2014). Over time, the chondroitinase ABC was released and showed an improvement in reducing the deposition of chondroitin sulfate proteoglycans (CSPGs) (CSPGs are a major class of axonal growth inhibitors) and eliminating the use of pumps or catheters (Assunção-Silva et al., 2014). It is also shown that if these agarose hydrogels containing chondroitinase were combined with NT-3 that there was locomotor recovery with axonal regeneration in injured rats (Kim et al., 2014).



(National; CID=11966311).

Figure 46. Chemical structure of Agarose.

Alginate. Alginate is also a linear polysaccharide like agarose that is derived from the cell walls of brown algae and is composed of repeating structures of (1-4) linked β -D-mannuronate acid (Figure 47, M) and α -L-guluronate acid (Figure 47, G). This polysaccharide has both biocompatibility and bioresorption properties, which allows it to be used in cell encapsulation, cell transplantation, and tissue engineering (Assunção-Silva et al., 2014; Kim et al., 2014). In a transection spinal cord injury model of young rats, the alginate provided a pathway for the severed axons and also decreased astrocytosis between the alginate and the spinal cord (Kim et al., 2014). In an acute cervical spinal cord of adult rats, the alginate was found to promote axon regeneration across the scaffold (Assunção-Silva et al., 2014). One issue that occurs with using this natural alginate is that it has a high degradation rate and cytotoxicity, and mammals do not possess the correct enzymes to degrade high molecular polymers of alginate. The addition of poly (lactic-co-glycolic acid) (PLGA) microspheres allows for a controlled

environment for enzymatic degradation (Assunção-Silva et al., 2014; Kim et al., 2014).

Another point to be aware of when using natural alginate is that they include toxic impurities and have to go through an extensive ultra-purification process before it is transplanted within the body safely (Kim et al., 2014).

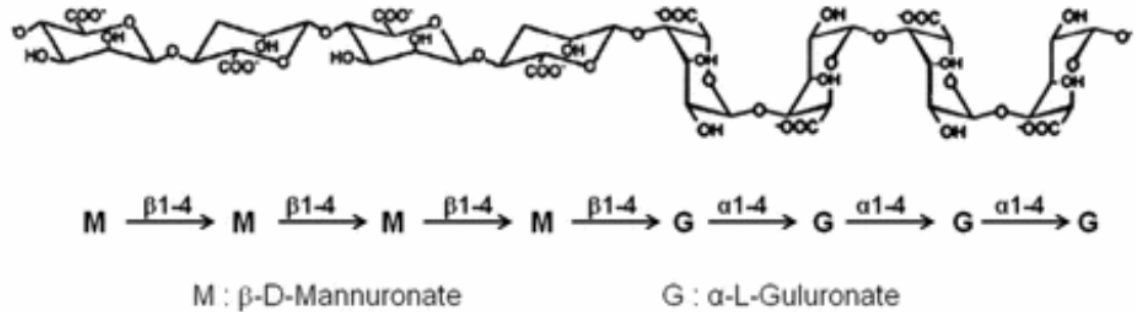
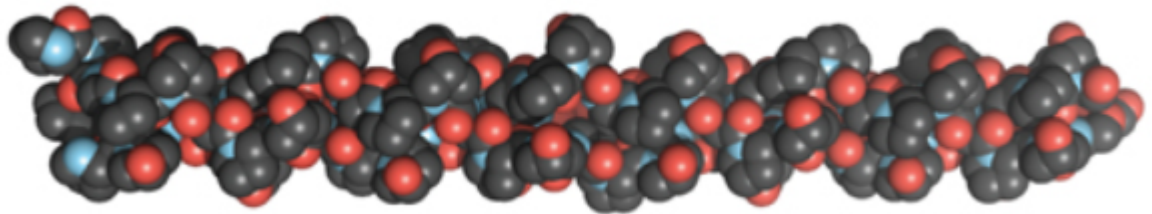


Figure 47. Chemical structure of alginate.

Collagen. Collagen is a protein found within the extra cellular matrix of mammals and accounts for about 25-30% of the total proteins. There are a total of 29 different collagen types. Collagen is used as a natural based hydrogel because of its binding sites that are used for cell adhesion, cell migration, proliferation, differentiation. They are also biocompatible, biodegradable, and noncytotoxic (Assunção-Silva et al., 2014; Kim et al., 2014). When looking at the mechanical properties of collagen, it has a very high mechanical strength that is closely related to that of soft tissue (Kim et al., 2014). One aspect of collagen that makes it easier to produce a hydrogel is that the gel formation can be produced by just changing the pH balance. Collagen is not only used in spinal cord

injuries, but in burns, wound dressings and nerve regeneration. There have been many studies conducted on different models using neurotrophic factors, among others, to deliver therapeutic cells. A recent study conducted in 2014, used collagen hydrogels as a vessel for the delivery of NT-3 in spinal cord injury rats. The results showed an aligned axonal regeneration, and an increase in the number of regenerating axons were observed in the vessels delivering the neurotrophin-3 (Assunção-Silva et al., 2014).

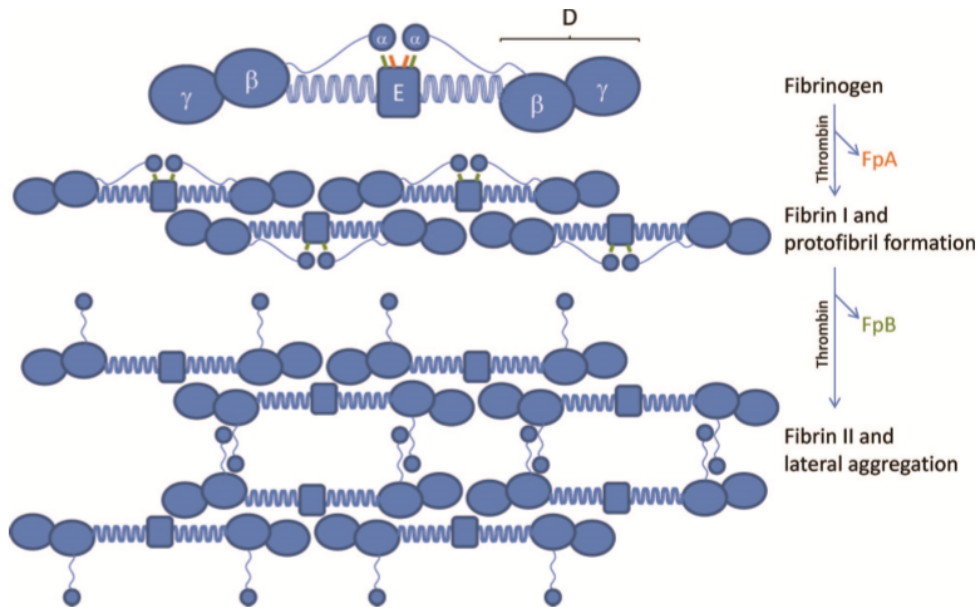


(Shoulders et al., 2009)

Figure 48. Collagen triple helix structure.

Fibrin. Fibrin is a fibrous protein that is involved during the clotting process of our body and acts as a binding agent between the molecules. It is produced during the coagulation process where fibrinogen has been severed by thrombin producing fibrin monomers. The process of fibrinogen and fibrin formation during the coagulation process is shown and explained in Figure 49 (Assunção-Silva et al., 2014; Kim et al., 2014). When fibrin is used in hydrogels for tissue engineering, it poses some advantages and disadvantages. One of the advantages is that the gelation of the hydrogel can be

controlled through different concentrations of thrombin during the coagulation process, offering researchers the possibility to maintain a liquid hydrogel during injection and once in the body a solid hydrogel. But on the other hand, these fibrin hydrogels originating from mammals degrade rapidly, posing a problem with contamination from blood-derived pathogens or prion proteins, and some studies report that inhibits neurite outgrowth and activates scar formation (Assunção-Silva et al., 2014). Despite these disadvantages, fibrin hydrogels have still been tested and showed promising results. Studies have been conducted on subacute, hemisected and severe, among others, using different growth factors, and stem cells, and all have shown some type of improvement, whether it be an increased neural fiber sprouting or some degree of axonal growth. Fibrin hydrogels have a very promising future in spinal cord injuries because they have the greatest potential for a minimally invasive approach for patients (Assunção-Silva et al., 2014; Kim et al., 2014).



(Undas et al., 2011)

Figure 49. Fibrinogen and fibrin formation. Fibrinogen is composed of $2A\alpha$, $2B\beta$, and 2γ -chains, which are arranged in a dimer of bilateral symmetry. The central E-region contains the N-termini of all 6 chains. The D-region, which is connected with the E-region by a coiled coil segment, is composed of the β - and γ -chain C-termini. The α -chain C-termini fold back on the coiled coil and interact with the E-region. Fibrin formation involves cleavage of FpA (fibrinopeptide, orange) by thrombin (fibrin I), which polymerizes into protofibrils. Subsequently, FpB (fibrinopeptide, green) is cleaved by thrombin (fibrin II). FpB cleavage is associated with release of the C-terminal α -domains, which interact for lateral aggregation (Undas et al., 2011).

Chitosan. Chitosan is also a linear polysaccharide that is composed of randomly distributed β -(1-4) linked D-glucosamine (deacetylated unit) and N-acetyl-D-glucosamine (acetylated unit) (Figure 50). Chitosan can be made from chitin found in crustacean shells. Crustacean shells are the second most abundant biopolymer, with cellulose being the first (Assunção-Silva et al., 2014). Since the origin of where chitosan is derived can change, the physicochemical properties change and are directly related from the source because of affect they have on the size and shape of the pores (Kim et al.,

2014). Chitosan hydrogels can be created by different bonding of the molecules, and can even form a hydrogel by itself through hydrogen bonds, hydrophobic interactions, and chitosan crystallites (Assunção-Silva et al., 2014; Kim et al., 2014). When looking at chitosan by itself, without any additives, it shows neuroprotective effect and helps aid physiological recovery in traumatic spinal cord injuries. Research shows when the chitosan hydrogel loaded with neural stem cells was transplanted in complete spinal cord transection and subacute spinal cord injury model of rats that there was an increase survival rates and regeneration of the spinal cord. These results only showed functional recovery when treated with growth factors and soluble Nogo-66 receptor in transection model and dibutyryl cyclic-AMP in the subacute model. But in acute model of rats, results showed enhancement of both functional recovery and nerve regeneration with chitosan hydrogels loaded with bone marrow stromal cells (Kim et al., 2014).

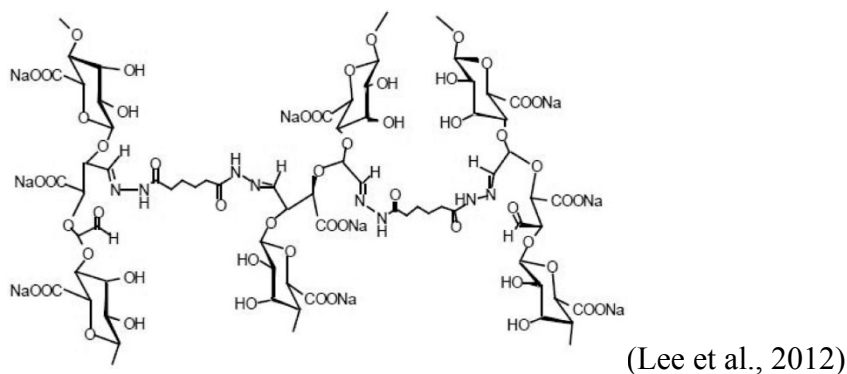


Figure 50. Chemical structure of chitosan.

Hyaluronic acid. Hyaluronic acid is a natural polysaccharide consisting of glucuronic acid and N-acetylglucosamine. Figure 51 below represents the chemical structure. It is used as a hydrogel because of its ability to be completely biodegradable, non-cytotoxic, and biocompatible, but it has weak mechanical properties and high degradation rate. To increase the mechanical properties other polymers are incorporated with the hyaluronic acid. Also, the surface of hyaluronic acid does not allow the cell to bind in an efficient manner, but this problem is overcome by modifying the acid to allow the cells to bind more easily. Researchers are trying to design the perfect hyaluronic acid hydrogel with different modification, because it is known that hyaluronic acid can help to reduce scar formation at the injury site. Some of the combinations that have been studied are high molecular weight hyaluronic acid, one modified with nogo-66 receptor antibody, and addition of brain derived neurotrophic factor (BDNF). The results showed that for the high molecular weight and modified with nogo-66, it reduced astrocytes activation and decreased chondroitin sulfate proteoglycans (CSPG) deposition *in vivo*. The hydrogel containing brain derived neurotrophic factor prevented an inflammatory reaction and increased motor functions in a rat spinal cord injury model (Kim et al., 2014).

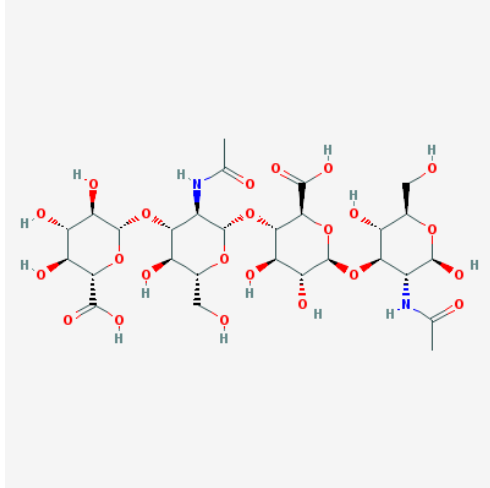


Figure 51. Chemical Structure of Hyaluronic Acid.

Self-assembling peptides. Another different approach from hydrogels and cell therapies in spinal cord injury research is the use of self-assembling peptides, which are nanomaterials that have the capability to form a scaffold by themselves when present within a solution that has similar properties to that of the extra cellular matrix (Kim et al., 2014). Depending on the contents of the solution through the self-assembling peptides, there can be changes to obtain a specific required response (Assunção-Silva et al., 2014). The self-assembling peptides are made up of short repeating units of amino acids that produce nanofibrous scaffolds in response to thermal or pH. These peptides are used because they are reabsorbable, allow biofunctionalizations, and can easily be made into a liquid injectable that will form a scaffold when injected into the tissue. Studies have shown that different self-assembling peptides have the ability to improve function and

histological recovery in an acute rat model and promotes neurological recovery (Kim et al., 2014).

Combinational Biomaterials

Combinational biomaterials are becoming the norm in spinal cord regeneration. Biomaterials alone can help to improve injury, as mentioned in previous sections in this chapter, with some limitations. These limitations as thought to be overcome by combining biomaterials with cell based therapies. Some of these combinations were mentioned briefly in the individual sections of both the cell based therapies and hydrogel based therapies and, will be discussed in a bit more detail in this section.

The first combination that will be discussed is using neural stem cells (NSC) with a poly-lactic-co-glycolic acid (PLGA). This scaffold was injected into spinal cord injury rats and results showed cell viability for a greater length of time and improved functional recovery of the rats according to Xiong et al., 2009 and Teng et al., 2002. Another study conducted by Rauch et al., 2009, used a hemisection spinal cord injury model to deliver both neural stem cells and endothelial cells. Researchers used two biomaterials containing poly-lactic-co-glycolic acid as the outer section and poly (ethylene glycol) / poly-L-lysine (PEG/PLL) as the inner section of this co-delivery system. The endothelial cells were present within this scaffold to promote vascularization, which in theory helped increase neural stem cells survival. Results of this study showed that there was an increase in the blood vessels at the injury site, but the survival of the neural stem cells did not increase.

The next combination using MSCS with a biomaterial poly (D, L-lactide-co-glycolide) / small intestinal submucosa (PLGA/SIS) in a complete transection spinal cord injury showed that it started nerve regeneration. Most successful studies using MSCs use macro porous hydrogels based on derivatives of with 2-hydroxyethyl methacrylate (HEMA), 2-hydroxypropyl methacrylamide (HPMA), or co-polymers of PHEMA. The results of these studies are very promising with the hydrogel promoting cell growth, axon growth in the proximal and distal stumps and reabsorption of the hydrogel by macrophages within the body and its replacement with newly formed tissue. This tissue was also found to contain connective tissue elements, blood vessels, astrocytic processes, and neurofilaments (Assunção-Silva et al., 2014).

The use of natural hydrogels to deliver mesenchymal stem cells have also been studied, but not in as much detail as synthetic hydrogels. These studies include the use of agarose, alginate, and fibrin among others. The results from these studies are not as promising as the use of synthetic hydrogels, but are still being studied to improve the results (Assunção-Silva et al., 2014). Using combinational biomaterials for spinal cord injuries holds much promise for the future, and future studies are needed to find cure for SCI.

Table 2

Therapeutic potential of combinational approaches based on cell therapy and biomaterials for spinal cord injury treatment (Assunção-Silva et al., 2014).

Cells	Biomaterial	<i>In vitro</i> improvements	<i>In vivo</i>	
			Functional improvements	Histological improvements
NSCs	PLA	✓	—	—
	PLGA	—	✓	✓
	Alginate	—	✓	✓
	Fibrin	✓	✓	✓
	Chitosan	✓	✓	✗
	Gellan-gum	✓	—	—
NSCs plus ECs	PLGA-PEG/PLL	—	✗	✓
NSCs plus OECs	Gellan-gum/GRGDS	✓	—	—
MSCs	PLGA/SIS	—	✓	✓
	HEMA, HPMA, and HPMA copolymers	—	✓	✓
	Agarose	—	✗	✓
	Alginate	✓	—	—
	Alginate/fibronectin	✓	—	—
	Matrigel	✓	—	—
	Fibrin	—	✓	✓
	Gellan-gum/GRGDS	✓	—	—
OECs	SAP-IKVAV	✓	—	—
	PHB-b-DEG	✓	—	—
	Alginate	✗	—	—
	Alginate/fibronectin	✓	—	—
	Matrigel	✓	—	—
OECs plus MSCs	Serum-derived albumin	—	✓	✓
SCs	PHB	✗	✗	✓
	PAN/PVC	—	✗	✓
	Alginate	✓	—	—
	Laminin/collagen	—	✓	✓
SCs plus OECs	PAN/PVC plus chABC delivery	—	✓	✓
	PLLA-PLLA oligomers	—	✗	✓
BM-MSC-SCs	Matrigel	✓	✓	✓

✓: improvements observed; ✗: no improvements observed; —: not studied.

Chapter 5

Using Bioengineered Scaffold Loaded with Neurotrophins to Enhance Functional Recovery after Locomotor Training in Spinal Cord Injury Animals

J. Witko¹, B. King¹, J. Vernengo², A. Singh³

1: Mechanical Engineering, Rowan University, Glassboro, NJ, USA

2: Chemical Engineering, Rowan University, Glassboro, NJ, USA

3: Mechanical Engineering, Rowan University, Glassboro, NJ, USA
Biomedical Engineering, Widener University, Chester, PA, USA

Abstract

Changes in monosynaptic reflex, often used to study spasticity, has been tested through the H-reflex in spinal cord injury (SCI) patients after rehabilitation training, such as body weight support treadmill training or cycling. The combinational effects of rehabilitation training and a bioengineered scaffold on spasticity in SCI animal model have not been studied. We used a clinically relevant animal model of spinal cord moderate contusion at T9/T10 with body weight support treadmill training and the bioengineered scaffold poly (N-isopropylacrylamide-) poly (ethylene glycol) (PNIPAAm-g-PEG) loaded with the growth factors BDNF/NT-3 to measure the efficiency of the combinational bioengineered approach to treat spasticity. Five animal groups were included in the study: sham, injury, SCI + body weight support treadmill training (BWSTT), SCI + PNIPAAm-g-PEG with BDNF/NT-3 (Transplant), and SCI + combination of body weight support treadmill training with PNIPAAm-g-PEG with BDNF/NT-3 (combinational). Results indicate that there was an increase in the overground BBB test scores from the BWSTT, and combinational groups from weeks 6-

8, but not in the transplant only or injury groups when compared to the sham. There was also a decrease in habituation of the H-reflex and restoration of rate depression properties in both the BWSTT and combinational groups. This allows new pathways to be opened to explore unique tissue-engineering approaches with promising clinical application for patients with incomplete SCI's.

Introduction

Spinal cord injury is a condition that affects about 40 million people worldwide (Assunção-Silva et al., 2014) with more than 11,000 new cases reported in the United States and Canada alone (Lam et al., 2007). The number one leading cause of spinal cord injuries are accidents while working (28%), followed by motor vehicle accidents (24%) and sporting/recreation (16%). Spinal cord injuries are also the second leading cause of paralysis (23%) (Christopher and Dana Reeve Foundation, April 2009). Due to the disruption within the motor and sensory systems after SCI, paralysis, spasticity, anesthesia, and hyper-reflexia below the lesion site is observed. Spasticity resulting from SCI due to changes in the motoneuron properties is observed in 65-78% (Adams et al., 2005) of SCI patients and is measured by the Hoffman or H-Reflex/monosynaptic reflex (Reese et al., 2006). The H-reflex is elicited by the synaptic activation of motoneurons by muscle afferents, following electrical stimulation of muscle nerves (Reese et al., 2006; Skinner et al., 1996). In normal patients, the H-wave amplitude decreases with increasing electrical stimulus (Reese et al., 2006), and after injury, becomes less sensitive which produces a higher H/M ratio (Lee et al., 2005).

Current treatments for spasticity after SCI include activity based rehabilitation therapies, such as body weight support treadmill training (BWSTT). The overall goal of this activity based rehabilitation therapy is to “target activation of the neuromuscular system below the level of the lesion, with the goal of retaining the nervous system to recover specific motor tasks” (Jones et al., 2012). This therapy focuses mainly on incomplete injuries because there is some preservation of the pathways below the level of injury, where as in a complete injury, there are no descending/spared pathways. Complete spinal cord injuries have never shown any recovery in over-ground walking, whereas body weight supported treadmill training has proven to enhance locomotor recover in incomplete injury patients (Lam et al., 2007). Since it has been proven that body weight supported treadmill training increased locomotor outcomes of incomplete spinal cord injuries, it shows that the level of recovery depends on the amount of spared descending pathways. To enhance the functional recovery while using this therapy, transplantation treatment strategies are added. These transplantation strategies have to 1) minimize the secondary injury 2) replace and minimize the survival of damaged cells and 3) alter the local environment to be more conducive for regeneration (Jones et al., 2012). To achieve the goals of transplantation strategies, neurotrophins growth factors, called neurotrophins, are used. Neurotrophins, such as BDNF and NT3, are neuroprotective and neuroregenerative agents that minimize tissue loss, promote regeneration and sprouting of injured axons, and help bridge the gap of injury (Boyce et al., 2014). Clinical transition of cell transplantation treatments secreting these neurotrophins still poses several problems including rejection, and release of the cells and the approaches used (Assunção-Silva et al., 2014). To overcome these problems, we propose using the bioengineered

scaffold poly (N-isopropylacrylamide)-poly (ethylene glycol) (PNIPAAm-g-PEG) loaded with neurotrophins. In past studies, PNIPAAm-g-PEG has shown to be highly biocompatible, and biodegradable, and has the ability to release a drug over a long duration of time. It can also be functionalized to secrete neurotrophins (Alexander et al., 2014; Comolli et al., 2009). In summary, this study aims to investigate changes in H reflex response in contused rats after combinational treatment strategy, using body weight support treadmill training and PNIPAAm-g-PEG scaffold releasing BDNF/NT-3.

Methods and Materials

Spinal cord injury (contusion) and animal care. All animal protocols were in accordance with NIH *Guide for the Care and Use of Laboratory Animals* and approved by Rowan School of Osteopathic Medicine Institutional Animal Care and Use Committee (IACUC). The study used a total of 38 adult female Sprague-Dawley rats (225-250 g, Harlan, NJ). They were housed 2-3 per cage containing alpha-dry bedding with a cardboard tube, on a 12-hour light-dark cycle, and had free access to food and water. The 38 rats were divided into 5 groups, as shown in Table 3. Groups 2-5 received SCI. Animals in these groups were anesthetized with an intraperitoneally (i.p.) injection of ketamine cocktail containing a mixture of ketamine (76 mg/kg, Fort Dodge Animal Health, Fort Dodge, IA), xylazine (7.6 mg/kg, Ben Venue Laboratories, Bedford, OH), and acepromazine maleate (0.6 mg/kg, Boehringer Ingelheim Vetmedica, Inc, St. Joseph, MO). Animals were shaved and then cleaned with alcohol and betadine, before T9/T10 laminectomy was performed to expose the dura. They received a moderate contusion injury from an impact device with a 10 gram, 2.0 mm diameter rod that dropped from 25

mm on exposed spinal cord. Subcutaneous fat was placed on the exposed dura preventing adhesions and 4.0 sutures closed the back muscles. The wound was closed with surgical wound clips. Rats were placed on a heating pad until conscious and moving regularly. Water bottles in the cages were replaced with long stems, and H₂O hydrogels and food were placed in the cage in the event that the rats could not reach food/water. After surgery, rats were injected subcutaneously with saline (3-5 ml) two times a day and Ampicillin (.3 cc, 22.7 mg/ml s.c., b.i.d.) once a day. Saline injections were given 10-12 hours apart, along with manually expressing the rat's bladder three times a day for 2 weeks after date of surgery. This minimized dehydration and urinary tract infection. Rats with signs of illness after 2 weeks post-surgery were given Children's Tylenol (.4 ml, 100 mg/kg) orally one time a day for 2 weeks or as needed.

Table 3

Number of animals in each group.

Group Number	Injury/Training Received	Number of Animals
Group 1	Sham	N=6
Group 2	Contused	N=8
Group 3	Contused + BWSTT	N=8
Group 4	Contused + Scaffold + Neurotrophins	N=8
Group 5	Contused + Scaffold + Neurotrophins + BWSTT	N=8

Transplantation. One-week post spinal cord injury Groups 4 and 5 received scaffold and neurotrophin transplants. Rats were anesthetized with the ketamine cocktail and prepared for surgery similar to the initial contusion surgery. The location of injury was identified and re-exposed, and approximately 5 ml of PNIPAAm-g-PEG loaded with BDNF ($0.5 \times 10^6 / 5 \mu\text{l}$) and NT-3 ($0.5 \times 10^6 / 5 \mu\text{l}$) was injected with a positive displacement pipette at the injury site. Post-operative care stayed the same as with the initial contusion injury, 2 weeks of saline, Ampicillin, and bladder expression.

Behavioral analysis. All rats were tested using the Basso, Beattie and Bresnahan (BBB, Basso et al., 1995) scale to measure their hindlimb function in an open field locomotion. Rats were video recorded for 4 minutes each in a circular enclosure and then scored based on their neurological rating scale, ranging from 0 (complete hindlimb paralysis) to 21 (normal hindlimb locomotion). The BBB test was conducted before the spinal cord injury (baseline), 2-3 days after surgery, and then each week thereafter until week 10 by a trained observer and scored by another blind observer.

Treadmill training. Figure 52 shows a custom-built treadmill with a load cell developed for this study. The load cell was attached to the body weight support (BWS) rod and read the actual load that the rat exerted on the rod during locomotion. Individual components of the custom treadmill are labeled and explained in Figure 53. Rats were secured to the BWS arm via a soft cloth vest and attached using Velcro strips and trained at 75% BWS at 7 cm/sec. This was done for rats in Groups 3 and 5 one-week post-injury

or transplant. Rats were trained 5 days a week, 1000 steps/day for up to 8 weeks as shown in Figure 5.3.

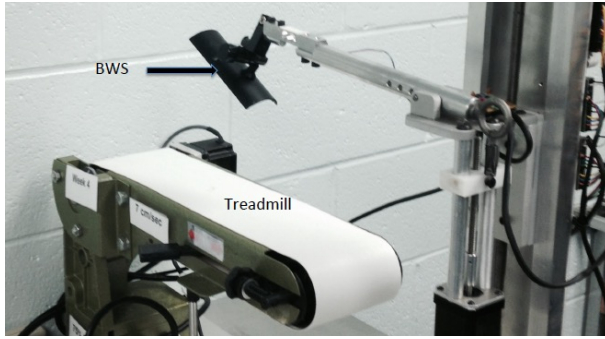


Figure 52. Custom treadmill and body weight support (BWS).



Figure 53. Custom body weight support (BWS) treadmill with components labeled. A) National Instruments myDAQ: paired with LabVIEW VI, the myDAQ issues commands to the motor controllers (B and C) and interprets the signal from the load cell amplifier (F), B) Treadmill Motor Controller: controls stepper motor used to drive the treadmill, C) Spring Tensioning Motor Controller: controls the stepper motor used to tension the spring, D) Power Supply: Supplies power to the motors, E) Treadmill Stepper Motor, F) Course Adjustment Knob: adjusts the height of the body weight support carriage, G) Animal Attachment Plate, H) Load Cell: measures the weight the animal is feeling after the spring provides assistance, I) Load Cell Amplification Circuit: amplifies the load cell signal before being processed by the my DAQ, J) Tension Spring: provides assistance to the animal when weight is supported, K) Spring Tensioning Motor: stepper motor that changes the tension of the assistance spring, L) Treadmill Belt, M) Treadmill Base, N) Body Weight Support Carriage: carriage attached to the course adjustment which moves the spring tensioning system, load cell, and variable angle specimen attachment.



Figure 54. Rat undergoing BWSTT.

Electrophysiology (H-reflex). Eight weeks after contusion or transplant, rats were anesthetized with ketamine cocktail, and their right hindlimbs were shaved, and then cleaned with alcohol. The right tibial nerve was exposed and lifted using a hook electrode (Figure 55), with active needle electrodes inserted between the fourth and fifth metatarsal, and the reference/recording electrode inserted in the skin of the fifth digit. The nerve was preserved using mineral oil throughout the test. The tibial nerve was stimulated using an A-M Systems Isolated Pulse Stimulator Model 2100 where the response was amplified with an A-M Systems Differential Amplifier Model 1700. The signal was sent to a Tektronix TDS 310 two channel oscilloscope and National Instruments USB-6212 BNC, which sent the information to the LabVIEW program loaded on the computer as shown in Figure 56. First the nerve was stimulated at .3 Hz to determine the threshold and maximum stimulus response levels. Once the threshold was found, the H-reflex of the tibial nerve was conducted at .3 Hz and 10 Hz at the particular stimulus. A 5-10-minute delay was introduced between the two tests to allow the nerve to return to baseline electrophysiological state.

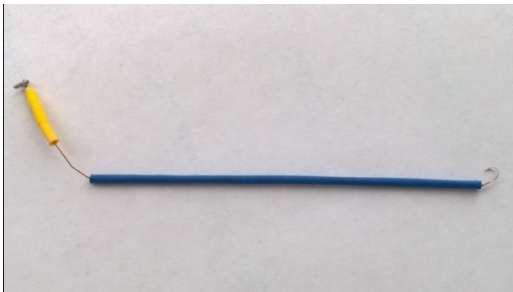


Figure 55. Bipolar hook electrode.

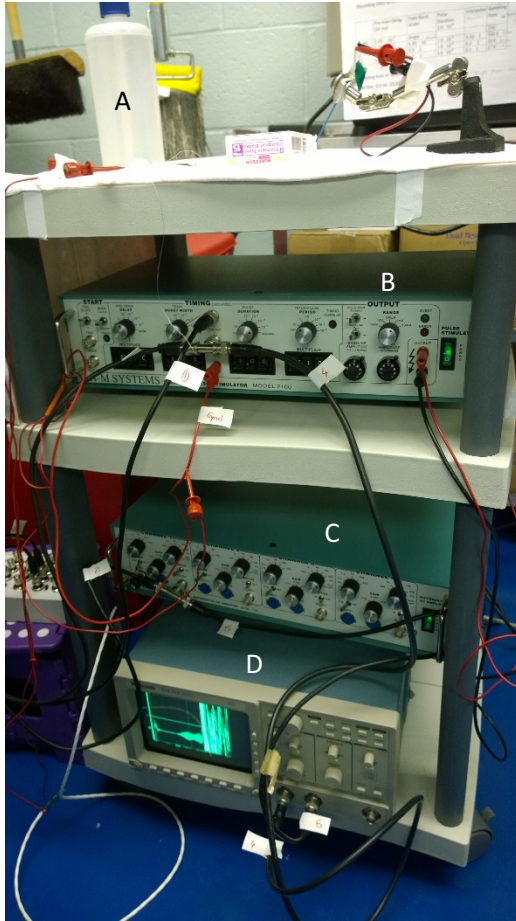


Figure 56. Set up of A-M Systems Isolated Pulse Stimulator Model 2100, A-M Systems Differential Amplifier Model 1700, and Tektronix TDS 310 oscilloscope used for H-reflex. A) Mineral oil, B) Stimulator, C) Amplifier, D) Oscilloscope.

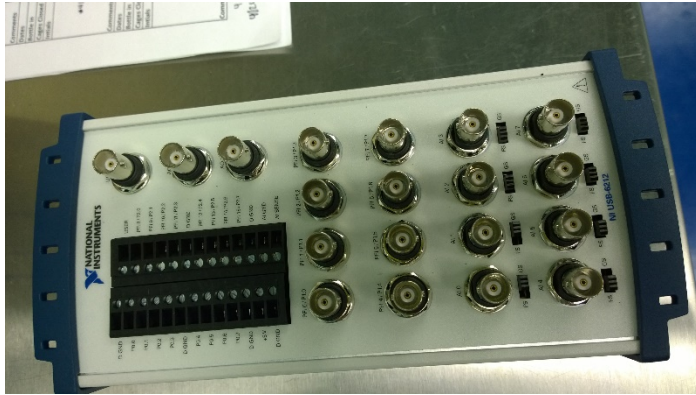


Figure 57. NI USB-6212 used to collect M and H waves.

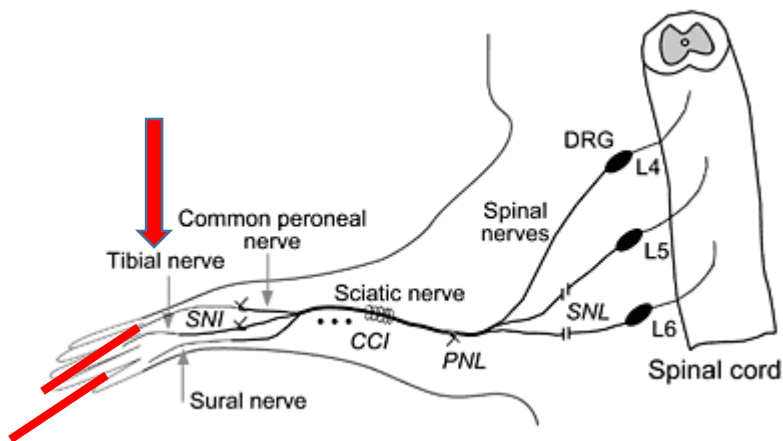


Figure 58. A schematic diagram of how the M and H waves are stimulated and the path it travels to the spinal cord to produce the response.

Statistical analysis. Statistical analysis was done using repeated measure ANOVA for BBB data between groups and time, with time taken as a repeated measure beginning at 1 week after training. The Turkey's test was used for post hoc analysis of parametric data, and the Mann-Whitney U test for nonparametric data. H-reflex was

analyzed using a one-way ANOVA between groups, followed by Turkey's post hoc test when appropriate. All values are expressed as mean +/- standard error of mean (SEM). All statistical analyses were performed using SPSS 11.5 for Windows Software, and significance was determined using a *p-value* of <0.05.

Results

Behavior test-overground BBB test. A baseline and weekly BBB scores are shown in Figure 59. Functional recovery was observed in BWSTT and combinational groups (Groups 3 and 5) but were not statically different from the Sham, Injury, and Transplant groups (Groups 1,2 and 4) (Figure 59).

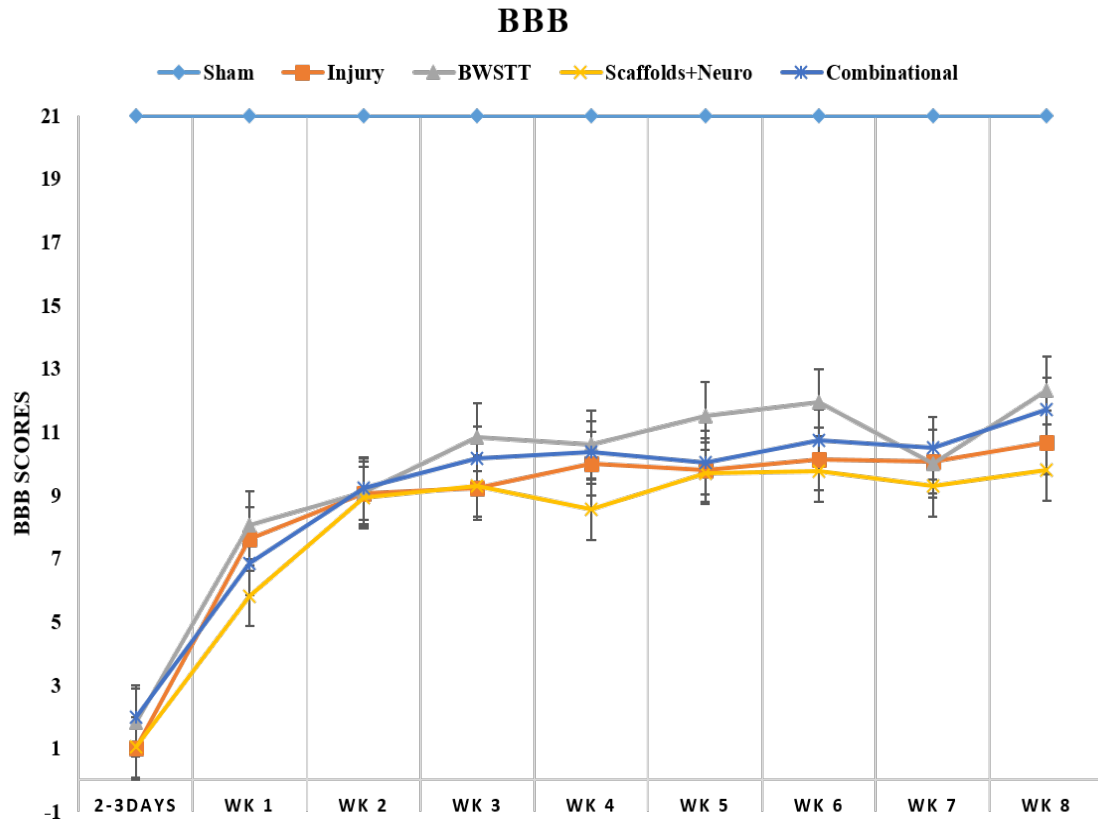


Figure 59. BBB Scores.

H-reflex. Figure 60 shows H-reflex response waveforms to stimulation at 0.3 and 10 Hz for all five groups. Figure 60A represents recording from a control animal stimulated at 0.3 Hz (the 100% response), along with (Figure 60B) the response at 10 Hz (group mean \pm SEM, 15.3 \pm 3.9% of the response at 0.3 Hz), and the response from an injury animal at 0.3 Hz (Figure 60C) (100%) and at 10 Hz (65.7 \pm 5.7%) (Figure 60D). Figure 60E and 60F show the H-reflex response of a transplant animal at 0.3 Hz (100%) and 10 Hz (58.7 \pm 8.8%). Figures 60G and 60H show the H-reflex response of a BWSTT animal at 0.3 Hz (100%) and 10 Hz (26.7 \pm 6.9%). Figures 60I and 60J show the H-reflex

response of a combinational animal at 0.3 Hz (100%) and 10 Hz (26.7±6.9%). These recordings demonstrate that in control animals, there is frequency-dependent depression, and this depression is lost in the injury and transplant groups, but not in the BWSTT and combinational groups.

Averages of the last 11 M and H responses were calculated for both stimulus frequency trains. Figure 61 shows the H/M ratio for each group at 10 Hz. This H/M ratio was plotted to determine the H-reflex rate depression seen in each group. Frequency dependent depression was observed to be restored in the BWSTT and combinational groups and not in the injury and transplant groups. Injury and transplant groups (*) were significantly different from control, BWSTT, and combinational groups (+) at the $p<0.05$ level. These results suggest that BWSTT and combinational treatment leads to a restoration of frequency dependent depression of the H-reflex. ANOVA of these groups showed statistically significant differences between experimental groups (df=4, $F=49.854$, $P<0.05$). Post hoc comparison between all groups showed significance at 10 Hz between the control, BWSTT, and combinational groups and the injury and transplant groups.

Figure 62 is a graph of the habituation of the H-reflex following stimulation at 0.3 and 10 Hz for the following groups of animals: Sham, Injury, Transplant, BWSTT, and Combinational. Statistically significant differences between injury and transplant (*) groups and the control, BWSTT, and combinational (+) groups were seen at the $p<0.05$ level for 10Hz. ANOVA of these groups showed statistically significant difference between experiment groups (df=4, $F=14.212$, $p<0.05$). Post hoc comparison also showed

the same significance at 10 Hz as the H/M ratio plot. The control, BWSTT, and combinational groups were significantly different from the injury and transplant groups.

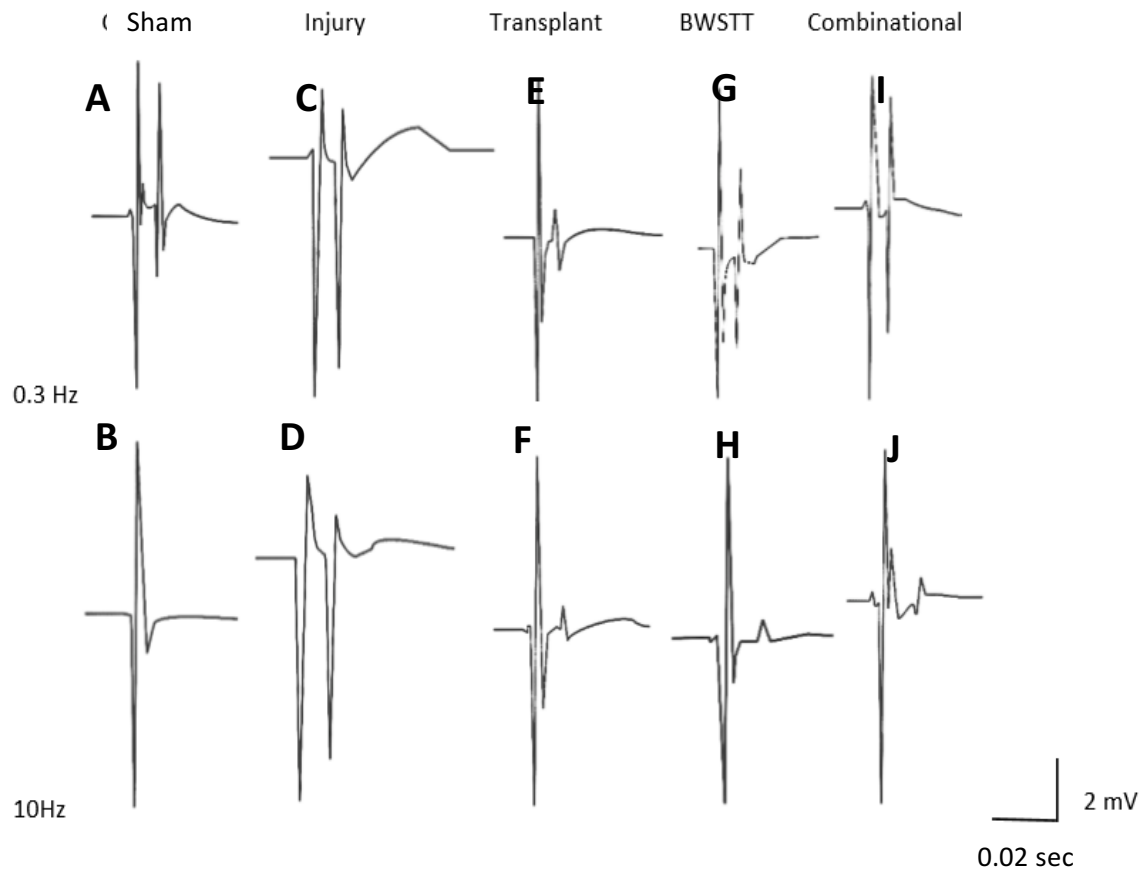


Figure 60. Averages of H-reflex recording at 0.3 and 10 Hz. The M-wave amplitude remains constant while the H-wave amplitude decreases with increasing stimulus frequency. A) H-reflex waveform response to stimulation at 0.3 Hz on a control rat. B) H-reflex waveform response to stimulation at 10 Hz in the same control rat. C) H-reflex waveform response to stimulation at 0.3 Hz in an injury only rat. D) H-reflex waveform response to stimulation at 10 Hz in the same injury only rat. There is a decrease in the frequency-dependent depression compared to control. E) H-reflex waveform response to stimulation at 0.3 Hz in transplant (scaffold and neurotrophins) animal. F) H-reflex waveform response to stimulation at 10 Hz in the same transplant rat. The transplant group also has a decrease in the frequency-dependent depression compared to control. G) H-reflex waveform response to stimulation at 0.3 Hz in a body weight support treadmill training (BWSTT) rat. H) H-reflex waveform response to stimulation at 10 Hz in the same BWSTT rat. I) H-reflex response waveform response to stimulation at 0.3 Hz in a combinational rat. J) H-reflex response waveform response to stimulation at 10 Hz in the same combinational rat. Note that the BWSTT and combinational groups had a return of frequency-dependent depression of the H-reflex. Calibration bars vertical 2 mV, horizontal 0.02 sec.

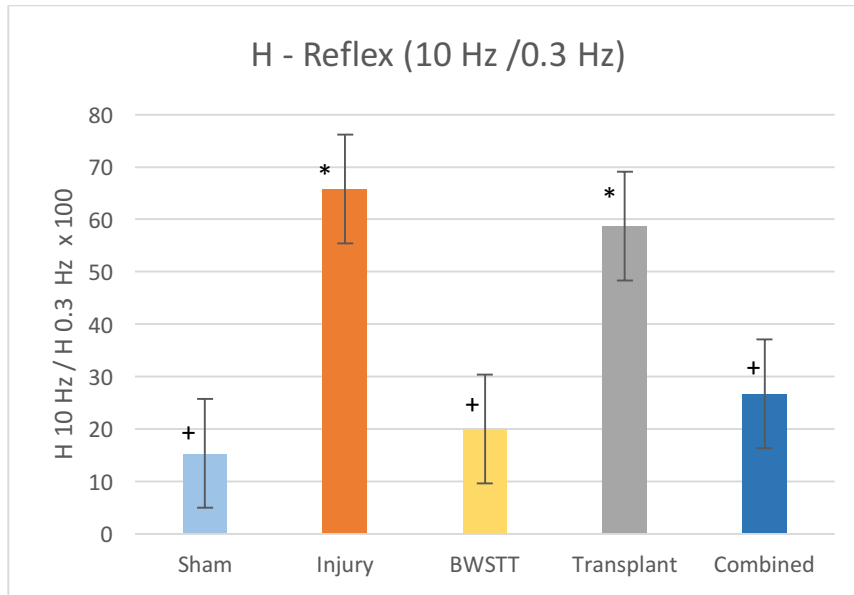


Figure 61. H ratio – 10/0.3 Hz for each group. The injury and transplant groups (*) are significantly different from the sham, BWSTT, and combinational groups (+) at the $P < 0.05$ level. *, +: Non-Significant.

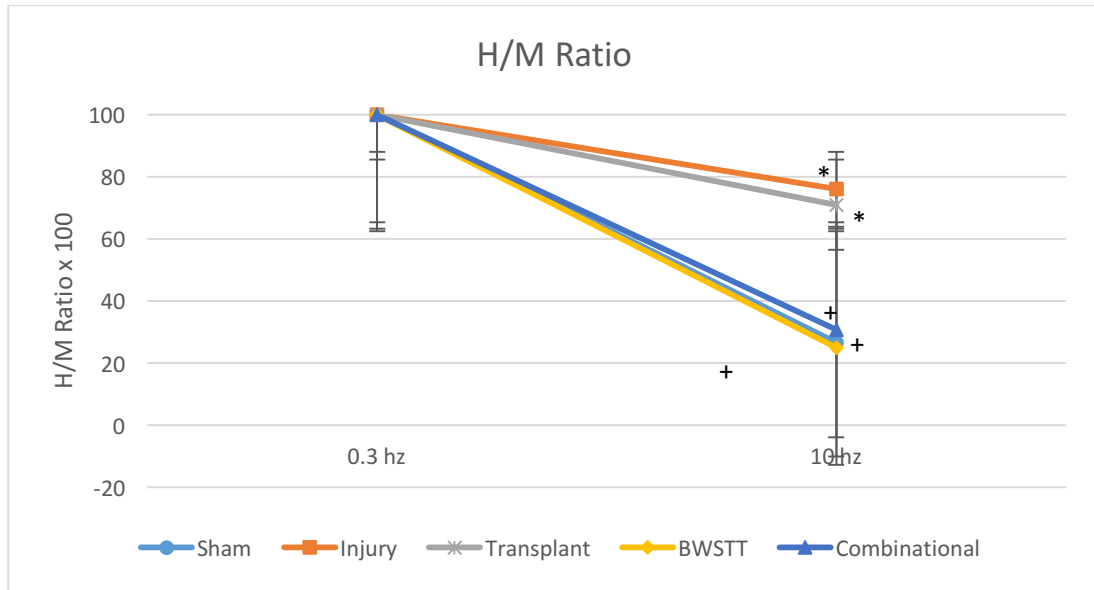


Figure 62. H/M Ratios at 0.3 and 10 Hz for control (circles), injury (square), BWSTT (diamond), transplant (asterisk) and combinational (triangle). Data normalized at 0.3 Hz indicates the injury and transplant groups (*) to be significantly different from the BWSTT, sham, and combinational groups, $P < 0.05$ level (+). *, +: Non-Significant.

Discussion

The hypothesis for this study is that neurotrophins secreting scaffold will (1) protect and minimize the secondary damage that the descending pathways undergo (2) promote growth of new pathways and (3) help achieve a better H-reflex response after body weight support treadmill training (BWSTT). Part 1 and 2 of the hypothesis will be proven later in phase 2: histology, part 3 was proven to be true according to results of part 1 presented in this paper.

The behavior analysis (BBB) showed no significance difference between groups. This is a course measurement of behavior recovery, that does not look at capturing

improvement in weight support and locomotion speed. This is why the second part of the study is kinematics analysis which is still ongoing. Kinematic analysis was tested at 75%, 65%, and 55% body weight support at a speed of 7cm/s and 10cm/s and this will help show if there is functional recovery within BWSTT and combinational groups.

Another thing to point out is why was there improvement of the H-reflex but not in the BBB scores (motor function). In motor functions, there are both poly and mono synaptic pathways that are involved, whereas the H-reflex is just a monosynaptic pathway (Lee et al., 2005; Gozariu et al., 1998). The monosynaptic pathways still give us critical information regarding spasticity which we know as a secondary complication after SCI (Adams et al., 2005).

The H-reflex has been a reliable and accurate measure of the changed spinal circuitry after spinal cord injury (SCI) in both contusion/compression (Lee et al., 2005; Magnuson et al., 1999; Skinner et al., 1996) and transection (Reese et al., 2006; Yates et al., 2008) models as well as in humans (Boorman et al., 1992; Phadke et al., 2006; Phadke et al., 2007; Rayegani et al., 2011; Schindler-Ivens et al., 2000; Yates et al., 2008). The contusion/compression models closely resemble the most common human spinal cord injuries (Blight et al., 2000; Magnuson et al., 1999), and can be used to assess all stages of the injury (spinal cord trauma, secondary tissue destruction, tissue repair process, stabilization of chronic lesion, and long-term disability) (Blight et al., 2000). The transection model is mainly used to test nerve fiber regeneration and cell transplantation (Blight, 2000). In the contusion/compression models, it is possible for the animals to regain some motor function, which is commonly observed in humans after SCI (Eaton,

2003). Our study used a moderate contusion injury, because we aimed to study the effects of bioengineering scaffold releasing neurotrophins and body weight supported treadmill training on H-reflex after incomplete injuries.

After SCI, the spinal circuitry changes and there is a reorganization (Reese et al., 2006) because of the loss of descending fibers modulating inhibitory fibers. These descending fibers are responsible for presynaptic inhibition of IA afferents onto motoneurons (Skinner et al., 1996). The H-reflex amplitude has shown to be proportional to the number of motoneurons that are activated at any stimulus, and the reflex measures the transmission between muscle afferents and the motoneurons (Skinner et al., 1996) and is influenced by the supraspinal control (Lee et al., 2005). After injury, the H-reflex response is exaggerated greatly (Phadke et al., 2007). The change in H-reflex amplitude at different stimulus frequency is the change in the excitability of the reflex pathways (Schindler-Ivens et al., 2000). At a higher frequency in a normal animal, a frequency-dependent depression is seen in the H-reflex, and after SCI, there is a decrease in the depression (Figure 60). This frequency-dependent depression results from the presynaptic inhibition due to lost descending fibers and the lack of changes in the motoneuronal excitability, which essentially controls the amplitude of the H-reflex (Skinner et al., 1996). Reese et al., 2006 reported that the decreased depression at low frequencies is related to a decrease in presynaptic inhibition. This draws our first hypothesis that by protecting and minimizing secondary damage of the descending pathways, a restoration of the H-reflex can occur.

It has been previously studied that the H-reflex is altered with rhythmic motions such as stepping, walking, running, and pedaling (Reese et al., 2006). Many studies have looked at incorporating an exercise regimen to produce a more normalized H-reflex depression because the exercise can compensate for the loss in presynaptic inhibition that happens after SCI, because the hindlimb/leg muscles are being alternately stretched in some form (Phadke et al., 2007; Skinner et al., 1996). Our study used a training regimen of BWSTT and the results showed that the BWSTT and combinational (Tx and BWSTT) groups did present a more normalized frequency rate depression as in the control group, when compared to the injury and transplant groups. These results were also reported by Skinner et al., 1996, where exercise helped to reorganize and preserve presynaptic inhibition producing an H-reflex amplitude with normal levels of frequency-dependent depression. In a similar study conducted by Reese et al., 2006, motorized bicycle exercise training (MBET) was shown to restore frequency-dependent depression of the H-reflex to normal level in the exercise, transected group. Boorman et al., 1992 study showed that H-reflex changes observed during pedaling and walking were due to presynaptic inhibition. It is also important to note that the level at which the spinal cord is transected can affect the H-reflex results at high frequencies. Skinner et al., 1996 supports the theory that at the T10 thoracic level, there is a reduced depression of the H-reflex at high frequencies. A study conducted by Reese et al., 2006 reported differently, in that their T10 transected group did not show any frequency-dependent depression at most stimulation frequencies. There have also been studies that have looked at how the severity effects the H-reflex. One particular study by Lee et al., 2005 showed that the changes that were observed in

the H-reflex results may be related to the severity of SCI. Our study used a moderate contusion injury across all of the groups.

Another aspect of SCI that becomes a problem to patients is spasticity. Spasticity can be seen in many forms such as hyperreflexia, clonus, clasp-knife responses, long-lasting cutaneous reflexes, and muscle spasms (Elbasiouny et al., 2010). One most commonly studied component of spasticity is hyperreflexia. The exact reason why hyperreflexia occurs is still unknown, but there have been reports of loss/decrease of presynaptic inhibition of Ia terminals, increase in postsynaptic receptor excitability, synapse growth and changes in intrinsic properties of alpha motoneurons (Reese et al., 2006; Yates et al., 2008) are involved. In humans, spasticity has been related to specific changes in excitability patterns of the soleus H-reflex (Phadke et al., 2007). Studies have shown that hyperreflexia is evident in animal models of SCI (Skinner et al., 1996), but does not happen immediately after SCI (Schindler-Ivens et al., 2000). It develops within 6-28 days after SCI in a contusion animal model (Yates et al., 2008) and has been shown to be evident even after 30 days (Reese et al., 2006). Since the hyperreflexia can be due to the loss/decrease of presynaptic inhibitions, researchers incorporate an exercise regimen that is known to compensate for the loss of presynaptic inhibitions and potentially decrease hyperreflexia. In our study, the H/M ratio was plotted for each group to see the habituation of the H-reflex. The lack of habituation shows that hyperreflexia may be present within those groups. The results showed that the injury and transplant groups presented very little habituation and the control, BWSTT, and combinational groups showed habituation. These results show that there was a possible increase in presynaptic

inhibition in the BWSTT and combinational groups producing a more normalized H-reflex response.

The combinational group used in our study has a combination of BWSTT and the bioengineered scaffold PNIPAAm-PEG loaded with neurotrophins (BDNF/NT-3). Biomaterials scaffolds, in general, are used to help bridge the gap between the lost tissue. They provide a site for an implant or host cells, and are capable of releasing therapeutic agents within the injured spinal cord, such as neurotrophins. These scaffolds also have the capability to preserve the local environment of the spinal cord through decreasing apoptosis of cells, inflammation and scar formation. The biomaterials are constructed from synthetic polymers that are easily blended together to create a unique biomaterial with the mechanical and physiochemical properties needed for its application (Kim et al., 2014). Some of PNIPAAm unique properties, which make it suitable for implantation within the spinal cord, are that it has compression modulus values in the range from 0.7 to 600 kPa and the self-ability to show thermal transitioning (Alexander et al., 2014). PEG also has a unique property that allows it to have an immune protecting effect on the spinal cord defects, because it helps to reseal cell membranes, which limits apoptosis (Assunção-Silva et al., 2014; Kim et al., 2014). Also, when implanted into the spinal cord, the PEG polymer is very resistant to recognition by the immune system not producing a response from the body (Assunção-Silva et al., 2014). This unique combination of PNIPAAm-PEG has been previously studied in spinal cords for cell transplantation, such as bioactive neurotrophins (Comolli et al., 2009; Grous et al., 2013;

Piantino et al., 2006) and load-bearing soft tissue applications (Alexander et al., 2014; Thomas et al., 2010).

These reported studies all used some form of the hydrogel PNIPAAm-PEG, except for Piantino et al., 2006. Piantino et al., 2006 looked at how PEG alone, coupled with NT-3, would improve recovery in a T8 laminectomy. The study reported improved locomotor recovery and greater axon growth when compared to control. Another study conducted by Grous et al., 2013 performed a cervical dorsolateral funiculotomy, and results showed that the cross-linked hydrogel PNIPAAm-g-PEG allowed axonal growth and successfully delivered BDNF into the injured spinal cord, while increasing recovery rate of fine motor function, when compared to control group (PNIPAAm-g-PEG only). Comolli et al., 2009 performed a similar study to Grous et al., 2013, but looked further into the neurotrophins and material properties of the neuronal tissue. The results showed that using PNIPAAm-PEG, loaded with NT-3 and BDNF neurotrophins were sustained for up to 4 weeks within the injury site, and bioactivity was confirmed after 4 weeks. Overall results from this study showed that PNIPAAm-PEG scaffold can be modified to match the mechanical properties of the neuronal tissue present within the spinal cord. Previous studies like Comolli et al., 2009 showed that PNIPAAm-PEG it is capable of releasing a drug over a long period of time and is biocompatible and biodegradable.

The growth factors NT-3 and BDNF are neurotrophins found in peripheral nerves and the spinal cord. They have shown to affect circuit behavior within the spinal cord. Long term treatment with these neurotrophins can provide a detour around the injury site of the spinal cord in neonatal and adult rats. Specifically looking at NT-3, it helps in the

survival of sensory afferent and it strengthens the group Ia synaptic projection to motoneurons. BDNF does not have an effect of the strength of the synaptic projections like NT-3, but it enhanced motor neuron excitability, which will produce a better H-reflex amplitude. It can also reduce synaptic inhibition (Boyce et al., 2014).

Conclusion

This study strengthens the results of previous studies in finding that an exercise regimen can help restore the frequency-dependent depression of the H-reflex (Lee et al., 2005; Reese et al., 2006; Skinner et al., 1996; Yates et al., 2008). Our study showed this restoration was present in the BWSTT and combinational groups, but not in the transplant group. The same effect was seen with the BBB test, such that the BWSTT and combinational groups exhibited functional recovery, but not the transplant group when compared to sham. There was also a decrease in habituation of the H-reflex, seen in both the BWSTT and combinational groups. These results open a new gateway for incomplete SCI patients through a unique tissue-engineering approach that has shown promise in clinical application. Our unique tissue engineering approach of using PNIPAA-m-PEG loaded with BDNF/NT-3 improved the H-reflex response in all aspects from habituation, spasticity, and frequency-dependent depression, but not as well as the BWSTT group. Future studies can combine this PNIPAA-m-PEG scaffold with other growth promoting agents, as well as different exercise regiments to explore the beneficial effects of the proposed combination treatment strategy in incomplete SCI animal models to see if a unique combination is proven more beneficial than BWSTT alone. This unique tissue-

engineering approach did not show a better result when compared to the BWSTT group, but did show promise when compared to sham and injury group.

Chapter 6

Future Work

There is much more future work that has to be done in order to cure spinal cord injuries. The study posed some limitations with respect to the bioengineered scaffold and rehabilitation techniques. Future work is needed to improve the study and the outcomes. Future studies should first look at the PNIPAAm-g-PEG with neurotrophins scaffold to access the changes in the anatomical and synaptic plasticity. These changes will access the neuroprotective and neroregenerative properties and to see if the scaffold was successful in establishing anatomical connections, while preserving spared descending pathways. If the PNIPAAm-g-PEG scaffold was found to be successful, then more studies should be conducted with that scaffold to improve the procedure and outcome of the studies. The scaffold injection process should be tested to access the amount of scaffold that was actually injected into the injury site. Problems arise with the scaffold leaking during injection. There needs to be a set procedure that can quantify and ensure the same amount of scaffold is injected into the injury site each time. Taking this into consideration can allow for better results and will eliminate the outliers that may have received more or less of the scaffold.

Future studies should also look at using different exercise regiments, such as robotic treadmill training because it is more accurate and precise during training (Querry et al., 2008). In our study this can be the reason why the BWSTT and combinational groups showed no difference statically. Another exercise regimen that can be tested with our bioengineered scaffold is motorized bicycle exercise. Skinner et al., 1996 and Reese

et al., 2006 studies showed that it was capable of restoring the H-reflex, so I would test for difference in the training and combinational groups because we did not see it in our study.

Studies should also look at different bioengineered scaffolds that have already proven helpful in some form for spinal cord injury repair. They should be tested to access their neuroprotective and neuroregeneration properties. Once these scaffolds are identified to have neuroprotective and neuroregeneration properties, they should be tested with different growth factors. Our transplant group using PNIPAAm-PEG loaded with BDNF/NT-3 did not show restoration of the H-reflex so a future study can look at replacing BDNF with NGF. NGF is known to prevent degeneration of neurons (Nerve) instead of encouraging neurogenesis (birth of neurons) like BDNF does (Patrick et al., 2011). Also combining NGF with NT-3 will allow different population to be affected by the neurotrophins (Nerve).

Another direction that future work can take is to study combinational biomaterials. These combinational biomaterials combine both cell-based therapies with hydrogel-based biomaterials. Since each part separately has shown to have some form of neuroprotective and neuroregenerative properties, they can be combined in a unique way to enhance these properties and to provide repair for spinal cord injury. There are many combinations that are able to be tested, but some may pose more ethical issues than others. This is the balance that researchers and society have to work with, but once there is a balance, combinational biomaterials have the best chance in spinal cord injury repair.

References

- Adams, M.M & Hicks, A.L. (2005). Spasticity after spinal cord injury. *Spinal Cord*, **43**:577-586.
- Alexander, A., Ajazuddin, Khan, J., Saraf, S. & Saraf, S. (2014). Polyethylene glycol (PEG)-Poly(N-isopropylacrylamide) (PNIPAAm) bases thermosensitive injectable hydrogels for biomedical applications. *European Journal of Pharmaceutics and Biopharmaceutics*, **(88)**: 575-585.
- Anatomy of the Spinal Cord (Section 2, Chapter 3) Neuroscience Online: An Electronic Textbook for the Neurosciences | Department of Neurobiology and Anatomy - The University of Texas Medical School at Houston. (n.d.). Retrieved February 17, 2016, from <http://neuroscience.uth.tmc.edu/s2/chapter03.html>
- Assunção-Silva, R.C., Gomes, E.D., Sousa, N., Silva, N.A. & Salgado, A.J. (2014). Hydrogels and cell Based Therapies in Spinal Cord Injury Regeneration. *Stem Cell International* **Article ID: 948040**: 24 pages.
- Basso, D.M., Beattie, M.S., Bresnahan, J.C. (1995). A sensitive and reliable locomotor rating scale for open field testing in rats. *Journal of Neurotrauma* **12**: 1-21.
- Blight, A.R. (2000). Animal Models of Spinal Cord Injury. *Top Spinal Cord Inj Rehabil*, **6(2)**: 1-13.
- Boorman, G., Becker, W.J., Morrice, B. & Lee, R.G. (1992). Modulation of the soleus H-reflex during pedaling in normal humans and in patients with spinal spasticity. *Journal of Neurology, Neurosurgery, and Psychiatry*, **55**: 1150-1156.
- Boyce, V.S. & Mendell, L.M. (2014). Neurotrophins and spinal circuit function. *Frontiers in Neural Circuits*, **59 (8)**: 1-7.
- Christopher and Dana Reeve Foundation, Paralysis Facts & Figures. (2009). Retrieved December 1, 2015, from http://www.christopherreeve.org/site/c.mtKZKGMWKwG/b.5184189/k.5587/Paralysis_Facts__Figures.htm
- Comolli, N., Neuguber, B., Fischer, I. & Lowman, A. (2009). In vitro analysis of PNIPAAm-PEG, a novel, injectable scaffold for spinal cord repair. *Acta Biomaterialia*, **5**: 1046-1055.
- Eaton, M. (2003). Common animal models for spasticity and pain. *Journal of Rehabilitation Research & Development*, **40(4)**: 41-54.

- Elbasiouny, S.M., Moroz, D., Bakr, M.M. & Mushahwar, V.K. (2010). Management of Spasticity After Spinal Cord Injury: Current Techniques and Future Directions. *Neurorehabilitation and Neural Repair*, **24(1)**: 23-33.
- Framptom, A.E. & Eynon, C.A. (2006). High dose methylprednisolone in the immediate management of acute, blunt spinal cord injury: what is the current practice in emergency departments, spinal units, and neurosurgical units in the UK?. *Emerg Med J*, **23**: 550-553.
- Gozariu, M., Roth, V., Keime, F., Bars, D. L. & Willer, J. (1998). An electrophysiological investigation into the monosynaptic H-reflex in the rat. *Brain Research*, **782**: 343-347.
- Grous, L.C, Vernengo, J., Jim, Y., Himes, B.T., Shumsky, J.S., Fischer, I. & Lowman, A. (2013). Implications of poly (N-isopropylacrylamide)-g-poly(ethylene glycol) with codissolved brain-derived neurotrophin factor injectable scaffold on motor function recovery rate following cervical dorsolateral funiculotomy in the rat. *J Neurosurg Spine*, **18**: 641-653.
- Hagen, E.M. (2015). Acute complications of spinal cord injuries. *World Journal of Orthopedics*, **6(1)**: 17-23.
- Hicks, A.L. & Ginia, K.A.M. (2008). Treadmill training after spinal cord injury: It's not just about the walking. *Journal of Rehabilitation Research & Development*, **45(2)**: 241-248.
- Hughenoltz, H. (2003). Methylprednisolone for acute spinal cord injury: not a standard of care. *CMAAJ*, **168 (9)**: 1145-1146.
- Hughenoltz, H., Cass, D.E., Dvorak, M.F., Fewer, D.H., Fox, R.J., Izukawa, D.M.S., Lexchin, J., Tuli, S., Bharatwal, N. & Short, C. (2002). High-dose methylprednisolone for acute closed spinal cord injury – only a treatment options. *The Canadian Journal of Neurological Sciences*, **29**: 227-235.
- Iwanami, A., Kaneko, S., Nakamura, M. (2005). Transplantation of human neural stem cells for spinal cord injury in primates. *Journal of Neuroscience Research*, **80(2)**: 182-190.
- Jones, M.L., Harness E., Denison, P., Tefertiller, C, Evans, N. & Larson, C.A. (2012). Activity-based Therapies in Spinal Cord Injury: Clinical Focus and Empirical Evidence in Three Independent Programs. *Top Spinal Cord Inj Rehabil*, **18 (1)**: 34-42.

- Takebeke, T.H., Kechner, H.E. & Knapp, P.A. (2005). The effect of passive cycling movements on spasticity after spinal cord injury: preliminary results. *Spinal Cord*, **42**: 483-488.
- Kakulas, B.A. (2004). Neuropathology: the foundation for new treatments in spinal cord injury. *Spinal Cord*, **42 (10)**: 549-563.
- Keirstead, H.S., Nistor, G., Bernal, G., Totoiu, M., Cloutier, F., Sharp, K. & Steward, O. (2005). Human Embryonic Stem Cell-Derived Oligodendrocyte Progenitor Cell Transplants Remyelinate and Restore Locomotion after Spinal Cord Injury. *The Journal of Neuroscience*, **25(19)**: 4694-4705.
- Kim, M., Park, S.R. & Choi, B.H. (2014). Biomaterial scaffolds used for the regeneration of spinal cord injury (SPI). *Histol Histopathol*, **29**: 000-000.
- Kirshblum, S.C., Burns, S.P., Biering-Sorensen, F., Donovan, W., Graves, D.E., Jha, A., Johansen, M., Jones, L., Krassioukov, A., Mulcahey, M.J., Schmidt-Read, M. & Waring, W. (2011). International standards for neurological classification of spinal cord injury (Revised 2011). *The Journal of Spinal Cord Medicine*, **34(6)**: 535-546.
- Knikou, M., Schmit, B. D., Chaudhuri, D., Kay, E. & Rymer, W. Z. (2007). Soleus H-reflex excitability changes in response to sinusoidal hip stretches in the injured human spinal cord. *Neuroscience Letters*, **423**: 18-23.
- Kundi, S., Bicknell, R. & Ahmed, Z. (2013). Spinal Cord Injury: Current Mammalian Models. *American Journal of Neuroscience*, **4(1)**: 1-12.
- Lam, T., Eng, J.J., Wolfe, D.L., Hsieh, J.T., Whittaker, M. & the SCIRE Research Team (2007). A systematic review of the efficacy of gait rehabilitation strategies for spinal cord injury. *Top Spinal Cord Inj Rehabil.*, **13(1)**: 32-57.
- Lee, J. K., Emch, G. S., Jognson, C. S. & Wrathall, J. R. (2005). Effect of spinal cord injury severity on alterations of the H-reflex. *Experimental Neurology*, **196**: 430-440.
- Lee, K.Y. & Mooney, D.J. (2012). Alginate: properties and biomedical applications. *Prog Polym Sci.*, **37(1)**: 106-126.
- Lu, P., Wang, Y., Graham, L., McHale, K., Gao, M., Wu, D., Brock, J., Blesch, A., Rosenzweig, E.S., Havton, L.A., Zheng, B., Conner, J.M., Marsala, M. & Tuszynski, M.H. (2012). Long-Distance Growth and Connectivity of Neural Stem Cells after Severe Spinal Cord Injury. *Cell*, **150(6)**: 1264-1273.

- Magnuson, D.S.K., Trinder, T.C., Zhang, Y.P., Burke, D., Morassutti, D.J. & Shields, C.B. (1999). Comparing Deficits Following Excitotoxic and Contusion Injuries in the Thoracic and Limbar Spinal Cord of the Adult Rat. *Experimental Neurology*, **156**: 191-204.
- Mahapatro, A. & Singh, D.K. (2011). Biodegradable nanoparticles are excellent vehicle for site directed in-vivo delivery of drugs and vaccines. *Journal of Nanobiotechnology*, **9**: 55.
- Martin, R., Sadowsky, C., Obst, K., Meyer, B. & McDonald, J. (2012). Functional electrical stimulation in spinal cord injury: from theory to practice. *Top Spinal Cord Inj Rehabil*, **12(1)**: 28-33.
- Moore, K.L., Dalley, A.F. & Agur, M.R. (1980) Clinically Oriented Anatomy. Retrieved from meded.lwwhealthlibrary.com.ezproxy.rowan.edu/book.aspx?bookid=739.
- Morita, S. (2014). Hydrogen-bonds structure in poly (2-hydroxyethyl methacrylate) studied by temperature-dependent infrared spectroscopy. *Frontiers in Chemistry*, **2**, 10. <http://doi.org/10.3389/fchem.2014.00010>
- Mukherjee, A. & Chakravarty, A. (2010). Spasticity mechanisms – for the clinician. *Frontiers in Neurology*, **149**.
- Nakazawa, K., Kawashima N. & Akai, M. (2006). Enhanced Stretch Reflex Excitability of the Soleus Muscle in Persons With Incomplete Rather Than Complete Chronic Spinal Cord Injury. *Arch Phys Med Rehabil*, **87**: 71-5.
- Nas, K., Yazmalar, L., Şah, V., Aydin, A. & Ö, K. (2015). Rehabilitation of spinal cord injuries. *World Journal or Orthopedics*, **6(1)**: 8-16.
- National Center for Biotechnology Information. PubChem Compound Database; CID=11966311, <https://pubchem.ncbi.nlm.nih.gov/compound/11966311> (accessed Oct. 26, 2015).
- National Center for Biotechnology Information. PubChem Compound Database; CID=3084050, <https://pubchem.ncbi.nlm.nih.gov/compound/3084050> (accessed Oct. 27, 2015).
- Nerve Regeneration - Neurotrophic Factors. (n.d.). Retrieved August 2, 2015, from http://biomed.brown.edu/Courses/BI108/BI108_2001_Groups/Nerve_Regeneration/Neurotrophic_Factors/Neurotrophic_Factors_Page_1.htm
- NINDS Spasticity Information Page. (2011, October 4). Retrieved November 18, 2015, from <http://www.ninds.nih.gov/disorders/spasticity/spasticity.htm>

- Nógrádi A, Vrbová G. Anatomy and Physiology of the Spinal Cord. In: Madame Curie Bioscience Database [Internet]. Austin (TX): Landes Bioscience; 2000-. Available from: <http://www.ncbi.nlm.nih.gov/books/NBK6229/>
- Patrick S. Murray and Philip V. Holmes, “An Overview of Brain-Derived Neurotrophic Factor and Implications for Excitotoxic Vulnerability in the Hippocampus,” *International Journal of Peptides*, vol. 2011, Article ID 654085, 12 pages, 2011. doi:10.1155/2011/654085
- Pease, R. W. (2006). *Merriam-Webster's medical dictionary*. Springfield, MA: Merriam-Webster.
- Phadke, C. P., Wu, S. S., Thompson F. J. & Behrman, A. L. (2007). Comparison of Soleus H-reflex Modulation after Incomplete Spinal Cord Injury in 2 Walking Environments: Treadmill with Body Weight Support and Overground. *Arch Phys Med Rehabil*, **88**: 1606-13.
- Phadke, C. P., Wu, S. S., Thompson, F. J. & Behrman, A. L. (2006). Soleus H-reflex modulation in response to change in percentage of leg loading in standing after incomplete spinal cord injury. *Neuroscience Letters*, **403**: 6-10.
- Piantino, J., Burdick, J.A., Goldberg, D., Langer, R. & Benowitz, L.I. (2006). An injectable, biodegradable hydrogel for trophic factor delivery enhances axonal regrowth and improves performance after spinal cord injury. *Experimental Neurology*, **201**: 359-367.
- Purves D, Augustine GJ, Fitzpatrick D, et al., editors. Neuroscience. 2nd edition. Sunderland (MA): Sinauer Associates; 2001. Damage to Descending Motor Pathways: The Upper Motor Neuron Syndrome. Available from: <http://www.ncbi.nlm.nih.gov/books/NBK10898/>
- Querry, R.G., Pacheco, F., Annaswamy, T., Goetz, L., Winchester, P.K. & Tansey, K.E. (2008). Synchronous stimulation and monitoring of soleus H reflex during robotic body weight-supported ambulation in subjects with spinal cord injury. *Journal of Rehabilitation Research & Development* **45**: 175-186.
- Radtke, C., Sasaki M., Lankford, K.L., Vogt, P.M. & Kocsis, J.D. (2008). Potential of olfactory ensheathing cells for cell-based therapy in spinal cord injury. *Journal of Rehabilitation Research & Development*, **45**: 141-152.

- Rauch, M.F., Hynes, S.R., Bertram, J., Redmond, A., Robinson, R., Williams, C., Xu, H., Madri, J.A. & Lavik, E., B. (2009). Engineering angiogenesis following spinal cord injury: A coculture of neural progenitor and endothelial cells in a degradable polymer implant leads to an increase in vessel density and formation of the blood-spinal cord barrier. *Eur J Neurosci*, **23(1)**: 132-145.
- Rayegani, S.M., Shojaee, H., Sedighipour, L., Soroush, M.R., Baghbani, M. & Amirani O.B. (2011). The effect of electrical passive cycling on spasticity in war veterans with spinal cord injury. *Frontiers in Neurology*, **39(2)**.
- Reese, N.B., Skinner, R.D., Mitchell, D., Yates, C., Barnes, C.N., Kiser, T.S. & Garcia-Till, E. (2006). Restoration of frequency-dependent depression of the H-reflex by passive exercise in spinal rats. *Spinal Cord*, **44**: 28-34.
- Sabapathy, V., Tharion, G. & Kumar, S. (2015). Cell Therapy Augments Functional Recovery Subsequent to Spinal Cord Injury under Experimental Conditions. **Article ID: 132172**: 12 pages.
- Schindler-Ivens, S. & Shields, R.K. (2000). Low frequency depression of H-reflexes in humans with acute and chronic spinal-cord injury. *Exp Brain Res*. **133(2)**: 233-241.
- Shoulders, M. D., & Raines, R. T. (2009). COLLAGEN STRUCTURE AND STABILITY. *Annual Review of Biochemistry*, *78*, 929–958.
<http://doi.org/10.1146/annurev.biochem.77.032207.120833>
- Skinner, R.D., Houle, J.D., Reese, N.B., Berry, C.L. & Garcia-Rill, E. (1996). Effects of exercise and fetal spinal cord implants on the H-reflex in chronically spinalized adult rats. *Brain Research* **729**: 127-131.
- Tam, R.Y., Fuehrmann T., Mitrousis N. & Shoichet, M.S. (2014). Regenerative Therapies for Central Nervous System Diseases: a Biomaterials Approach. *Neuropsychopharmacology* **39**: 169-188.
- Teng, Y.D., Lavik, E.B., Qu, X., Park, K.I., Ourednik, J., Zurakowski, D., Langer, R. & Snyder E. Y. (2002). Functional recovery following traumatic spinal cord injury mediated by a unique polymer scaffold seeded with neural stem cells. *PNAS*, **99(5)**:3024-3029.
- Tewarie, R.S.N., Hurtado, A., Bartels, R.H., Grotenhuis, A. & Oudegs, M. (2008). Stem Cell-Based Therapies for Spinal Cord Injury. *J Spinal Cord Med*. **32(2)**: 105-114.

- Thomas, J.D, Fussell, G., Sarkar, S., Lowman, A.M. & Marcolongo, M. (2010). Synthesis and recovery characteristics of branched and grafted PNIPAAm-PEG hydrogels for the development of an injectable load—bearing nucleus pulposus replacement. *Acta Biomaterialia*, **6**: 1319-1328.
- Tucker, K. J., Tuncer, M. & Türker, K. S. (2005). A review of the H-reflex and M-wave in the human triceps surae. *Human Movement Science*, **24**: 667-688.
- Ulbrich, K. & Šubr, V. (2010). Structural and chemical aspects of HPMA copolymers as drug carriers. *Advanced Drug Delivery Reviews*, **62(2)**: 150-166.
- Undas, A. & Ariëns, R.A.S. (2011). Fibrin Clot Structure and Function. *Arteriosclerosis, Thrombosis, and Vascular Biology*, **31**: 88-99.
- Voerman, G.E., Gregoric, M. & Hermens, H. J. (2005). Neurophysiological methods for the assessment of spasticity: The Hoffmann reflex, the tendon reflex, and the stretch reflex. *Disability and Rehabilitation*, **27 (1/2)**: 33-68.
- Xiong, Y., Zeng, Y., Zeng, C., Du, B., He, L., Quan, D., Zhang, W., Wang, J., Wu, J., Li, Y. & Li, J. (2009). Synaptic transmission of neural stem cells seeded in 3-dimensional PLGA scaffolds. *Biomaterials*, **30**: 3711-3722.
- Yates, C., Charlesworth, A., Allen, S.R., Reese, N.B., Skinner, R.D. & Garcia-Rill, E. (2008). The onset of hyperreflexia in the rat following complete spinal cord transection. *Spinal Cord* **46**: 798-803.

Appendix

Definitions

Adipocyte – Fat cell

Afferent – Bearing or conducting inward; specifically: conveying impulses toward the central nervous system

Aliphatic – Of, relating to, or being an organic compound (as an alkane or alkene) having an open-chain structure

Angiogenesis – The formation and differentiation of blood vessels

Anterior – Relating to or situated near or toward the head or toward the part in headless animals most nearly corresponding to the head; situated toward the front of the body

Antidromic – Proceeding or conducting in a direction opposite to the usual one – used especially of a nerve impulse or fiber

Apoptosis – A genetically directed process of cell self-destruction that is marked by the fragmentation of nuclear DNA and is a normal physiological process eliminating DNA-damages, superfluous, or unwanted cells – called also programmed cell death

Arachnoid – A thin membrane of the brains and spinal cord that lies between the dura mater and the pia mater

Astrocytes – A star shaped cell; especially: and comparatively large much-branched neuroglial cell

Axon – A usually long and single nerve-cell process that usually conducts impulses away from the cell body

Bioengineered - The application of biological techniques (as genetic recombination) to create modified versions of organisms

Blood-Brain Barrier – A barrier created by the modification of brain capillaries (as by reduction in fenestration and formation of tight cell-to-cell contacts) that prevents many substances from leaving the blood and crossing the capillary walls into the brain tissue

Cardiac Output – The volume of blood ejected from the left side of the heart in one minute

Cerebrospinal Fluid - A liquid that is comparable to serum but contains less dissolved material, that is secreted from the blood into the lateral ventricles of the brain, and that serves chiefly to maintain uniform pressure within the brain and spinal cord

Chondrocyte – A cartilage cell

Clonus – A series of alternating contractions and partial relaxations of a muscle that in some nervous diseases occurs in the form of convulsive spasms

Dendrite – Any of the usually branching protoplasmic process that conducts impulses toward the body of a nerve cell

Distal – Situated away from the part of attachment or origin or a central point as a: located away from the center of the body b: located away from the mesial plane of the body

Dorsal – Being or located near, on, or toward the upper surface of an animal (as a quadruped) opposite the lower or ventral surface; being or located near, on, or toward the back or posterior part of the human body

Dura Mater – The tough fibrous membrane lined with endothelium on the inner surface that envelops that brain and spinal cord external to the arachnoid and pia mater that in the spinal cord is separated from the bone by a considerable space and contains no venous sinuses

Efferent – Conducting outward from a part or organ specifically: conveying nervous impulses to an effector

Endoneurial – Endoneurium – The delicate connective tissue network holding together the individual fibers of a nerve

Endoneurium – The delicate connective tissue network holding together the individual fibers of nerve trunk

Epineurium – The external connective tissue sheath of a nerve trunk

Extension – The stretching of a fractured or dislocated limb so as to restore it to its natural position: an unbending movement around a joint in a limb (as the knee or elbow) that increases the angle between the bones of the limb at the joint

Extracellular – Situated or occurring outside a cell or the cells of the body

Fibrocartilage – Cartilage in which the matrix, except immediately about the cells, is largely composed of fibers like those of ordinary connective tissue; also: a structure or part composed of such cartilage

Flexion – A bending movement around a joint in a limb (as the knee or elbow) that decreases the angle between the bones of the limb at the joint

Glial – Glia – Supporting tissue that intermingles with the essential elements of nervous tissue especially in the brain, spinal cord, and ganglia and is composed of a network of fine fibrils and of flattened stellate cells with numerous radiating fibrillary processes

Habituation – A form of non-associative learning characterized by a decrease in responsiveness upon repeated exposure to a stimulus

Hemorrhaging – A copious discharge of blood from the blood vessels

Hydrogel – A gel in which the liquid is water

Hydrophilic – of, relating to, or having a strong affinity for water

Hyper-excitability – The state or condition of being unusually or excessively excitable

Hyperextension – To extend so that the angle between bones of a joint is greater than normal; also: to extend (as a body part) beyond the normal range of motion

Hyperreflexia – Over activity of physiological reflexes

Inflammation – A local response to cellular injury that is marked by capillary dilatation, leukocyte infiltration, redness, heat, pain, swelling, and often loss of function and that serves as a mechanism initiating the elimination of noxious agents of damaged tissue

Intramedullary – Situated or occurring within a medulla; especially: involving use of the marrow space of a bone support

Kyphosis - Exaggerated backward curvature of the thoracic region of the spinal column

Laminae – A thin plate or layer especially of an anatomical part

Laminectomy – Surgical removal of the posterior arch of a vertebra

Lateral – Of or relating to the side; especially, of a body part: lying at or extending toward the right or left side: lying away from the median axis of the body

Leukocyte – White blood cell, a cell (as a macrophage) of the tissues comparable to or derived from a leukocyte

Lordosis – Exaggerated forward curvature of the lumbar and cervical regions of the spinal column

Lymphocyte – Any of the colorless weakly motile cells originating from stem cells and differentiating in lymphoid tissue (as of the thymus or bone marrow) that are the typical cellular elements of lymph, include the cellular mediators of immunity, and constitute 20 to 30 percent of the white blood cells of normal human blood

Macrophage – A phagocytic tissue cell of the immune system that may be fixed or freely motile, is derived from a monocyte, functions in the destruction of foreign antigens, and serves as an antigen-presenting cell

Matrix – The extracellular substance in which tissue cells (as of connective tissue) are embedded

Medial Malleolus – A strong pyramid shaped process of the tibia that projects distally on the medial side of its lower extremity at the ankle

Median – Situated in the middle; specifically: lying in a plane dividing a bilateral animal into right and left halves

Metatarsal – Of, relating to, or being the part of the human foot or of the hind foot in quadrupeds between the tarsus and the phalanges that in humans comprises five elongated bones, which form the front of the instep and ball of the foot

Mixed Nerve – A nerve containing both sensory and motor fibers

Monocyte – A large white blood cell with finely granulated chromatin dispersed throughout the nucleus that is formed in the bone marrow, enters the blood, and migrates into the connective tissue where it is differentiated into a macrophage

Monomer – A chemical compound that can undergo polymerization

Monosynaptic – Having or involving a single neural synapse

Motor – Of or relating to, or being a motor neuron or a nerve containing motor neurons; of, relating to, concerned with, or involving muscular movement

Multipolar – Having several dendrites

Myelinated – Having a myelin sheath

Myelination – The process of acquiring a myelin sheath; the condition of being myelinated

Nerve Fiber – Any of the processes (as an axon or a dendrite) of a neuron

Neuroglia – **glia**: Supporting tissue that is intermingled with the essential elements of nervous tissue, especially in the brain, spinal cord, and ganglia and is composed of a network of fine fibrils and of flattened stellate cells with numerous radiating fibrillar processes

Neurolemma – **Neurilemma** : The outer layer surrounding a Schwann cell of a myelinated axon

Neuron – One of the cells that constitute nervous tissue, that have the property of transmitting and receiving nervous impulses, and that possess cytoplasmic

processes which are highly differentiated frequently as multiple dendrites or usually as solitary axons, and which conduct impulses toward and away from the cell body

Neuroprotective - Serving to protect neurons from injury or degeneration

Neurotransmitter – A substance that transmits nerve impulses across a synapse

Neurotrophin – Neurotrophic factor: Any of a group of neuropeptides (as nerve growth factor) that regulate the growth, differentiation, and survival of certain neurons in the peripheral and central nervous system

Neutrophil – A granulocyte that is the chief phagocyte white blood cell

Olfactory Bulb – A bulbous anterior projection of the olfactory lobe that is the place of termination of the olfactory nerves

Olfactory Nerve – Either of the pair of nerves that are the first cranial nerves, that serve to conduct sensory stimuli from the olfactory organ to the brain, and that arise from the olfactory cells and terminate in the olfactory bulb

Oligodendrocyte – A glial cell resembling an astrocyte, but smaller with few and slender processes having few branches and forming the myelin sheath around axons in the central nervous system

Orthodromic – Proceeding or conducting in a normal direction – used especially of a nerve impulse or fiber

Osteoblast – Bone forming cell

Paralysis – Complete or partial loss of function especially when involving the power of motion or of sensation in any part of the body

Perineurium –The sheath of connective tissue that surrounds a bundle of nerve fibers

Phagocyte – A cell (as a macrophage or neutrophil) that engulfs and consumes foreign material (as microorganisms) and debris (as dead tissue cell)

Pia Mater – The delicate and highly vascular membrane of connective tissue investing the brain and spinal cord, lying internal at the arachnoid and dura mater, dipping down between the convolutions of the brain, and sending an ingrowth into the anterior fissure of the spinal cord

Pluripotent – Not foxes as to developmental potentialities; especially: capable of differentiating into one of many cell types

Polymer – A chemical compound or mixture of compounds formed by polymerization and consisting essentially of repeating units

Posterior – Situated behind: as a: situated at or toward the hind part of the body: caudal b: dorsal – used of human anatomy in which the upright posture makes dorsal and caudal identical

Process – A part of the mass of an organism or organic structure that projects outward from the main mass

Soleus – A broad, flat muscle of the calf of the leg that lies deep to the gastrocnemius, arises from the back and upper part of the tibia and fibula and from a tendinous arch between them, inserts by a tendon that unites with that of the gastrocnemius to form the Achilles tendon, and acts to reflex the foot

Stroke Volume – The volume of blood pumped from a ventricle of the heart in one beat

Synapse – The place at which a nervous impulse passes from one neuron to another

Tibial Nerve – The large nerve in the back of the leg that is a continuation of the sciatic nerve and terminates at the medial malleolus in the lateral and medial plantar nerves

Pease, R. W. (2006). *Merriam-Webster's medical dictionary*. Springfield, MA: Merriam-Webster.